

N 65-33268

(ACCESSION NUMBER)

124
(PAGES)

(NASA OR NASA-OR AD NUMBER)

(THRU)

1
(CODE)01
(CATEGORY)

FACILITY FORM 602

NA

RESEARCH MEMORANDUM

EXPERIMENTAL AND THEORETICAL DETERMINATION OF
FORCES AND MOMENTS ON A STORE AND ON A STORE-PYLON
COMBINATION MOUNTED ON A 45° SWEPT-WING-FUSELAGE
CONFIGURATION AT A MACH NUMBER OF 1.61

By Odell A. Morris, Harry W. Carlson,
and Douglas J. Geier

Langley Aeronautical Laboratory
Langley Field, Va.

ADMINISTRATIVE - EFFECTIVE 1-15-64
Authorized: Memo Geo. Drobka NASA HQ.
Code ATSS-A Dtd. 3-12-64 Subj: Chang
in Security Classification Marking.

GPO PRICE \$

CSFTI PRICE(S) \$

Hard copy (HC)

Microfiche (MF)

NATIONAL ADVISORY COMMITTEE
FOR AERONAUTICS

WASHINGTON

January 30, 1958

Declassified by authority of NASA
Classification Change Notices No. 2-2-82
Dated ** 1-1-84

REF ID: A60118

NATIONAL ADVISORY COMMITTEE FOR AERONAUTICS

RESEARCH MEMORANDUM

EXPERIMENTAL AND THEORETICAL DETERMINATION OF
FORCES AND MOMENTS ON A STORE AND ON A STORE-PYLON
COMBINATION MOUNTED ON A 45° SWEEP-WING—FUSELAGE
CONFIGURATION AT A MACH NUMBER OF 1.61

By Odell A. Morris, Harry W. Carlson,
and Douglas J. Geier

SUMMARY

33268

An investigation of store-pylon forces and moments has been conducted in the Langley 4- by 4-foot supersonic pressure tunnel at a Mach number of 1.61. Separate forces and moments were measured simultaneously on a store and on a store-pylon combination for a number of pylon-mounted store locations below the wing of a 45° swept-wing—fuselage combination. Tests were made through an angle-of-attack range of -4° to 12° and an angle-of-sideslip range of -12° to 12° . The basic model configuration, which was almost identical to the model used in reference 1, simulates a heavy-bomber-type airplane with a large ogive cylinder store.

The results of the investigation indicate that the most important source of store-pylon side forces is the pylon itself. When immersed in a strong sidewash field, the pylon can assume a large load and also produce a large incremental load upon the store. Both tend to increase rapidly with increasing angle of attack or angle of sideslip. Location of the store-pylon combination in a sidewash field of strong intensity may also result in powerful secondary effects on the normal force and axial force of the store. The large unstable pitching moments obtained for the sweptforward store-pylon installations at moderate angles of attack indicate that release of an unfinned store from a forward store location could be hazardous. Tests with two stores mounted on the same wing panel show that the presence of the inboard store-pylon combination causes significant decreases in the outboard store and store-pylon side forces produced by angle of attack. The theory as used here provides a useful estimation of the angle-of-attack-induced store or store-pylon side force. However, the side force is underestimated at the inboard wing positions and is overestimated at the outboard positions.

Further

DECLASSIFIED - EFFECTIVE 1-15-64
Authority: Memo Geo. Drobka NASA HQ.
Code ATSS-A Dtd. 3-12-64 Subj: Chang
in Security Classification Marking.

for Check back
ABST card

INTRODUCTION

As a result of the wide use of external stores and nacelles on high-speed aircraft, extensive experimental investigation of the nature and origin of store loads has been conducted by the National Advisory Committee for Aeronautics. Previous investigations (see refs. 1, 2, and 3) have shown that at supersonic speeds the interference from the various aircraft components may produce large performance penalties and also large structural loads. The side forces are often the critical design load because of their magnitude and the inherent weakness of the pylon support to lateral loads and bending moments. The theoretical work of reference 4 indicated that store side-force loads may be calculated by linear theory with reasonable accuracy. However, the experimental data available for correlation were somewhat limited, particularly in the case of pylon-induced store loads. To the authors' knowledge, no supersonic data for the loads on the pylon itself were in existence.

The results of these and other investigations have indicated a need for additional experimental data on pylon-induced store loads and on pylon loads as well as a need to provide additional checks on the theoretical methods for the prediction of these loads. The present investigation extends the range of the tests of references 1 and 2 to obtain data on pylon-mounted store configurations over a wide angle-of-attack and angle-of-sideslip range at a Mach number of 1.61. The store and wing-fuselage combination of this investigation are geometrically identical to the model used in reference 1 with the exception of the fuselage afterbody. A pylon was not employed in the previous tests.

This report presents the forces and moments (five components) measured on the store in the presence of the pylon, and the forces and moments (three components) on the store-pylon combinations. The tests were conducted for a number of spanwise and chordwise store positions using several different store-pylon combinations for an angle-of-attack range of -4° to 12° and for an angle-of-sideslip range of -12° to 12° at angles of attack of 0° , 4° , and 8° . Correlations between the calculated and experimental store and store-pylon side-force loads are also included; some of these results have previously been presented in reference 5.

SYMBOLS

$C_{A,s}$ axial-force coefficient of store, F_A/qF

$C_{m,s}$ pitching-moment coefficient of store about store midpoint,
 M_y/qFl

$C_{N,s}$	normal-force coefficient of store, F_N/qF
$C_{n,s}$	yawing-moment coefficient of store about store midpoint, M_Z/qFl
$C_{n,s}'$	yawing-moment coefficient of store about pylon midpoint at wing chord plane, M_Z/qFl
$C_{Y,s}$	side-force coefficient of store, F_Y/qF
$C_{M,sp}$	bending-moment coefficient of store-pylon combination about pylon root at wing chord plane, M_B/qFl
$C_{n,sp}$	yawing-moment coefficient of store-pylon combination about pylon midpoint at wing chord plane, M_Z/qFl
$C_{Y,sp}$	side-force coefficient of store-pylon combination, F_Y/qF
\bar{c}	mean aerodynamic chord
F	maximum frontal area of store, 0.0123 sq ft
F_A	axial force, lb
F_N	normal force, lb
F_Y	side force, lb
l	store length, 12 in.
M_B	bending moment, in-lb
M_Y	pitching moment, in-lb
M_Z	yawing moment, in-lb
q	free-stream dynamic pressure, lb/sq ft
V	free-stream velocity, fps
x	chordwise position of store midpoint measured from nose of fuselage, in.
y	spanwise position of store center line, measured from fuse- lage center line, in.

- z vertical position of store center line, measured from wing chord plane, in.
- α angle of attack, deg
- β angle of sideslip, deg

APPARATUS AND TESTS

Models and Equipment

The principal dimensions of the models and the general arrangement of the test setup are shown in figure 1. The 45° swept-wing—fuselage—store combination was designed to simulate a heavy-bomber-type airplane with a large external store. The dimensions of this configuration were identical to those of the semispan model used in references 1 and 2 except for the cylindrical afterbody on the present fuselage.

The wing, fuselage, and stores were constructed of metal and the stores were supported by wing-mounted pylons attached to each wing panel. Slots were milled into the wing to provide a flat mounting surface for the pylons at each store position tested. Also, a slot along the span of each wing panel fitted with small cover plates provided a passage for the store and pylon balance leads into the fuselage.

The store mounted under the right wing panel contained an internal five-component strain-gage balance which measured the forces and moments on the store in the presence of the pylon. The store under the left wing panel was mounted to a three-component strain-gage balance enclosed within the pylon fairing which measured the forces and moments on the complete store-pylon combination. The swept and unswept pylons used in the tests had symmetrical 9-percent-thick circular-arc sections parallel to the free air stream. The 9-percent thickness of the pylon, which was somewhat larger than desired, was necessary in order to permit installation of the pylon balance. The overall dimensions of the store-pylon combination used for each wing panel were identical; however, they were quite different internally. (See cutaway drawing, fig. 1(c).) For the three-component pylon balance, the pylon was merely a fairing which enclosed the strain-gage beam and a different pylon was required for each store position tested in order to maintain a constant clearance (about $1/16$ inch) between the pylon and wing surface. Two separate three-component pylon strain-gage balances were necessary in order to instrument both the swept and unswept pylons.

For mounting the five-component store balance on the opposite wing panel, the pylon was a solid strut (except for a small hole which allowed

passage of the store-balance leads to the wing) and the same two pylons (the unswept and swept) were interchangeable for any of the store positions tested. A clearance gap of approximately 1/16 inch was provided at the store-pylon juncture to allow for balance deflection under loads. (See fig. 1(c).)

Tests

The complete wing-store model combination was mounted on the standard rotary sting of the Langley 4- by 4-foot supersonic pressure tunnel, which allowed the model to be pitched or yawed through a wide range of positions. For each store position, tests were made through an angle-of-attack range of -4° to 12° ($\beta = 0^{\circ}$) and through an angle-of-sideslip range of -12° to 12° at constant angles of attack of 0° , 4° , and 8° . However, for some positions, the angle ranges were restricted by the load limits of the test equipment or by fouling of the balance due to deflection under load.

The fifteen store-pylon configurations tested are shown in figure 2; figure 3 shows the positive direction of the measured forces and moments. For all model configurations tested, symmetrical store locations about the fuselage center line were employed. For all tests, in order to insure boundary-layer transition from laminar to turbulent flow, a 1/4-inch-wide strip of No. 60 carborundum grains and shellac was located on both surfaces of the wing at the 10-percent-chord point, on the fuselage nose 1/2 inch from the tip, and on the store nose 1/4 inch from the tip.

The tests were conducted in the Langley 4- by 4-foot supersonic pressure tunnel at a Mach number of 1.61 with a stagnation pressure of 5 pounds per square inch absolute and a corresponding Reynolds number of 1.4×10^6 per foot. Also, repeat tests were conducted at a stagnation pressure of 10 pounds per square inch absolute with a corresponding Reynolds number of 2.7×10^6 per foot. Comparison of the data taken at both pressures showed good agreement. (See fig. 4.)

Accuracy of Data

The angles of attack and sideslip have been corrected for deflection of the balance and sting under load. No correction has been made for the effect of gaps at the wing-pylon and at the store-pylon junctures which allow clearance for balance deflection. However, the effect of these gaps on the accuracy of the data is believed to be small.

An estimate of the probable accuracy of the present data as determined from an inspection of repeat test points and static-deflection calibration is as follows:

α , deg	± 0.2
β , deg	± 0.2
x, in.	± 0.025
y, in.	± 0.05
z, in.	± 0.025

Store:

$C_{A,s}$	± 0.02
$C_{N,s}$	± 0.02
$C_{m,s}$	± 0.02
$C_{Y,s}$	± 0.05
$C_{n,s}$	± 0.02

Store-pylon combination:

$C_{Y,sp}$	± 0.06
$C_{n,sp}$	± 0.02
$C_{M,sp}$	± 0.02

PRESENTATION OF DATA

The isolated store axial-force, normal-force, and pitching-moment coefficients for the store with and without fins (reported in refs. 1, 2, and 6) are presented in figure 5. Figure 6 presents schlieren photographs for some of the model configurations tested.

The bulk of the store and store-pylon data is plotted against angle of attack and angle of sideslip for the various store positions and is presented in figures 7 to 32. The figures are plotted with the data for two, three, or four store positions in each figure with the store-pylon configuration used being identified by the symbol opposite the small-scale drawings in each figure. The fifteen store-pylon combinations tested are grouped in such a manner as to show the various effects of the different store-pylon positions and combinations; thus, in a number of the figures, some of the data are repeated for ease of comparison. The store yawing-moment coefficients that are plotted against angle of attack are presented both about the store midpoint and about the pylon center at the wing-pylon juncture for convenience in making comparison with the store-pylon data. Spanwise and chordwise comparison plots of the store and store-pylon data, together with store data of references 1 and 2, are

presented in figures 33 and 34, respectively. Comparison of the experimental and calculated store and store-pylon side-force loads is presented in figures 35 to 38.

A general index of the data figures presenting the results is as follows:

	Figure
Stagnation pressure plots	4
Isolated store data	5
Schlieren photographs	6
Store coefficients plotted against α	7 to 13
Store-pylon coefficients plotted against α	14 to 19
Store coefficients plotted against β	20 to 26
Store-pylon coefficients plotted against β	27 to 32
Store spanwise and chordwise comparison plots	33 and 34
Comparison of store and store-pylon side forces	35
Theoretical components of side force	36
Comparison of theoretical and experimental side force	37 and 38

RESULTS AND DISCUSSION

Experience shows that the structural design of the pylon and its attachment to both the wing and the store are generally determined by the side forces on the store and store-pylon assembly. The side-force loads are important structurally because they produce large bending moments in a direction of least structural strength and large yawing (twisting) moments on the pylon. The following discussion is therefore directed principally toward the variations in side force, which is considered the fundamental component. Also included in this discussion is a comparison of the measured side forces with those computed by using the methods of references 4 and 5.

Variation of the Forces and Moments With Angle of Attack

Effects of store position.- For most test positions of the basic store, large changes in the magnitudes of all of the measured store and store-pylon forces and moments occurred with increases in angle of attack and with changes in store spanwise and chordwise position. (See figs. 7, 8, and 14.)

Of the components measured, the most significant changes were shown for the store and store-pylon side-force coefficients. The side-force curves for both the store and store-pylon combination showed essentially linear variation with increases in angle of attack. However, the slopes of the store-pylon curves were at least two to three times greater (depending upon store position) than those of the store.



In most cases, the bending-moment coefficients show sizable increases with increasing angle of attack (fig. 14(b)). It can be calculated that the center of pressure of the store-pylon assembly moves downward about 20 percent of the pylon span (assuming span is equal to 2.09 inches) from about the pylon-midspan location as the angle of attack is increased from 0° to 12° .

Relative to the performance problem imposed by the use of stores, it should be noted that for the forward store location (figs. 7(a) and 8(a)) the store axial-force coefficient decreases with increasing angle of attack, whereas an equally large increase was shown for the most rearward location. The increase in axial-force coefficient with span position (fig. 7(a)) will be discussed in a later section. Of course, no conclusions can be drawn about overall airplane performance without the corresponding wing-fuselage data. The pitching-moment data of figure 8(b) and the normal-force data of figure 8(a) are of interest when there is concern over the release characteristics of a jettisoned store. The data indicate that because of the large positive pitching-moment coefficients obtained at moderate airplane angles of attack, release from a forward location would be hazardous. (Also, see fig. 7(b).) The large moments could cause a nose-up store attitude at which enough lift might be generated to force the store to strike the pylon or wing. At the rearward location (fig. 8(b)), although the pitching-moment coefficients are not large, the normal-force coefficient may in itself make a satisfactory release difficult. For the midchord positions, the negative initial moments should aid in obtaining satisfactory releases.

Effects of store fins and store tail cone.- For the two store-pylon configurations tested, addition of the tail cone had only small and generally negligible effects on the measured store characteristics (figs. 10, 11, 16, and 17). In general, addition of the fins to the basic store caused large changes in all the coefficients except side-force coefficient at store positions where the fins were placed in a low sidewash region. (See figs. 9 to 12 and 15 to 18.) The large changes which occurred for $C_{N,s}$, $C_{m,s}$, and $C_{A,s}$ due to the fins, however, were primarily a result of the changes shown by the isolated-store fin data. (See fig. 5.) The determination of whether the addition of fins to the store at the midchord location would increase the possibility of a satisfactory release would require a detailed study. The large negative moment would aid release, but the positive normal force would tend to make release more difficult.

Effect of pylon location.- When the unswept pylon was moved from a forward to a rearward location while maintaining the same store position, the largest changes occurred for store normal-force coefficient and for the store and store-pylon side-force coefficients (figs. 13 and 19). At the higher angles of attack, the side-force coefficients for



the rearward pylon position were less than in the forward position, whereas the store normal-force coefficient showed an increase. The pylon in the forward location is in a sidewash region of greater intensity (shown by the higher store-ylon side-force loads in fig. 19); in this position, the presence of the pylon results in larger decreases in the store normal-force coefficient.


Interference effect of an inboard store on an outboard store.- Figures 12 and 18 show the effect on the outboard store and store-ylon loads of adding an inboard store at the location indicated in figure 2. Only small changes in store axial-force, pitching-moment, and yawing-moment coefficients were produced by the presence of the inboard store. However, a significant increase in store normal-force coefficient and a significant decrease in store and store-ylon side-force coefficients were measured as the angle of attack was increased. In addition to the interference effects produced by the flow field of the inboard store and pylon, this installation is believed to act as a "fence" which reduces the outward wing sidewash due to angle of attack. Consequently, these interference effects produced by the inboard store reduced the store side-force coefficient and increased the store normal-force coefficient on the outboard store.

Variation of the Forces and Moments

With Angle of Sideslip

For the basic store position, the store and store-ylon data (figs. 20, 21, and 27) show large changes in the measured coefficients with increases in β . The most noteworthy changes occurred for the store and store-ylon side-force coefficients and for store normal-force coefficients. Large increases in the store and store-ylon side-force coefficients with increases in sideslip angle were accompanied by large decreases in store normal-force coefficients. In general, for the store and store-ylon side force, the effects of the combined α and β (shown for angles of attack of 4° and 8°) are additive when the store is located on the rearward wing panel ($-\beta$ range for store, $+\beta$ range for the store-ylon combination) and thus results in even larger loads on the store and store-ylon combination than previously shown by the data taken at $\beta = 0^\circ$.

Effect of store position.- Examination of the coefficients of figures 20, 21, and 27 also shows that the effects of store spanwise and chordwise position are sizable, with the variation of the coefficients being somewhat more pronounced for store chordwise movement than for store spanwise movement over the range of positions tested. The effects of store position are generally smaller than the effects produced by variation in angle of sideslip. In the case of the store and store-ylon side-force coefficients, the changes over the range of store positions



tested are about one-third as large as the changes due to angle of sideslip at the extreme angles of 12° tested. (See fig. 38.)

Effect of store fins and store tail cone.- The data of figures 22 to 25 and 28 to 31 show that addition of the store fins caused moderate to large incremental changes in all of the store and store-pylon coefficients measured, with the incremental changes in $C_{A,s}$, $C_{N,s}$, and $C_{m,s}$ (for most cases) being little affected by angle of sideslip. However, in the case of the store and store-pylon side-force and yawing-moment coefficients, the addition of the fins produces large increases in the slope of the curves as would be expected.

Again, addition of the faired tail cone caused only small and generally negligible effects on all the coefficients except store axial-force coefficient.

Effect of pylon location.- Examination of the data of figures 26 and 32 shows that a change in pylon position produces only small to moderate changes in the measured coefficients with variation in β except in the case of the coefficients $C_{N,s}$ and $C_{n,sp}$. The large slope change shown for the store-pylon yawing-moment curve would be expected since the moments were computed about the pylon center. For store normal-force coefficient, moving the pylon rearward caused unusually large increases in the coefficients in the negative β range and only small changes in the positive β range.

Interference effect of an inboard store on an outboard store.- Figures 25 and 31 show that the addition of the inboard store produced large changes in all the coefficients (except $C_{y,s}$) which increase with angle of sideslip when the store was on the rearward wing panel (that is, positive β for the store-pylon coefficients and negative β for the store coefficients). However, when the model was yawed so that the store was located on the forward wing panel, the incremental changes in $C_{N,s}$, $C_{m,s}$, and $C_{y,sp}$ for the outboard store decreased gradually with increasing sideslip angle until the differences became small or negligible at the higher angles. This results from the fact that the flow due to sideslip tends to cancel the side flow due to wing angle of attack and the flow due to the inboard store; thus, the outboard store undergoes no sizable change in interference originating from the inboard-mounted store.

Relative Contribution of the Store and Pylon Toward

Total Store-Pylon Loads

In order to show the relative contribution of the store and pylon toward some of the total store-eylon loads, the comparison plots of figures 33 and 34 were prepared by using the store data of references 1 and 2 (with no pylon) and the present store data. For the spanwise comparison plots (fig. 33), the most important effects of the pylon were on the store and store-eylon side force and store axial force. This figure, which illustrates more clearly the breakdown in side-force loads, shows that the pylon carries the largest proportion of the total side-force load, with the variation due to spanwise position being relatively small in comparison with the large changes caused by the addition of the pylon. The large changes which occurred in store axial force due to the presence of the pylon were substantially greater for the outboard store positions than for the inboard store positions. Changes in $C_{m,s}$, $C_{n,s}$, $C_{N,s}$ were generally variable along the span and were small. In considering these effects, it should be noted that the pylon location is moved forward slightly on the store with outboard store movement. With variation in store chordwise position (fig. 34), the presence of the pylon also caused large increases in the store and store-eylon side force. Also, the presence of the pylon produced large increases in store axial force; however, the incremental increases were only little affected by store chordwise position and pylon sweep.

Figure 35 has been prepared to show the relative contribution of the store and store-eylon side force to the total load over the β range. Data at an angle of attack of 4.1° are presented for six test configurations. In general, it is seen that for the β range of these tests, as well as for the α range, the pylon carries a load as large as or larger than that on the store.

Theoretical Consideration

Store and store-eylon side forces have been estimated by using the methods of references 4, 5, and 7. The wing-fuselage flow-field information has been obtained from a number of sources. The wing-thickness static-pressure distributions were determined by differentiating velocity potential with respect to x by using methods similar to those shown in reference 8, numerical integration being substituted for the graphical integration used therein. Wing-thickness sidewash was found by differentiating that velocity potential with respect to y . Fuselage-thickness effects were found to be small and are not included in this analysis. The wing-angle-of-attack sidewash has been computed by using the formulas of reference 9.

The estimation of the complete side-force load on a store-pylon installation immersed in a nonuniform flow requires consideration of a number of factors whose relative importance will be shown later. The buoyant side force acting on the store was found by a graphical integration over the store surface of the static pressures due to the wing thickness. The potential side force due to the thickness and angle-of-attack sidewash distribution along the store center line was calculated by using the method of reference 10. The viscous side force due to the thickness and angle-of-attack sidewash distribution along the store center line was determined by a graphical integration of the crossflow drag over the length of the store (ref. 7). The pylon side force and the store side force caused by the presence of the pylon were calculated by the method given in reference 5, which simply uses an average of the sidewash over the surface of the pylon and assumes that the presence of the pylon in no way alters the flow.

Figure 36 has been prepared to illustrate the relative importance of the various theoretical components of the store-pylon side force; one of the configurations of this test has been used as an example. Store or store-pylon side force has been plotted as a function of airplane angle of attack. Contributions to the total store-pylon side force are made cumulatively. Each curve is identified by a component of the theory and represents the sum of that component and all components listed below it. The one outstanding feature of this figure is the overpowering effect of the pylon on the total store-pylon side force.

In figure 37 the theoretical side force is compared with experimental side force for eight of the configurations tested. Again, the store or store-pylon side force has been plotted as a function of airplane angle of attack. In figure 37(a) data for the store and sweptforward pylon are presented for the spanwise positions. The theory is seen to underestimate the experiment at the inboard station and overestimate it at the outboard station. An examination of the schlieren photographs (fig. 6) shows that the shock from the wing-leading-edge—fuselage juncture appears to be a significant distance ahead of the leading edge instead of being behind as is the Mach line used in the theory. The schlieren photographs of figure 6(a) show that the wing-leading-edge shock angle for the wing-fuselage combination is unaffected by the presence of the store and pylon. Accordingly, the wing-angle-of-attack flow field was recalculated for a Mach number of 1.4 for which the Mach angle equaled the measured shock angle. Use of this theoretical sidewash distribution resulted in an improved prediction of the slope of the store-pylon side-force curves as was shown in reference 5.

Also shown in figure 37(a) are data for a store and rearward-swept pylon. Store-pylon data are not presented here because the pylon yawing-moment data taken during this run, which were obviously in error, throw

doubt on the validity of the side-force measurements. Unfortunately, the data were published in reference 5 before the error was discovered.

In figure 37(b) data are shown for four more configurations illustrating the effect of fins, a store tail cone, and a change in pylon location for a fixed store position. Since the store or store-pylon load is determined predominantly by the sidewash acting on the pylon, it is interesting to note the change in loading with a change in pylon location, everything else remaining constant. The large effect of the relocation and the degree to which it could be predicted is shown in the upper half of figure 37(b). The discrepancies between experiment and theory may be caused by the failure of the actual sidewash to reach fully the theoretical peak values near the leading edge. This was demonstrated in reference 5 when, as mentioned before, the subsonic-leading-edge type of sidewash distribution was found to give a better agreement.

A comparison of the data for the closed store afterbody (that is, tail cone on) with that of the boattail afterbody showed little or no change. Although for isolated bodies the slender-body concept is greatly dependent on the degree of boattailing, that factor was relatively unimportant in this case because of the small contribution of the potential side force.

The remaining configuration treated in figure 37(b) is one with a finned store which is the same in other respects as an earlier configuration. The increase in the slope of the curve has been fairly well predicted but the theory predicts a change in intercept that is not realized.

A simplified procedure has been applied to the calculation of the side-force variation with sideslip angle. The pylon and pylon-induced store side force, the store potential side-force, and the store viscous side force were computed for a uniform sidewash angle equal to the angle of sideslip. Thus, the theoretical side force due to sideslip is dependent only on pylon area, store geometry, and the ratio of pylon span to store diameter. Since the theory shows the same results for all configurations of these tests except those having store afterbody changes, the theory and data from the configurations tested are shown in figure 38 on one set of axes. In this figure, the store or store-pylon incremental side force due to sideslip is plotted as a function of sideslip angle for an angle of attack of 4° . The theory is seen to overestimate by a substantial margin the experimental data for the configurations shown. However it should be noted that the experimental side force at constant α is primarily a function of β rather than of configuration. A more accurate prediction of the effects of angle of sideslip may possibly be obtained by considering the effects of the changes in leading-edge sweep. (See ref. 11.)

In general, the theory as used here provides a useful estimation of the angle-of-attack-induced store or store-pylon side force. However, the side force is underestimated at the inboard wing positions and is overestimated at the outboard positions. The simplified treatment of the sideslip effects yielded an overestimation of the side-force increment ranging from 50 percent to 100 percent. Also, it has been shown that with a large pylon, as employed in these tests, a theoretical treatment of the pylon effect alone gives a prediction which is improved only slightly by the addition of all the other theoretical considerations.

CONCLUSIONS

Forces and moments have been measured at a Mach number of 1.61 on a store and on a store-pylon combination for a number of pylon-mounted store positions below the wing of a 45° swept-wing-fuselage combination. Theoretical calculations of store and store-pylon side forces have been compared with experimental data. Results of the investigation indicate the following conclusions:

1. The most important source of store-pylon side force is the pylon itself. When immersed in a strong sidewash field, the pylon can assume a large load and also produce a large incremental load upon the store. Both tend to increase rapidly with increasing angle of attack or angle of sideslip.
2. Location of the store-pylon combination in a sidewash field of strong intensity may also result in powerful secondary effects on the normal force and axial force of the store.
3. The large unstable pitching moments obtained for the sweptforward store-pylon installations at moderate angles of attack indicate that release of an unfinned store from a forward store location could be hazardous.
4. Tests with two stores mounted on the same wing panel show that the presence of the inboard store-pylon combination causes significant decreases in the outboard store and store-pylon side forces produced by angle of attack.
5. The theory as used here provides a useful estimation of the angle-of-attack-induced store or store-pylon side force. However, the side force is underestimated at the inboard wing positions and is overestimated at the outboard positions.

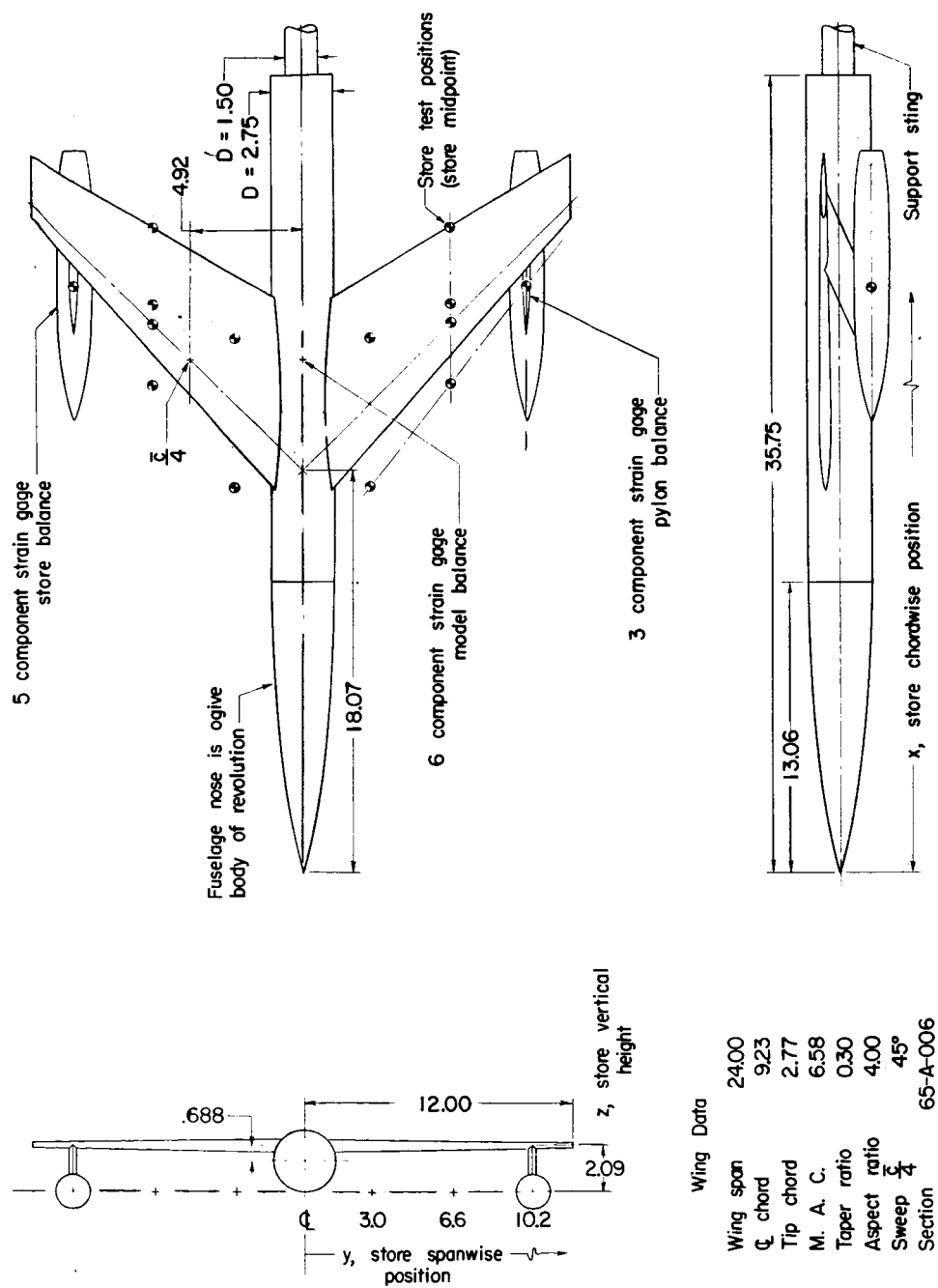
Langley Aeronautical Laboratory,
National Advisory Committee for Aeronautics,
Langley Field, Va., October 25, 1957.

REFERENCES

1. Smith, Norman F., and Carlson, Harry W.: The Origin and Distribution of Supersonic Store Interference From Measurement of Individual Forces on Several Wing-Fuselage-Store Configurations. I.- Swept-Wing Heavy-Bomber Configuration With Large Store (Nacelle). Lift and Drag; Mach Number, 1.61. NACA RM L55A13a, 1955.
2. Smith, Norman F., and Carlson, Harry W.: The Origin and Distribution of Supersonic Store Interference From Measurement of Individual Forces on Several Wing-Fuselage-Store Configurations. II.- Swept-Wing Heavy-Bomber Configuration With Large Store (Nacelle). Lateral Forces and Pitching Moments; Mach Number, 1.61. NACA RM L55E26a, 1955.
3. Guy, Lawrence D., and Hadaway, William M.: Aerodynamic Loads on an External Store Adjacent to a 45° Sweptback Wing at Mach Numbers From 0.70 to 1.96, Including an Evaluation of Techniques Used. NACA RM L55H12, 1955.
4. Bobbitt, Percy J., Malvestuto, Frank S., Jr., and Margolis, Kenneth: Theoretical Prediction of the Side Force on Stores Attached to Configurations Traveling at Supersonic Speeds. NACA RM L55L30b, 1956.
5. Bobbitt, Percy J., Carlson, Harry W., and Pearson, Albin O.: Calculation of External-Store Loads and Correlation With Experiment. NACA RM L57D30a, 1957.
6. Smith, Norman F.: The Origin and Distribution of Supersonic Store Interference From Measurement of Individual Forces on Several Wing-Fuselage-Store Configurations. VI.- Swept-Wing Heavy-Bomber Configuration With Stores of Different Sizes and Shapes. NACA RM L55L08, 1956.
7. Allen, H. Julian: Estimation of the Forces and Moments Acting on Inclined Bodies of Revolution of High Fineness Ratio. NACA RM A9I26, 1949.
8. Carlson, Harry W., and Geier, Douglas J.: The Origin and Distribution of Supersonic Store Interference From Measurement of Individual Forces on Several Wing-Fuselage-Store Configurations. V.- Swept-Wing Heavy-Bomber Configuration With Large Store (Nacelle). Mach Number 2.01. NACA RM L55K15, 1956.
9. Bobbitt, Percy J., and Maxie, Peter J., Jr.: Sidewash in the Vicinity of Lifting Swept Wings at Supersonic Speeds. NACA TN 3938, 1957.

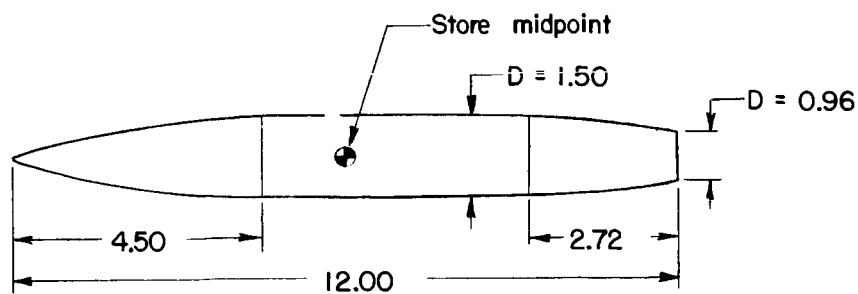
037122

10. Moskowitz, Barry: Approximate Theory for Calculation of Lift of Bodies, Afterbodies, and Combinations of Bodies. NACA TN 2669, 1952.
11. Goldstein, S., and Ward, G. M.: The Linearised Theory of Conical Fields in Supersonic Flow, With Applications to Plane Aerofoils. Aero. Quarterly, vol. II, pt. I, May 1950, pp. 39-84.

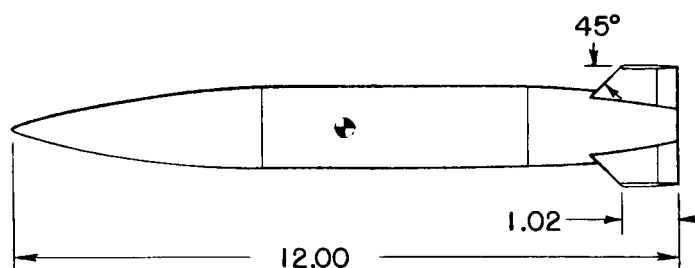
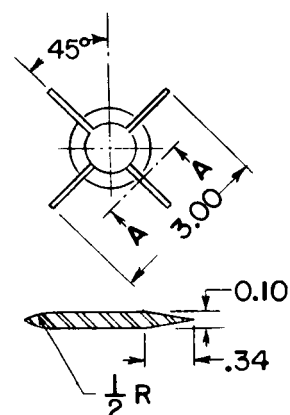


(a) Dimensions of wing-fuselage model combination and store positions investigated.

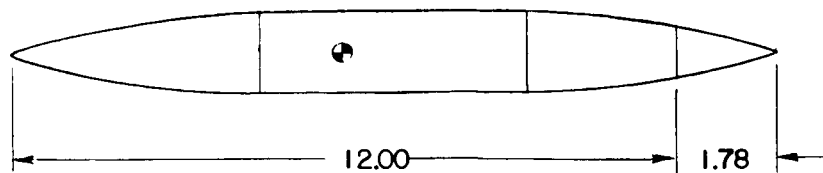
Figure 1.- Details of model and stores. (All dimensions in inches.)



Basic store configuration

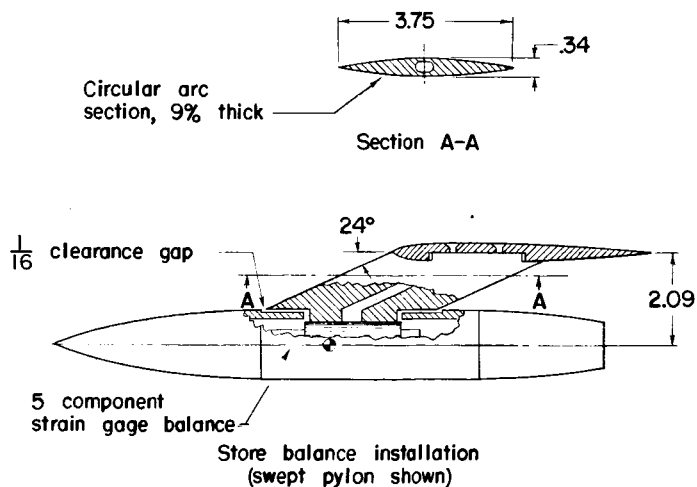
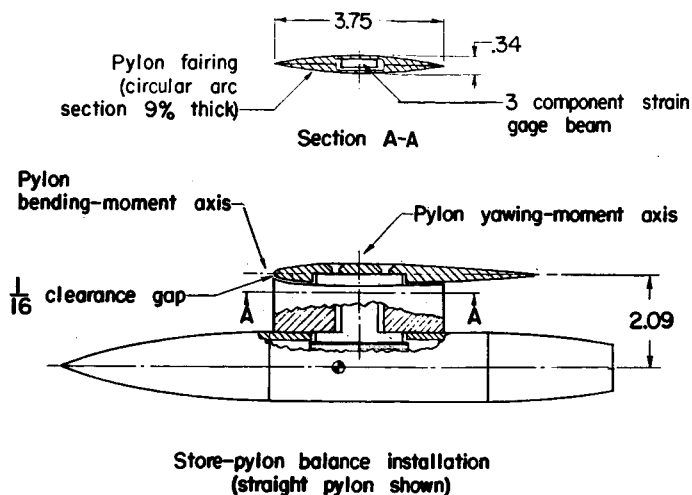
Basic store with
fins added

Section A-A, typ.

Basic store with
tail cone added

(b) Dimensions of store configurations tested. (Store nose and after-body are ogive bodies of revolution.)

Figure 1.- Continued.



(c) Dimensions of pylons and details of balance installations.

Figure 1.- Concluded.

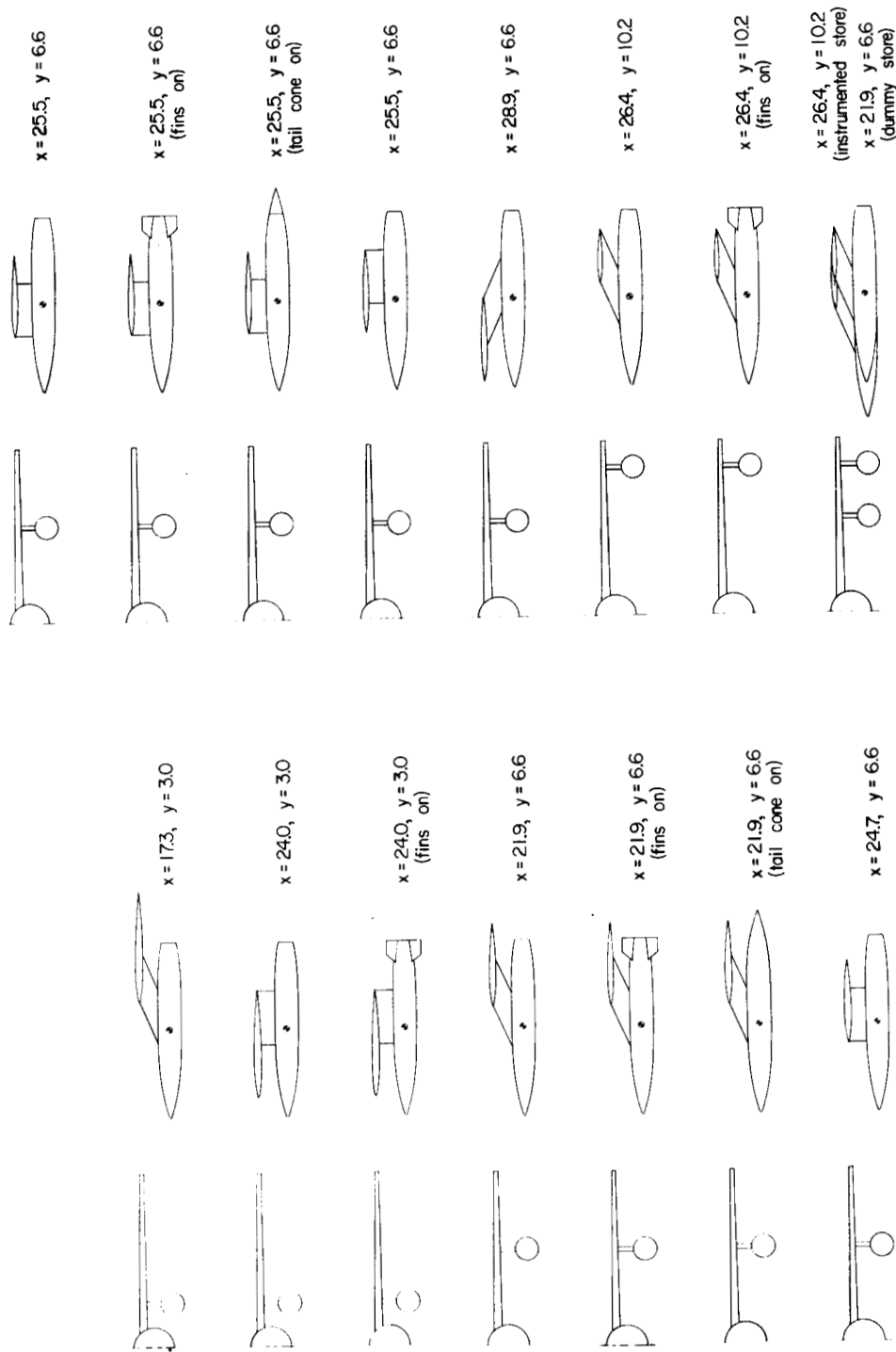


Figure 2.- Store-pylon configurations tested. (Values of x and y given in inches.)

CONFIDENTIAL

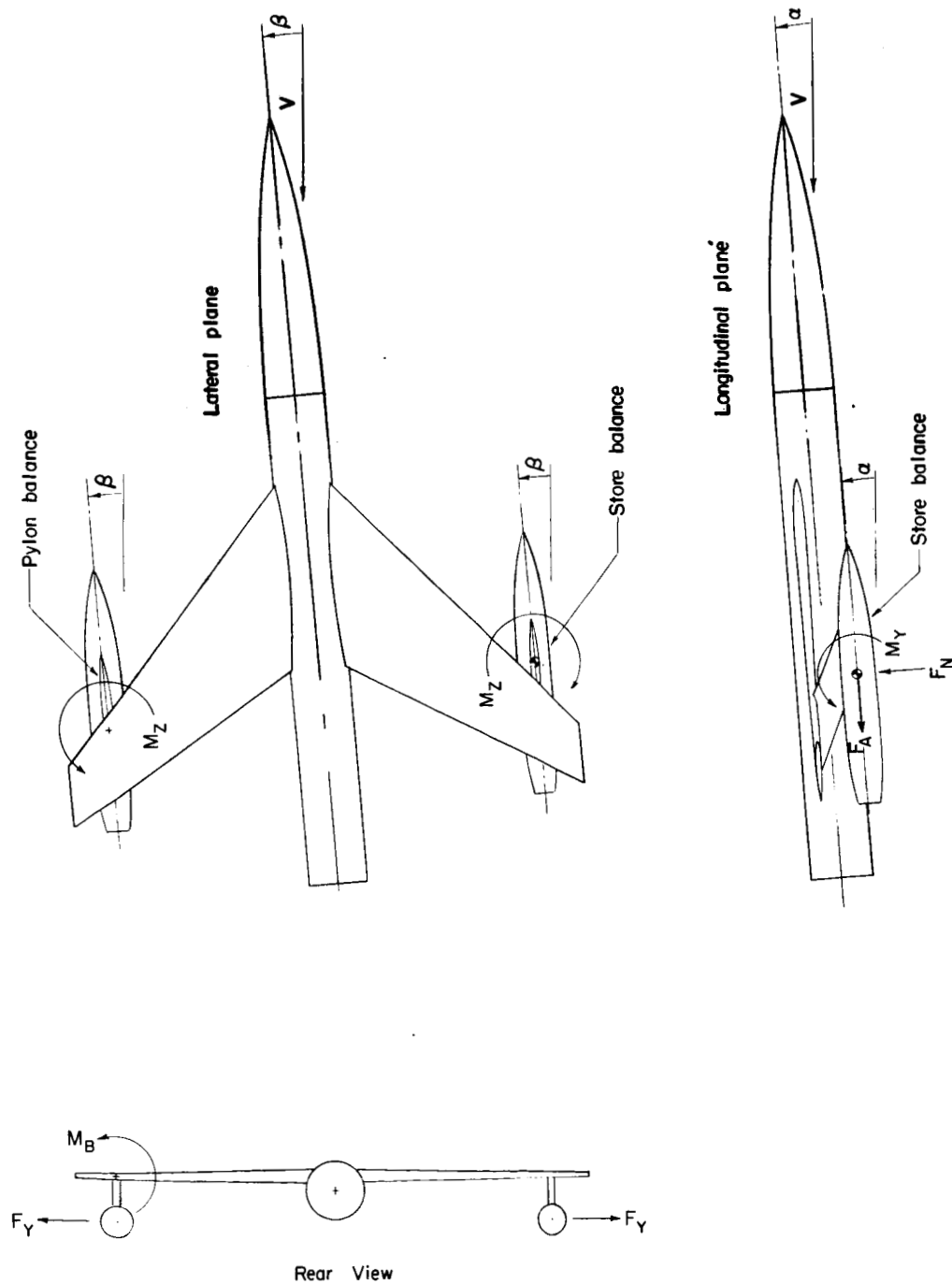
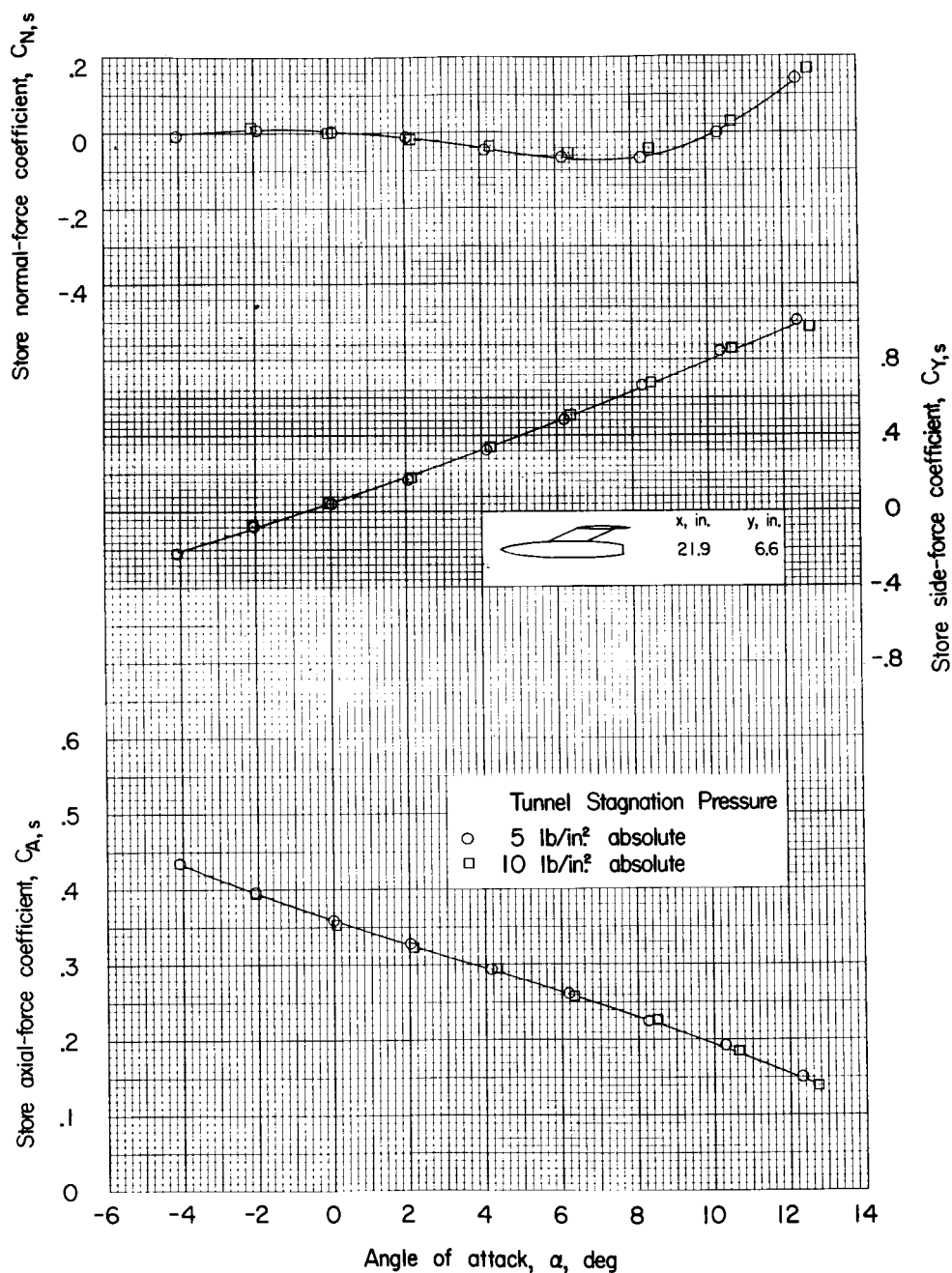
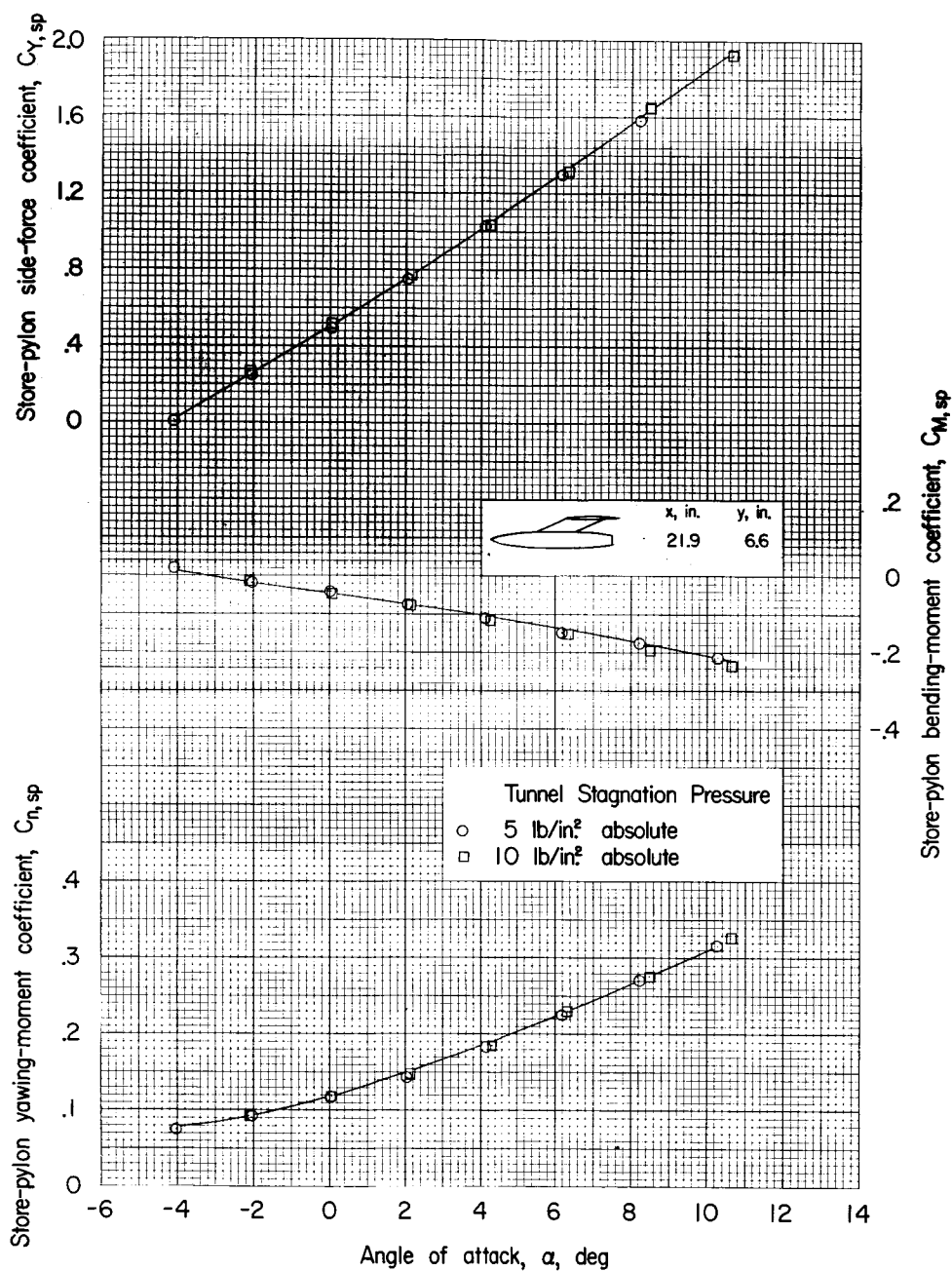


Figure 3.- Positive direction of forces and moments on the store and store-pylon combination.



(a) Store coefficients.

Figure 4.- Effect of tunnel stagnation pressure on the aerodynamic characteristics of the store and store-pylon combination for a representative tunnel run.



(b) Store-pylon coefficients.

Figure 4.- Concluded.

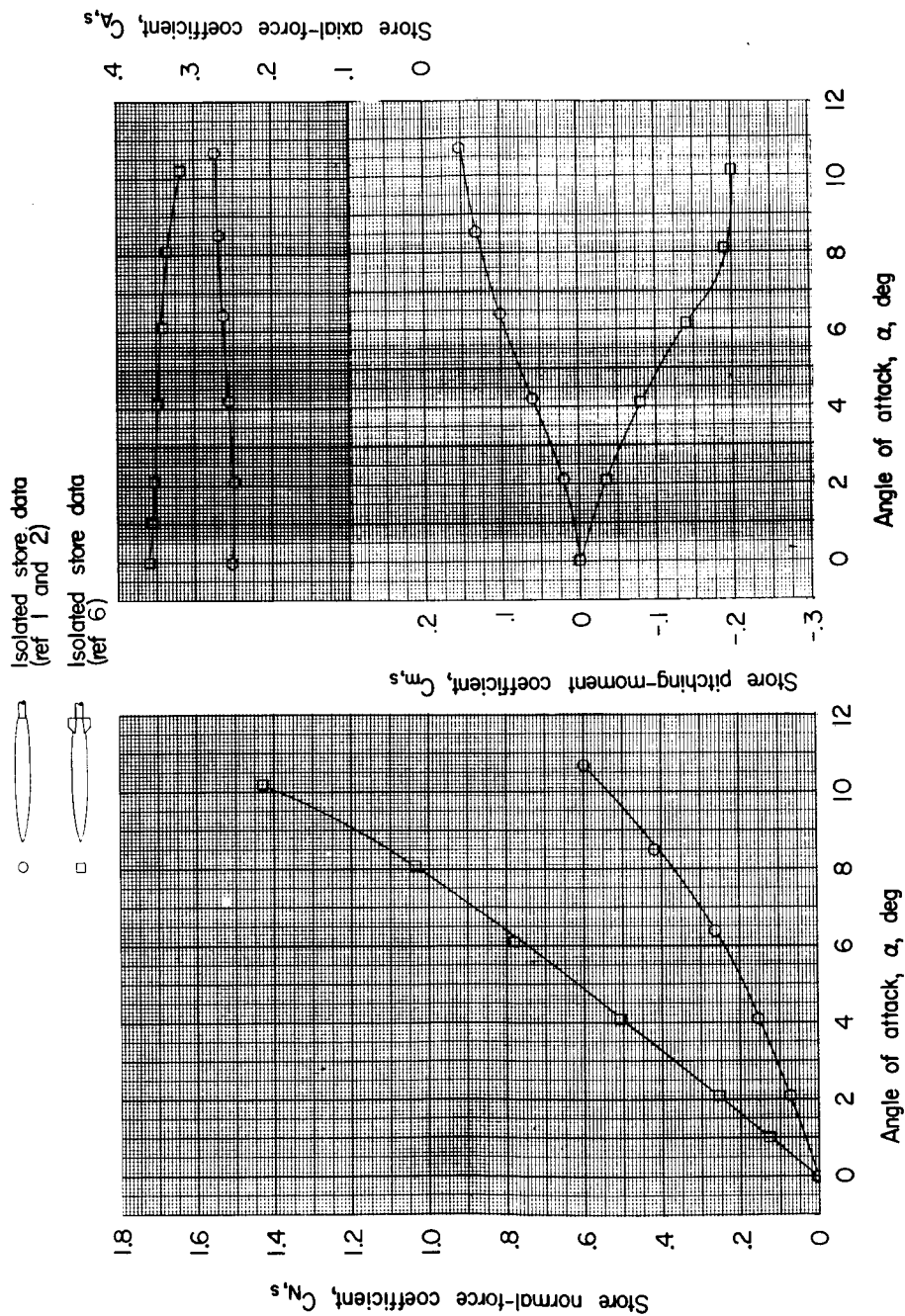
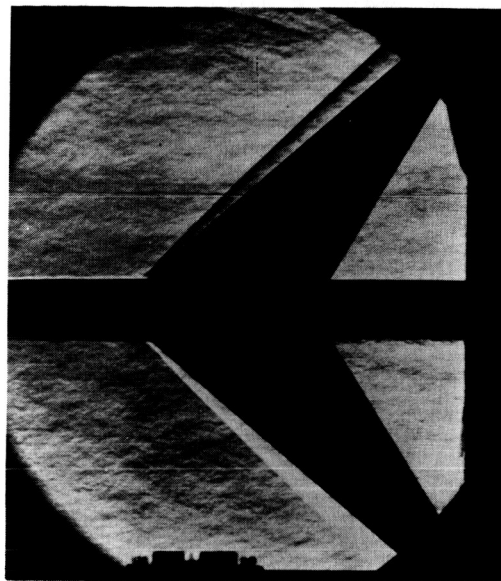
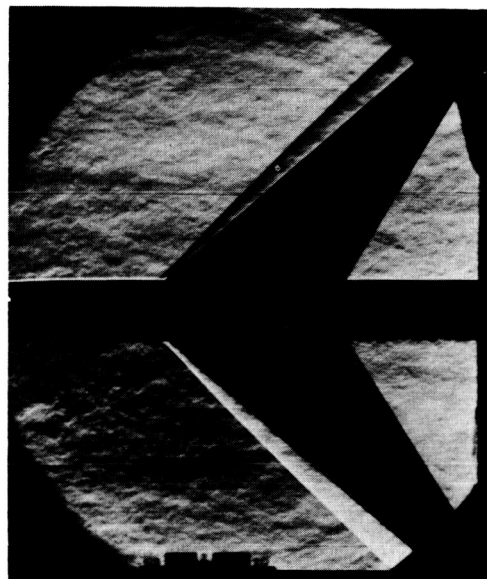


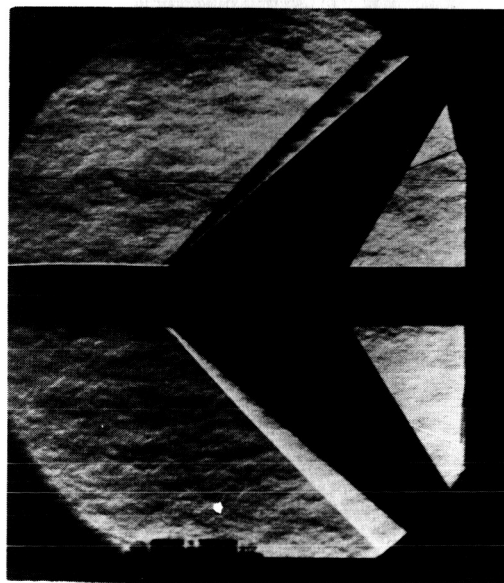
Figure 5.- Aerodynamic characteristics of isolated store.



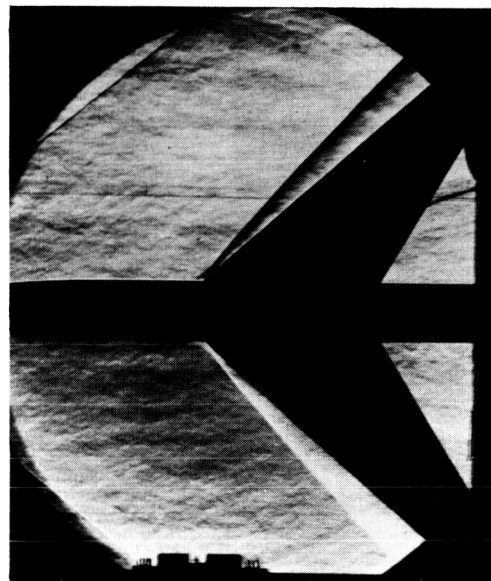
$\alpha = 0^\circ$



$\alpha = 4.1^\circ$



$\alpha = 8.2^\circ$

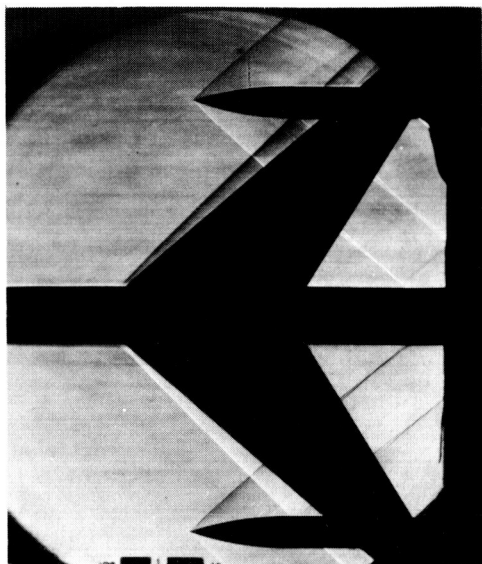
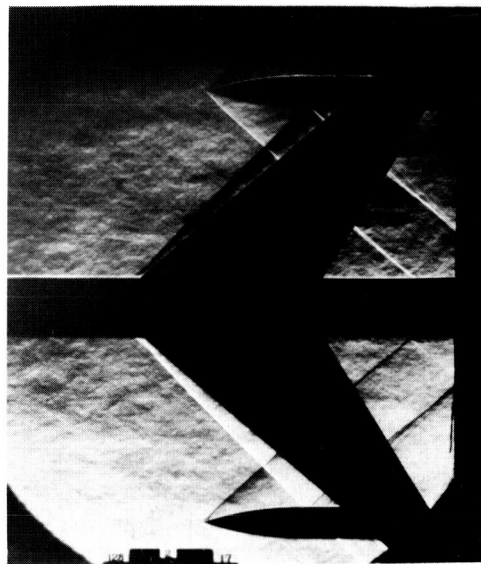
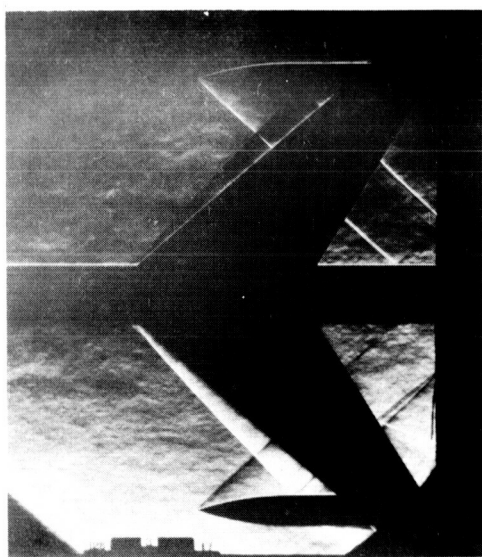
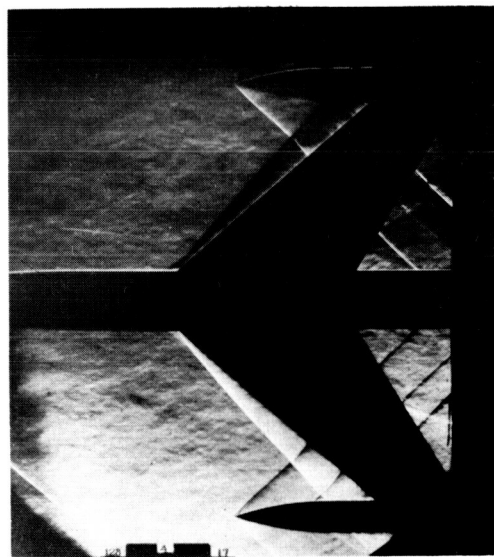


$\alpha = 12.3^\circ$

(a) Wing-fuselage alone.

L-57-1643

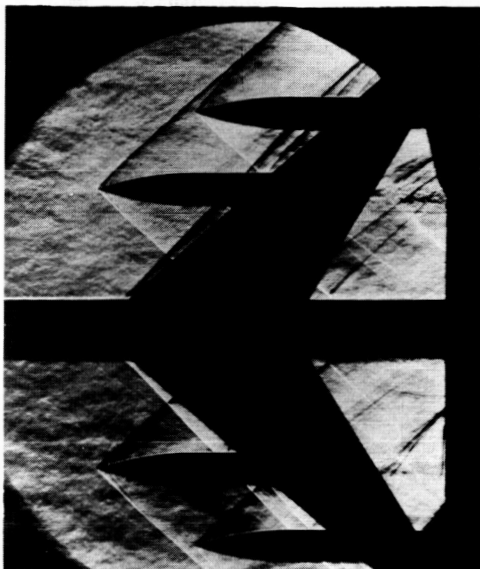
Figure 6.- Schlieren photographs of several model combinations.

 $\alpha = 0^\circ$  $\alpha = 4.1^\circ$  $\alpha = 8.2^\circ$  $\alpha = 12.3^\circ$

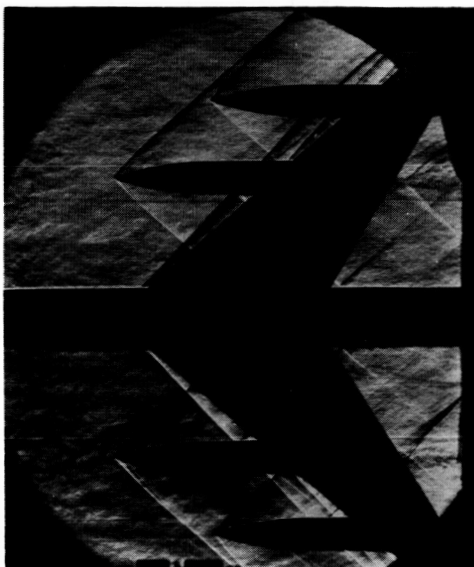
(b) Swept-eylon store combination: $x = 26.4$ inches; $y = 10.2$ inches. L-57-1644

Figure 6.- Continued.

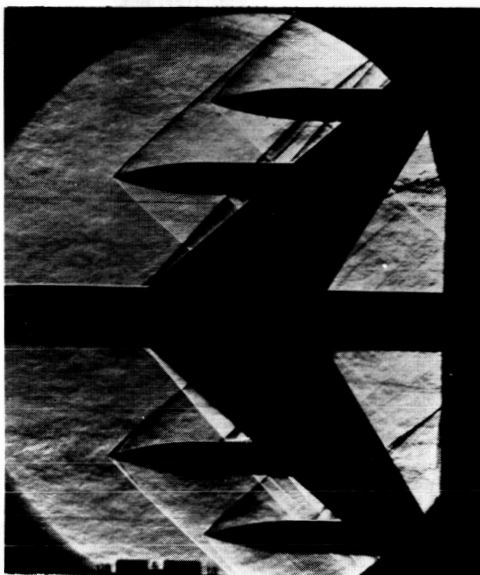
CONFIDENTIAL



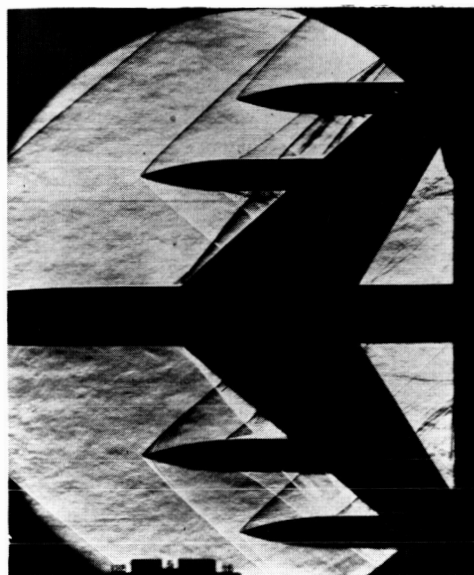
$\alpha = 0^\circ$



$\alpha = 4.1^\circ$



$\alpha = 8.2^\circ$



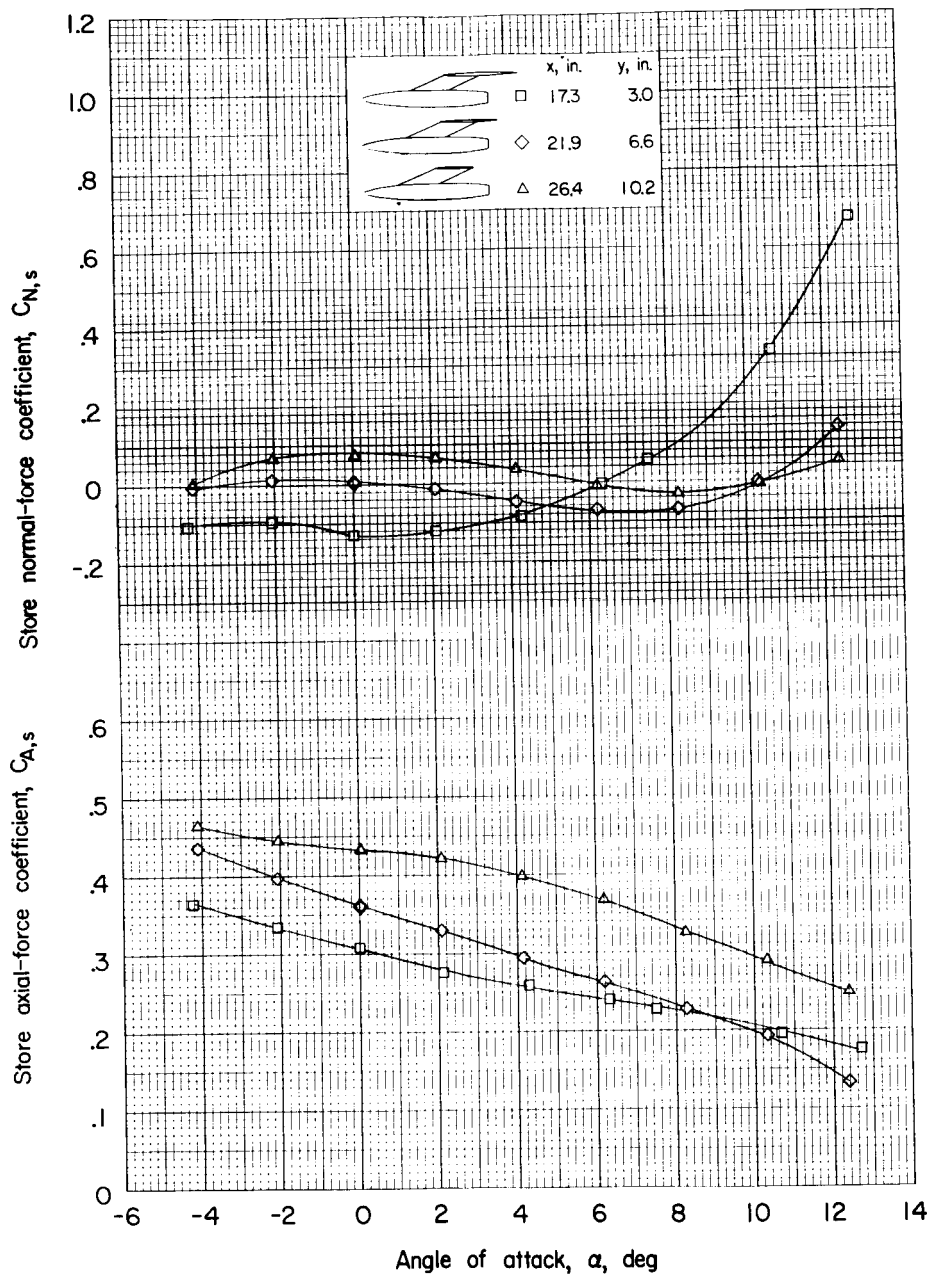
$\alpha = 12.3^\circ$

L-57-1645

(c) Swept-ylon store combination: $x = 26.4$ inches; $y = 10.2$ inches.
 Dummy store: $x = 21.9$ inches; $y = 6.6$ inches.

Figure 6.- Concluded.

CONFIDENTIAL



(a) Variation of $C_{N,s}$ and $C_{A,s}$ with α .

Figure 7.- Aerodynamic characteristics of the store in the presence of the wing-fuselage combination for three spanwise store positions.

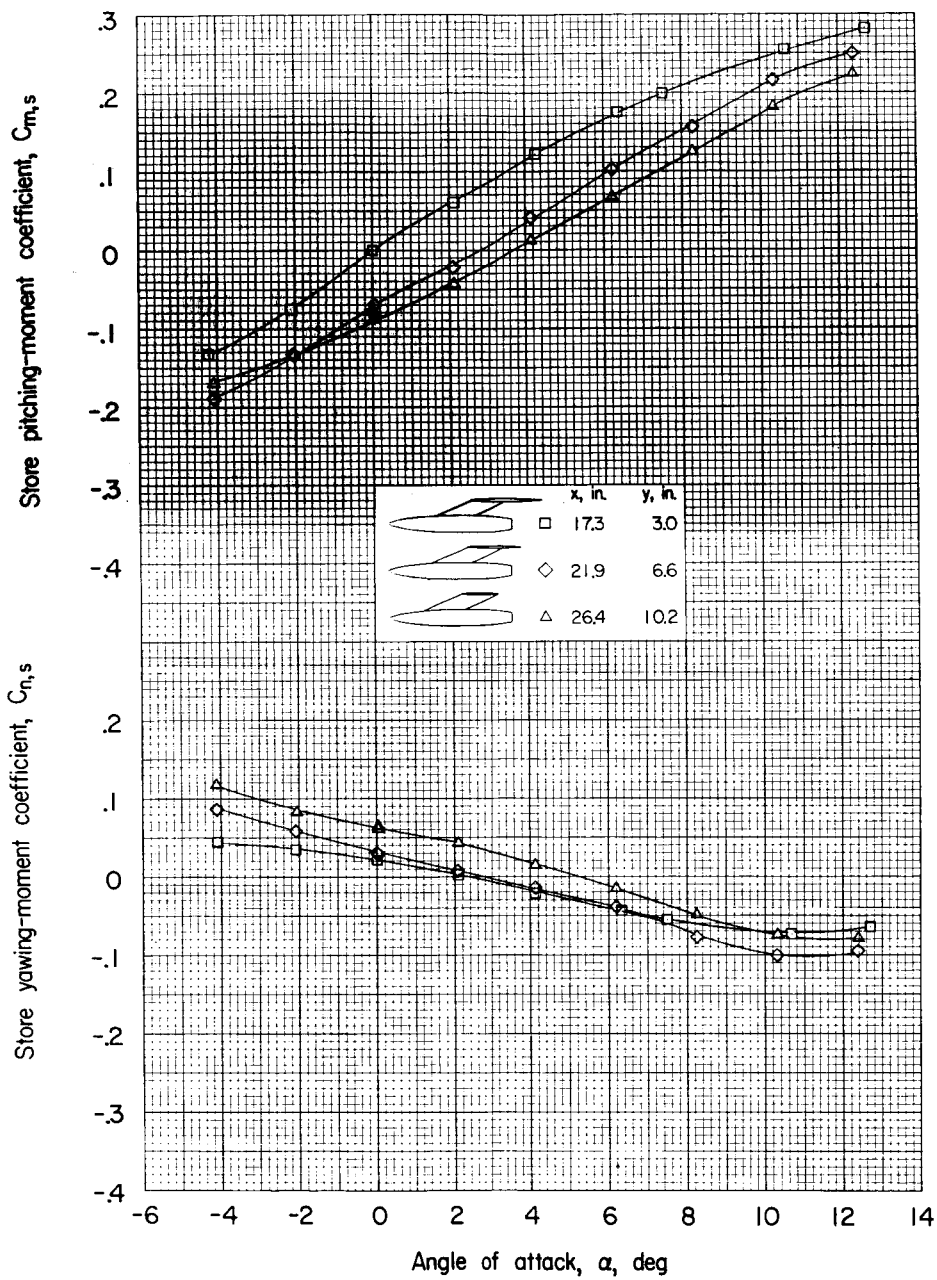
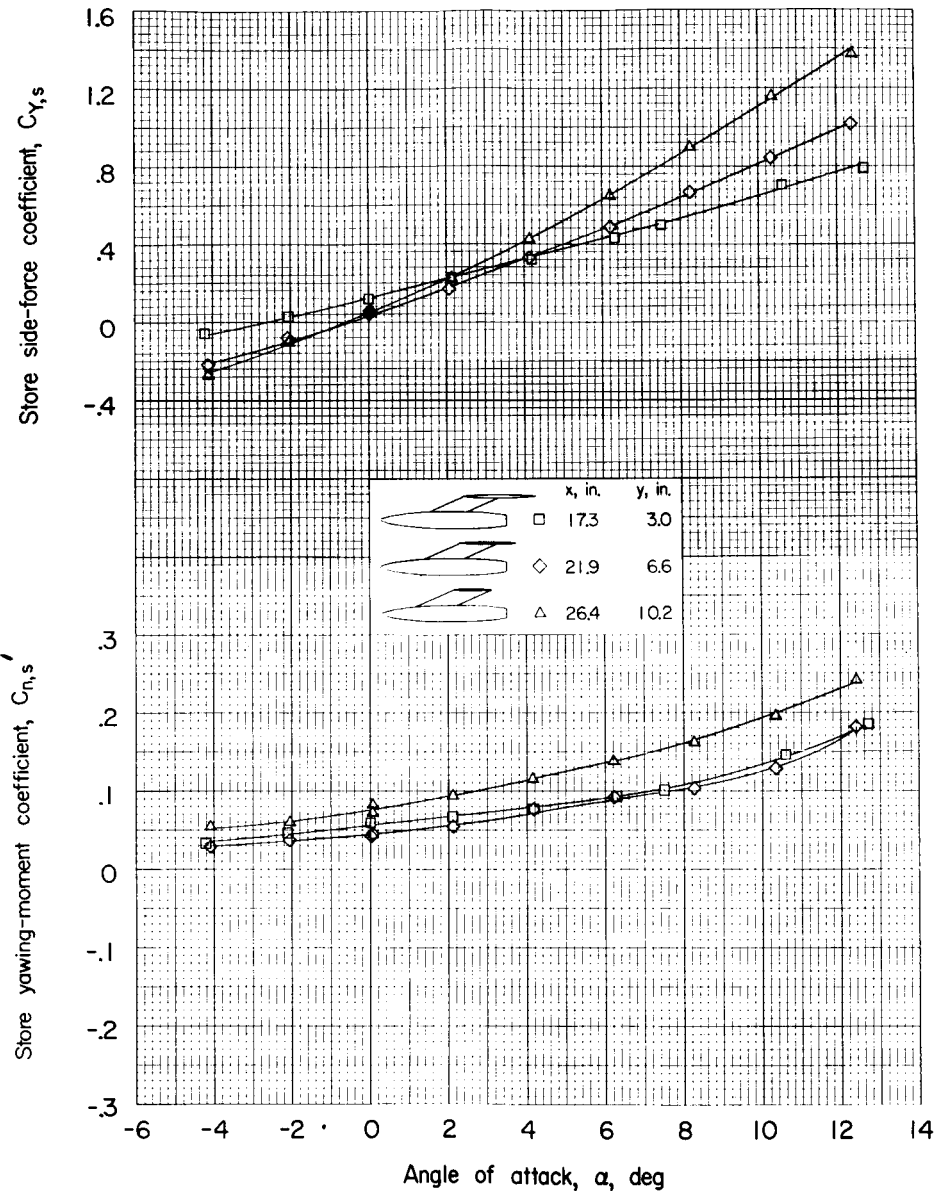
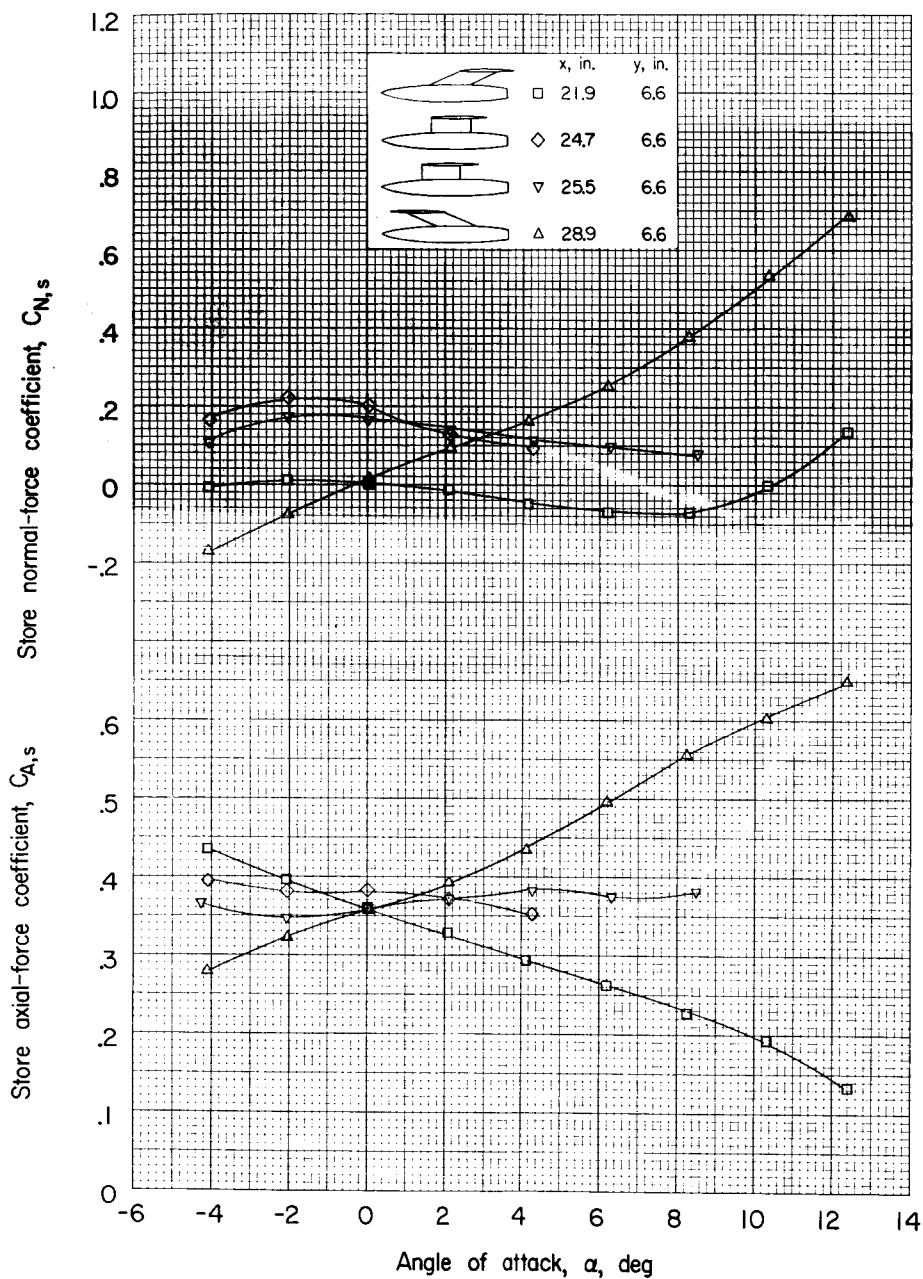
(b) Variation of $C_{m,s}$ and $C_{n,s}$ with α .

Figure 7.- Continued.



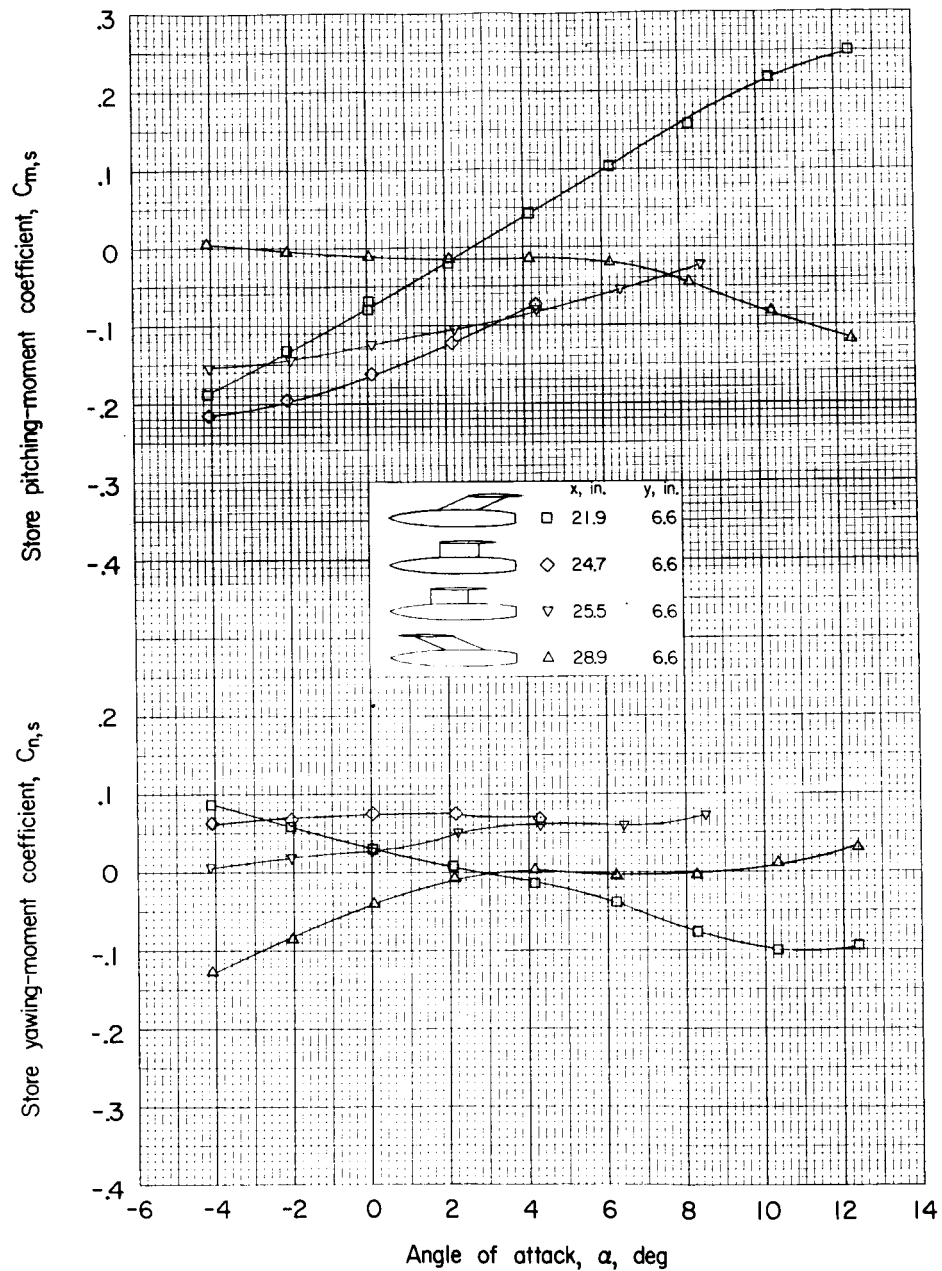
(c) Variation of $C_{Y,s}$ and $C_{n,s}'$ with α .

Figure 7.- Concluded.



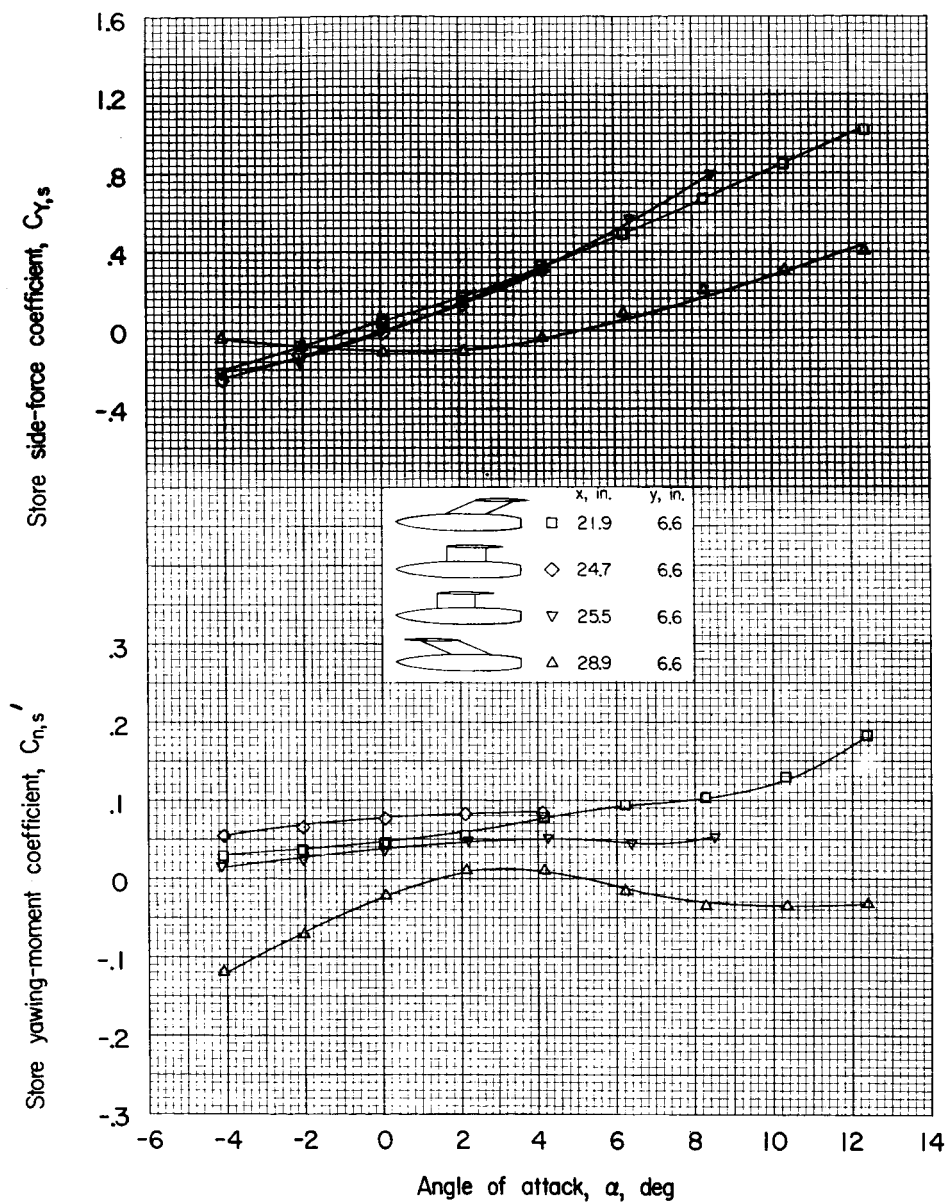
(a) Variation of $C_{N,s}$ and $C_{A,s}$ with α .

Figure 8.- Aerodynamic characteristics of the store in the presence of the wing-fuselage combination for four chordwise store positions.



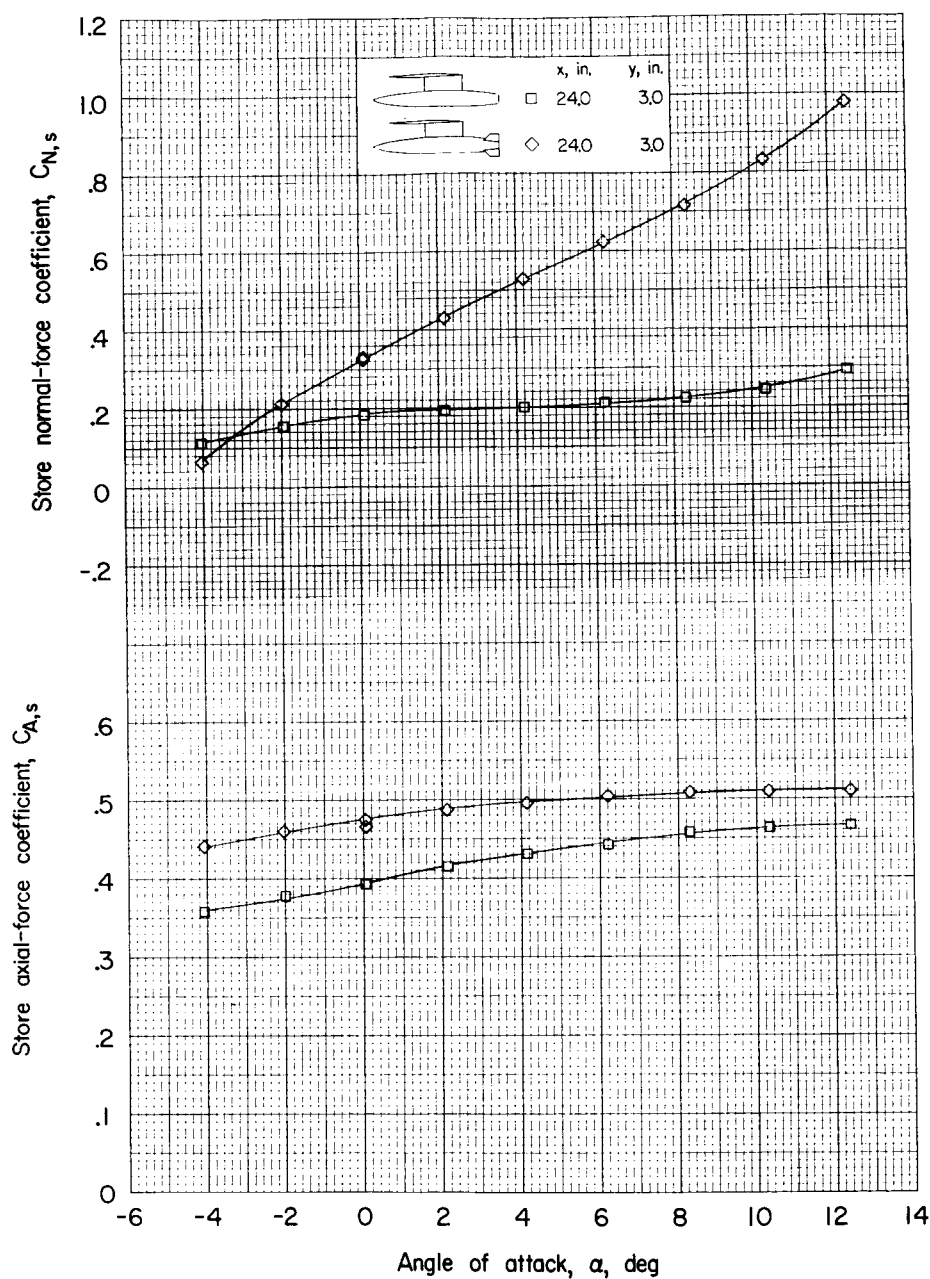
(b) Variation of $C_{m,s}$ and $C_{n,s}$ with α .

Figure 8.- Continued.



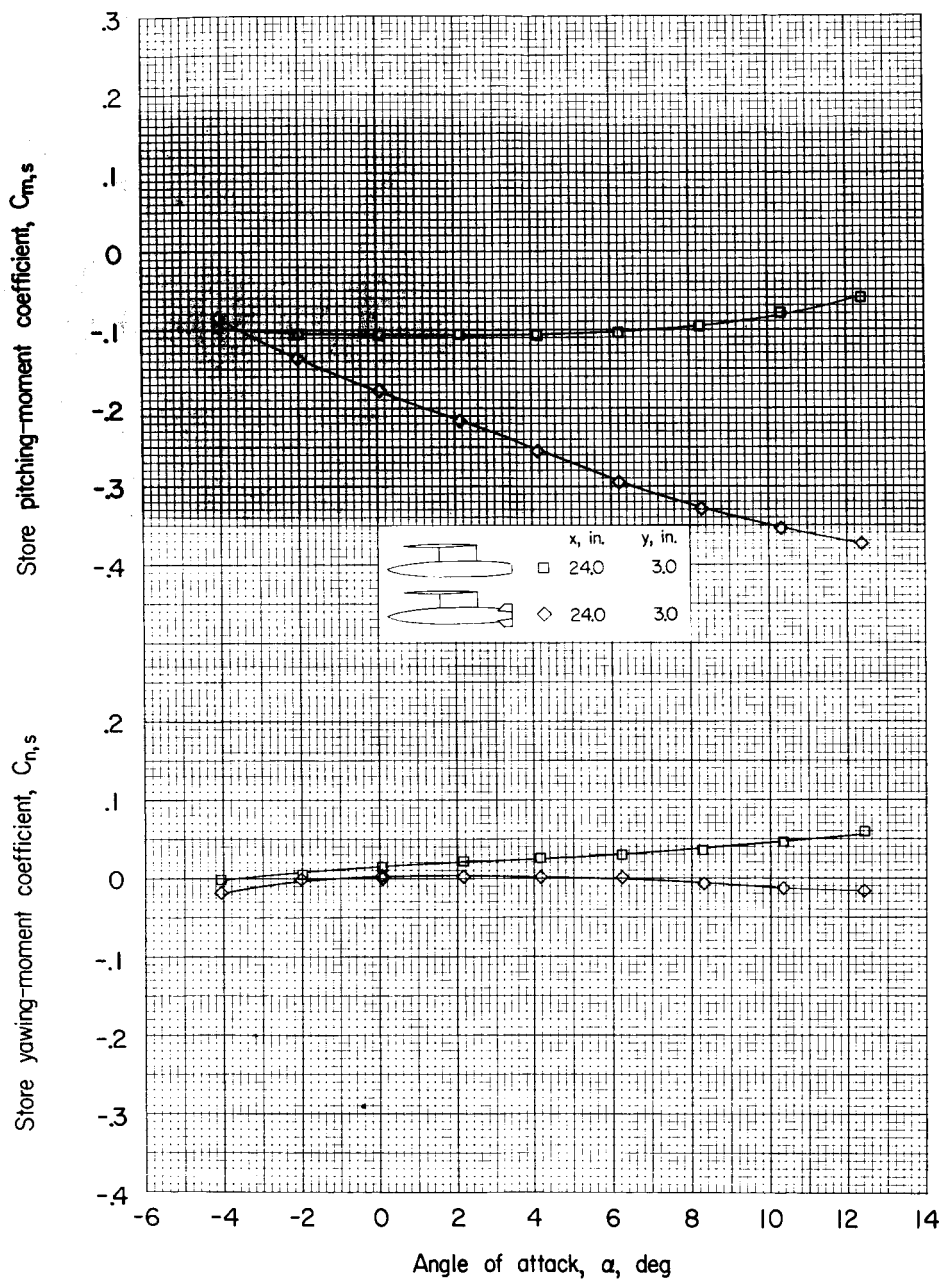
(c) Variation of $C_{Y,s}$ and $C_{n,s'}$ with α .

Figure 8.- Concluded.



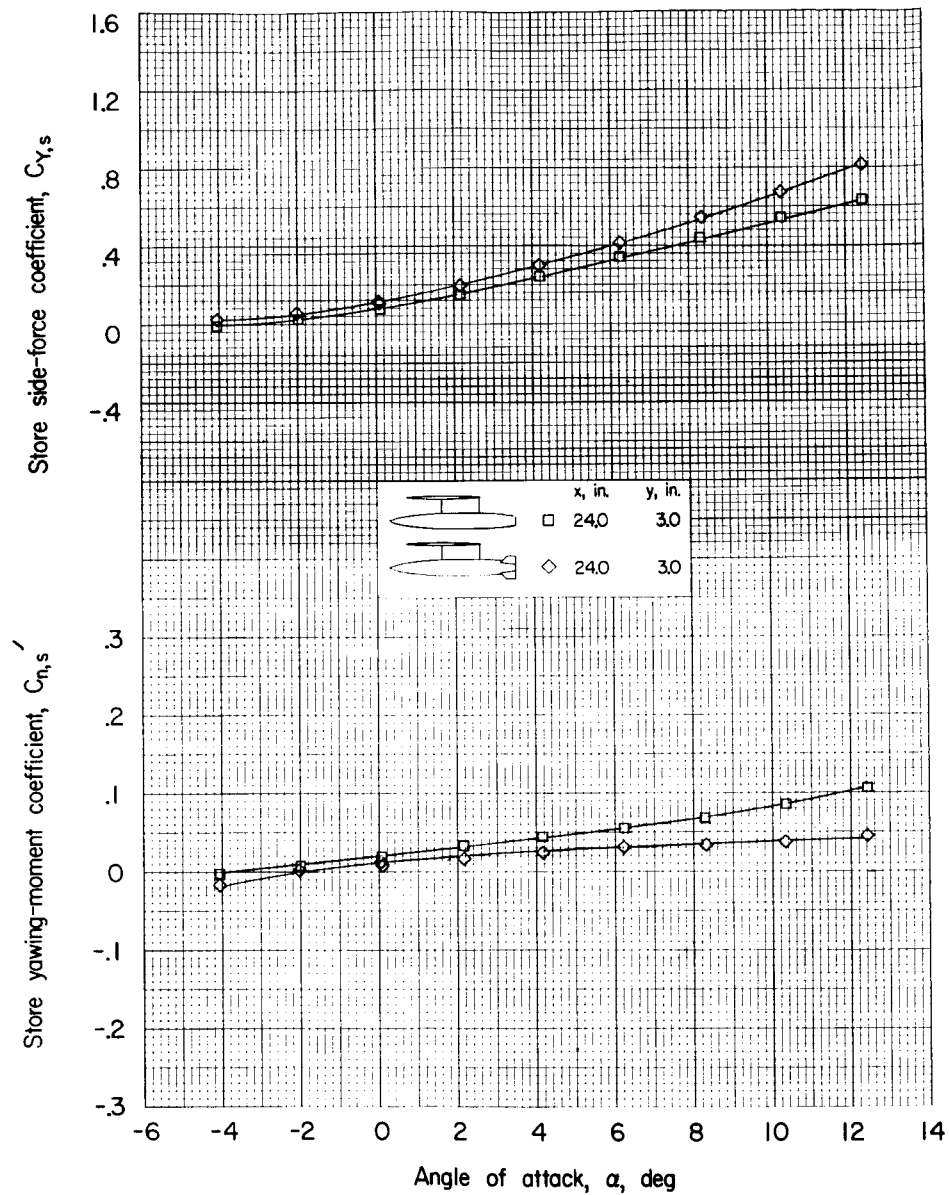
(a) Variation of $C_{N,s}$ and $C_{A,s}$ with α .

Figure 9.- Effect of the store fins on the aerodynamic characteristics of the store in the presence of the wing-fuselage combination.



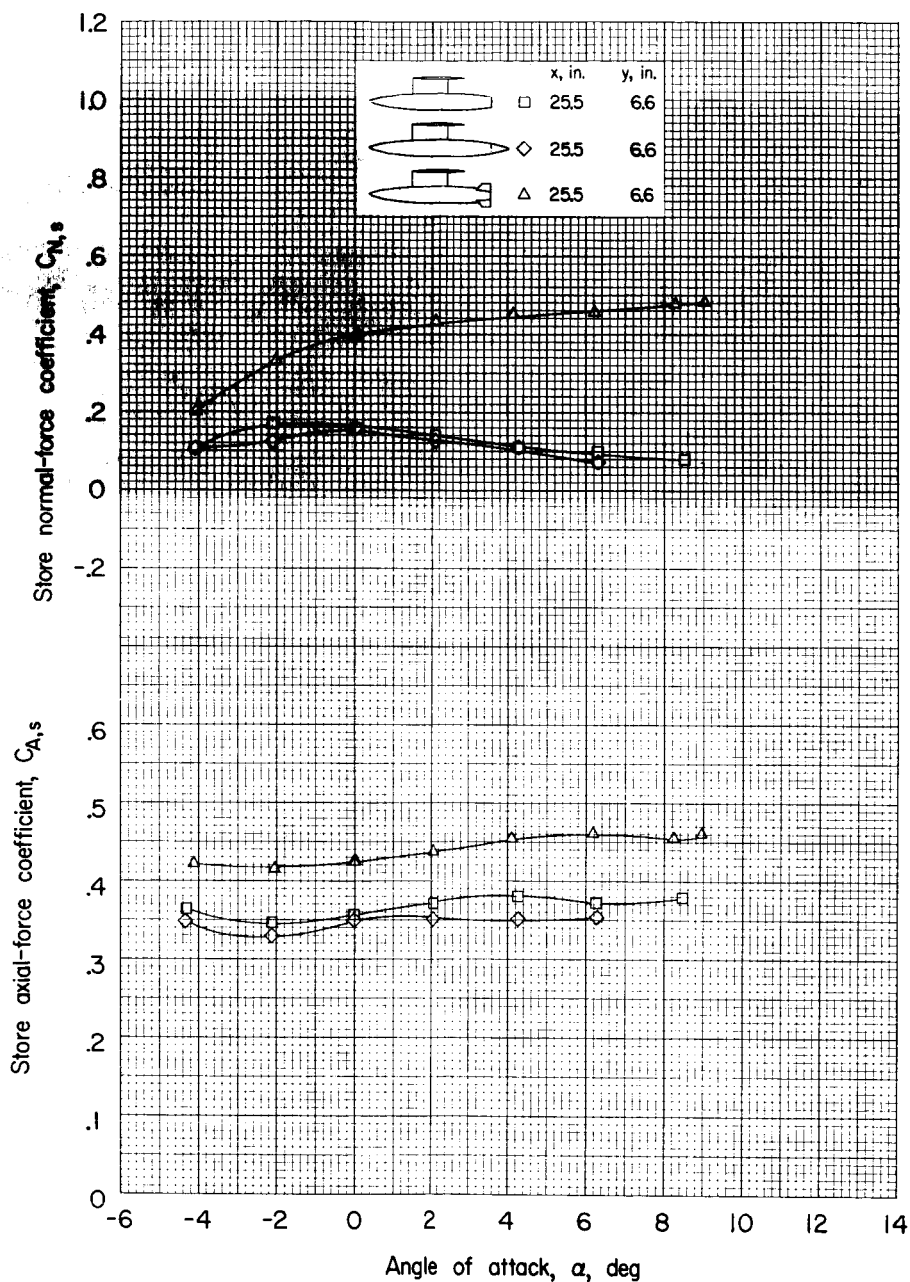
(b) Variation of $C_{m,s}$ and $C_{n,s}$ with α .

Figure 9.- Continued.



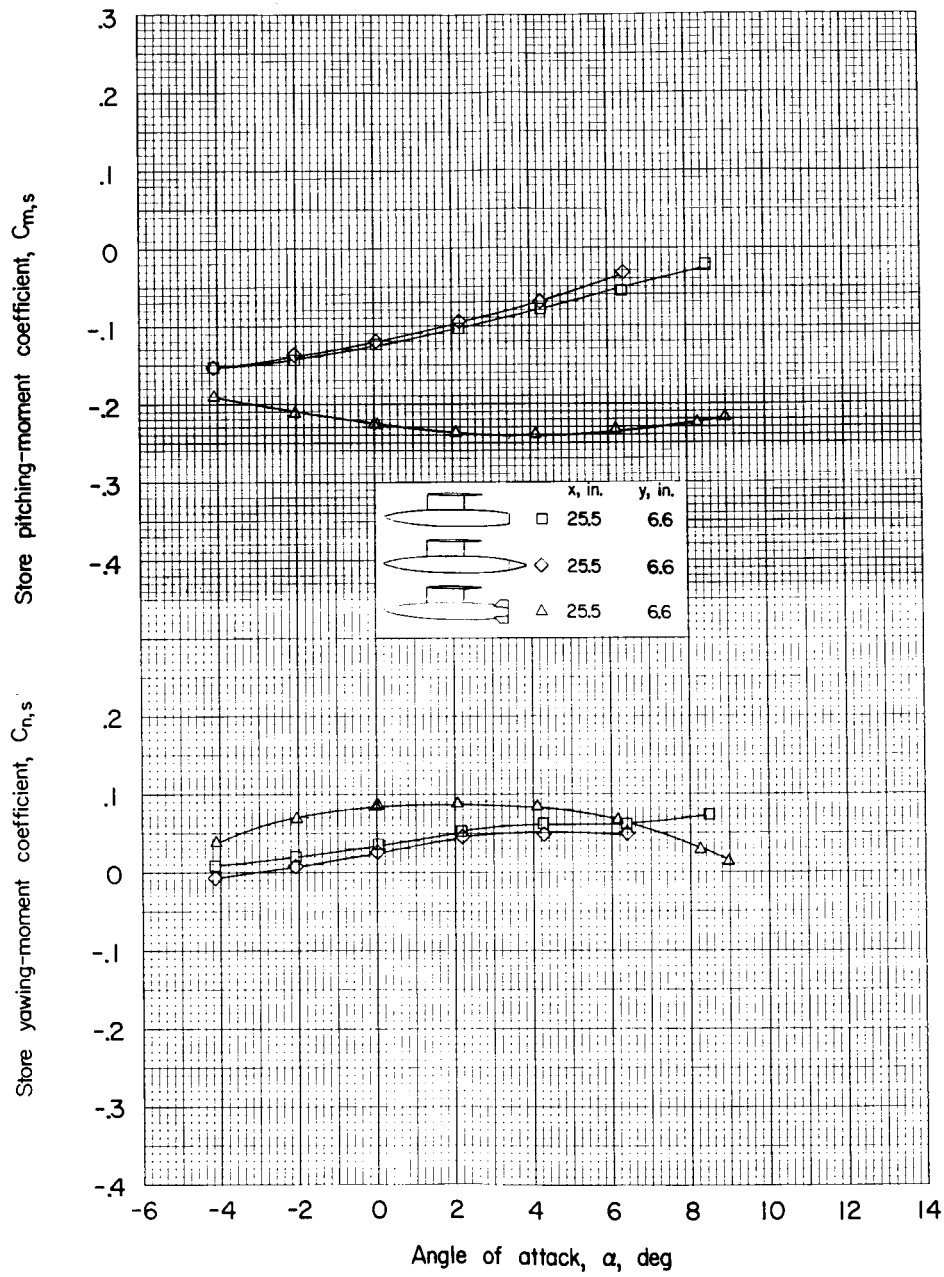
(c) Variation of $C_{Y,s}$ and $C_{n,s}'$ with α .

Figure 9.- Concluded.



(a) Variation of $C_{N,s}$ and $C_{A,s}$ with α .

Figure 10.- Effect of store fins and store tail cone on the aerodynamic characteristics of the store in the presence of the wing-fuselage combination.



(b) Variation of $C_{m,s}$ and $C_{n,s}$ with α .

Figure 10.- Continued.

CONFIDENTIAL

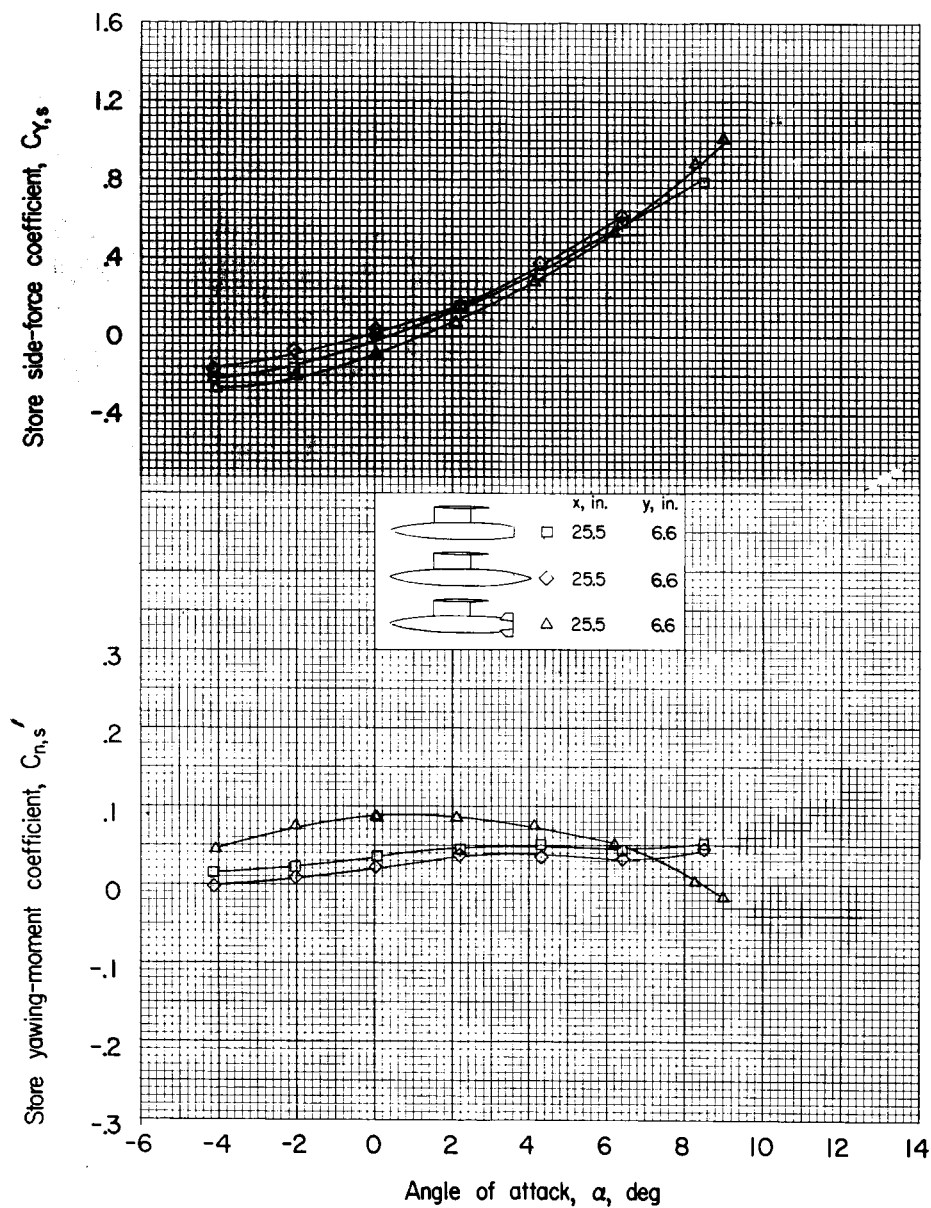
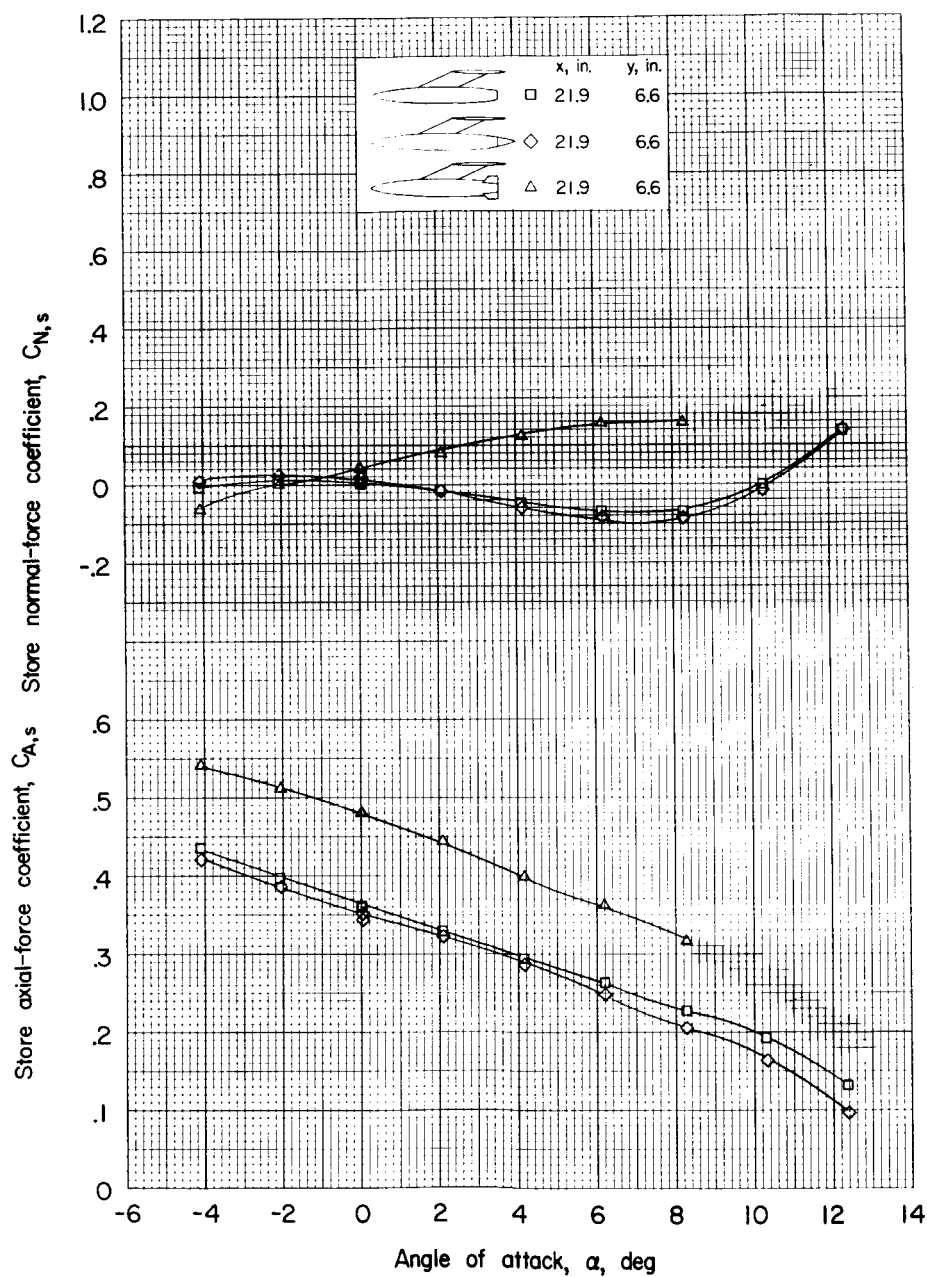
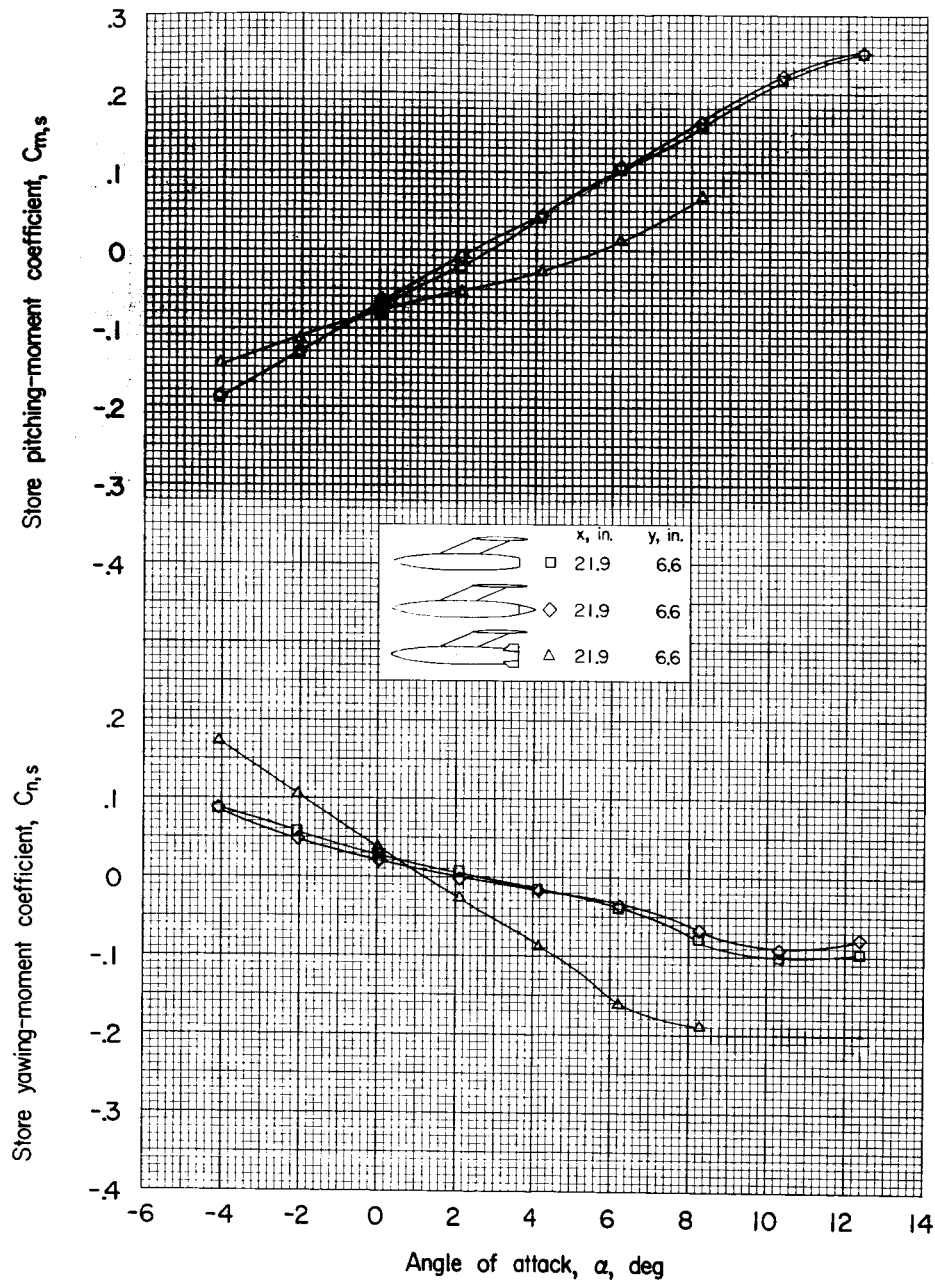
(c) Variation of $C_{Y,s}$ and $C_{n,s}'$ with α .

Figure 10.- Concluded.



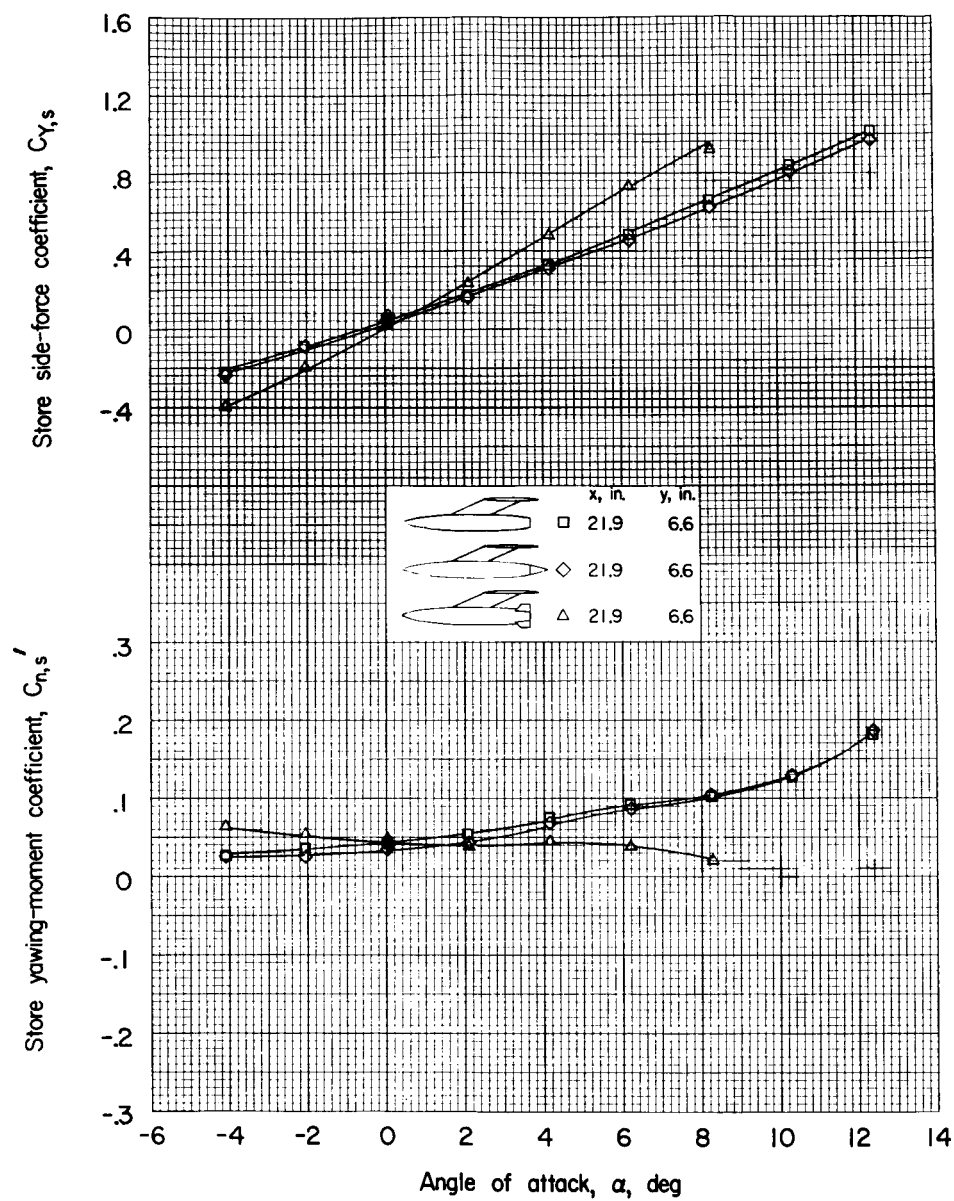
(a) Variation of $C_{N,s}$ and $C_{A,s}$ with α .

Figure 11.- Effect of store fins and store tail cone on the aerodynamic characteristics of the store in the presence of the wing-fuselage combination.



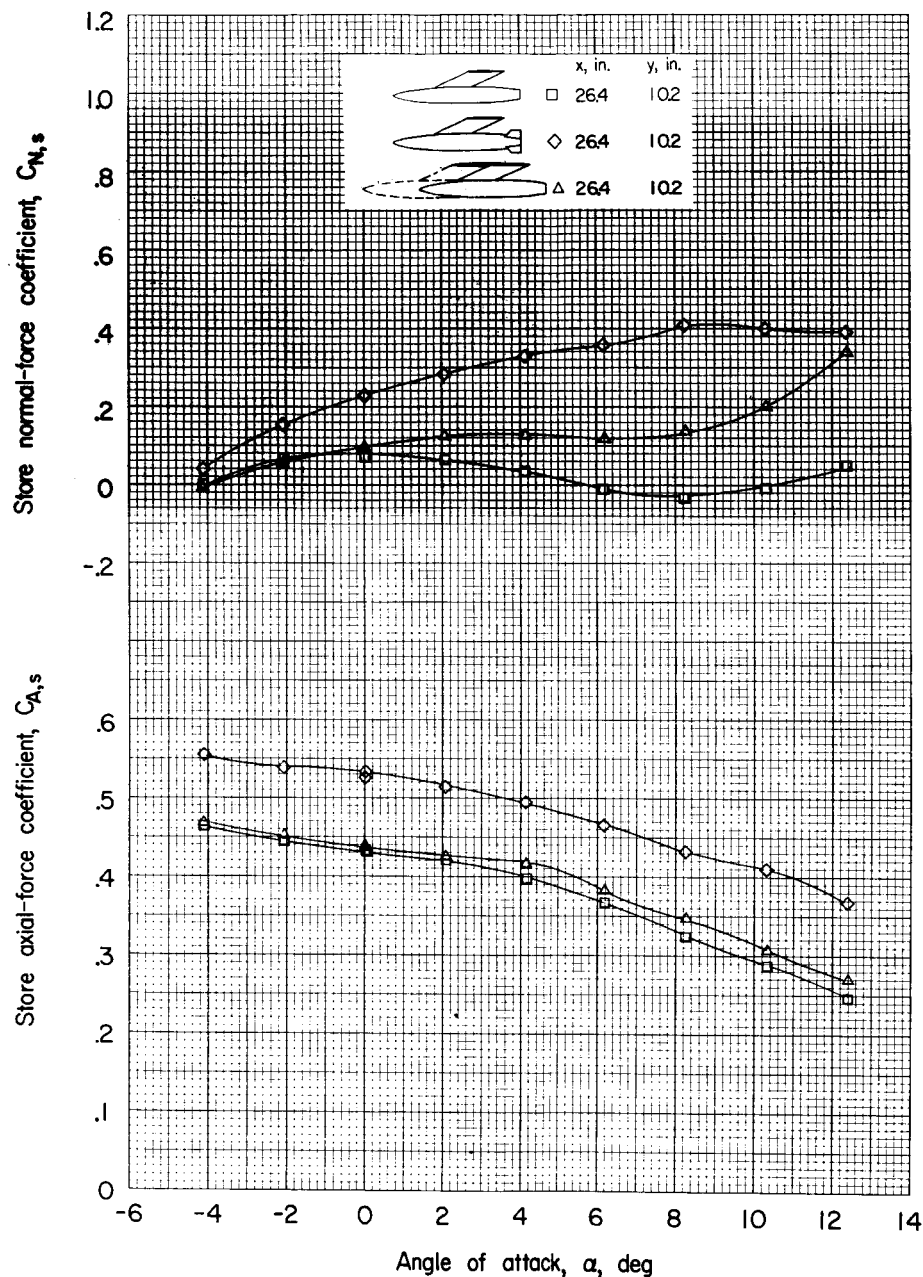
(b) Variation of $C_{m,s}$ and $C_{n,s}$ with α .

Figure 11.- Continued.



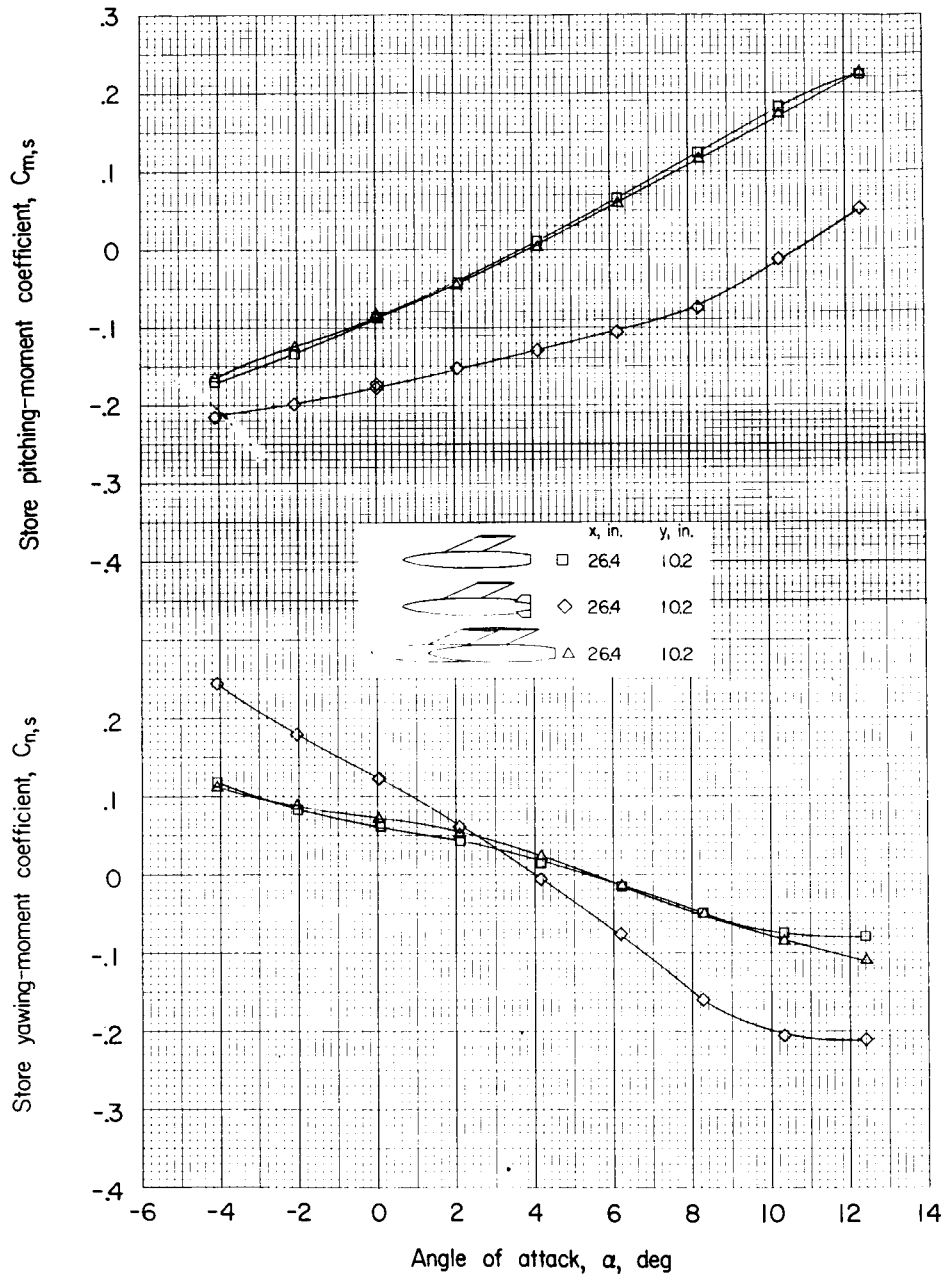
(c) Variation of $C_{Y,s}$ and $C_{n,s}'$ with α .

Figure 11.- Concluded.



(a) Variation of $C_{N,s}$ and $C_{A,s}$ with α .

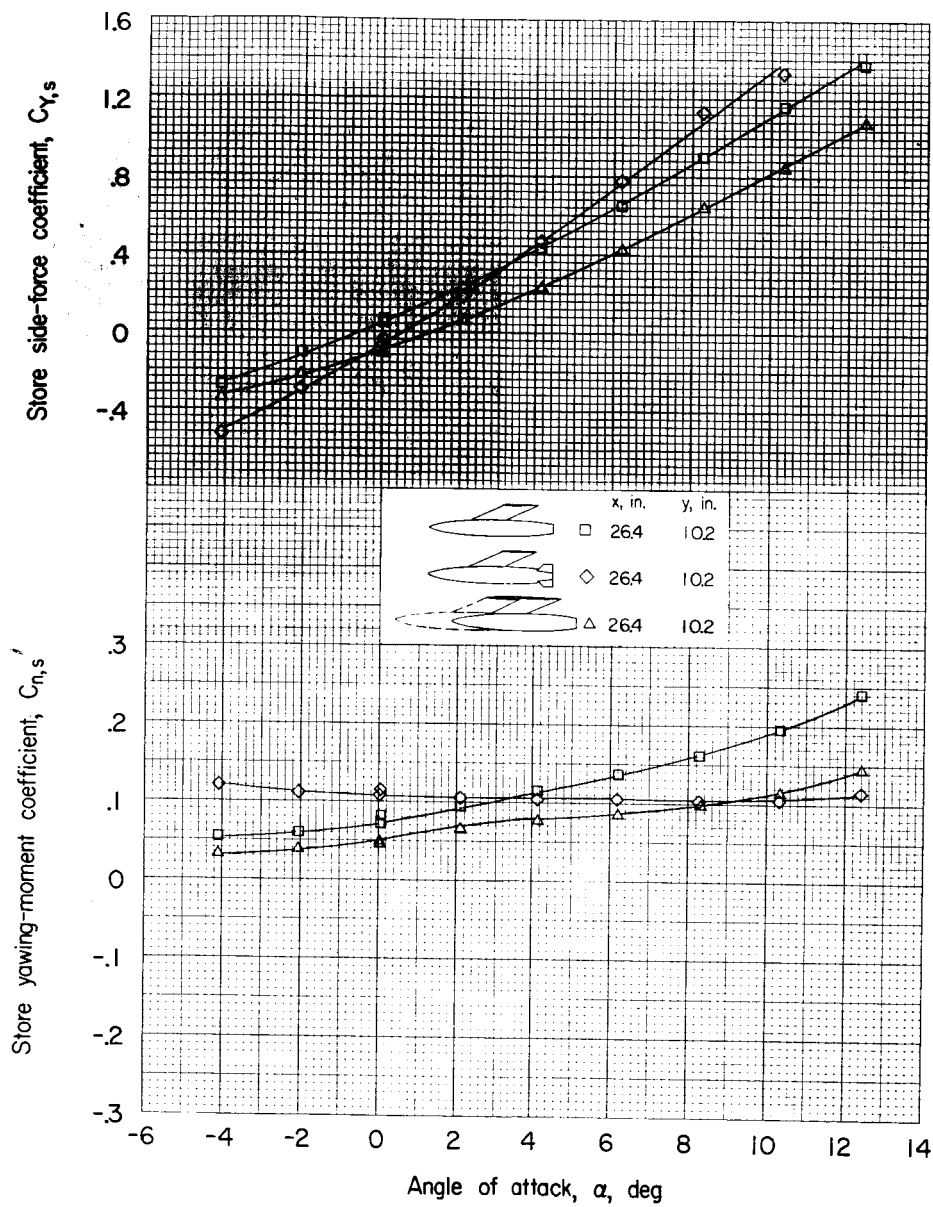
Figure 12.- Effect of store fins and inboard and outboard store interference on the aerodynamic characteristics of the store in the presence of the wing-fuselage combination.



(b) Variation of $C_{m,s}$ and $C_{n,s}$ with α .

Figure 12.- Continued.

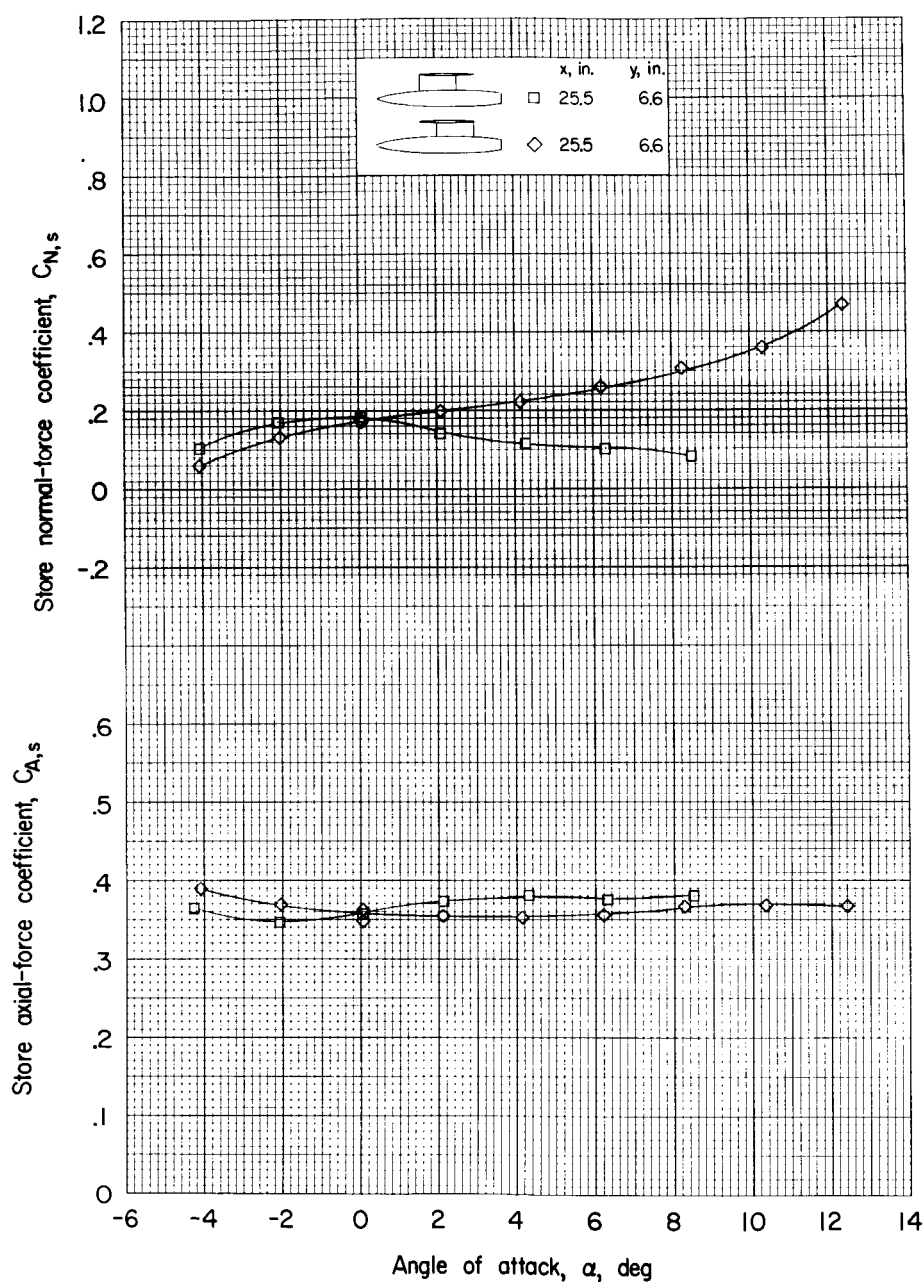
SECRET



(c) Variation of $C_{Y,s}$ and $C_{n,s'}$ with α .

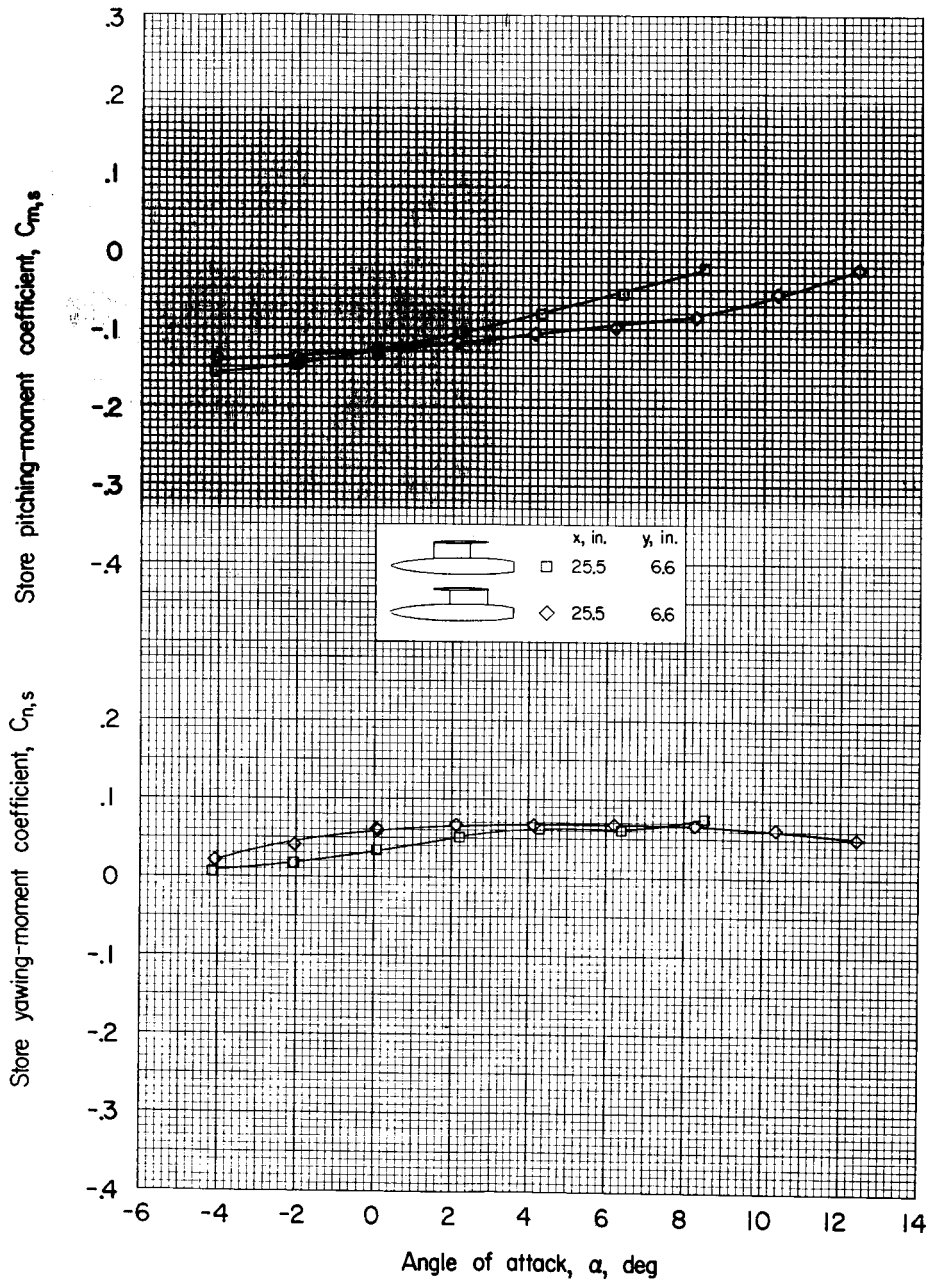
Figure 12.- Concluded.

SECRET



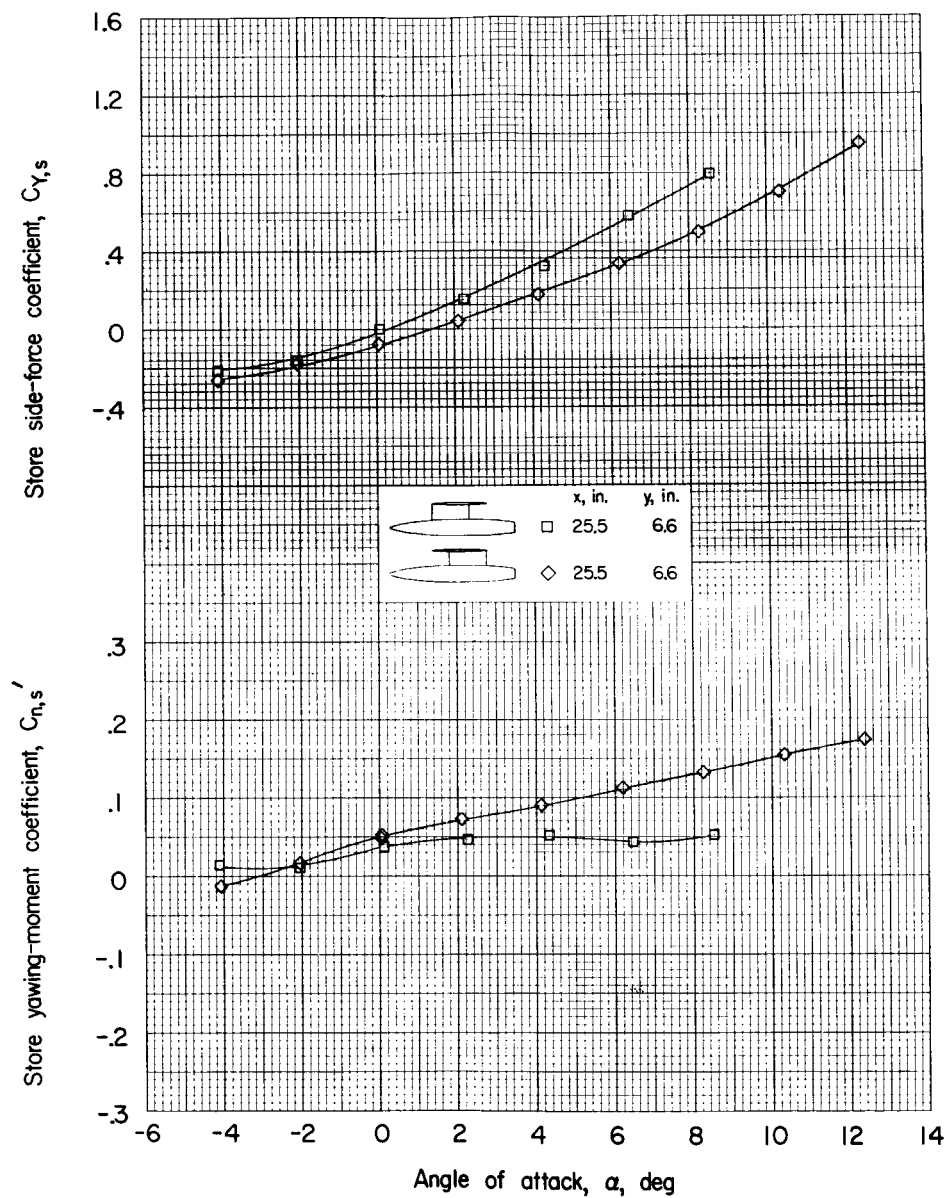
(a) Variation of $C_{N,s}$ and $C_{A,s}$ with α .

Figure 13.- Effect of pylon location on the aerodynamic characteristics of the store in the presence of the wing-fuselage combination.



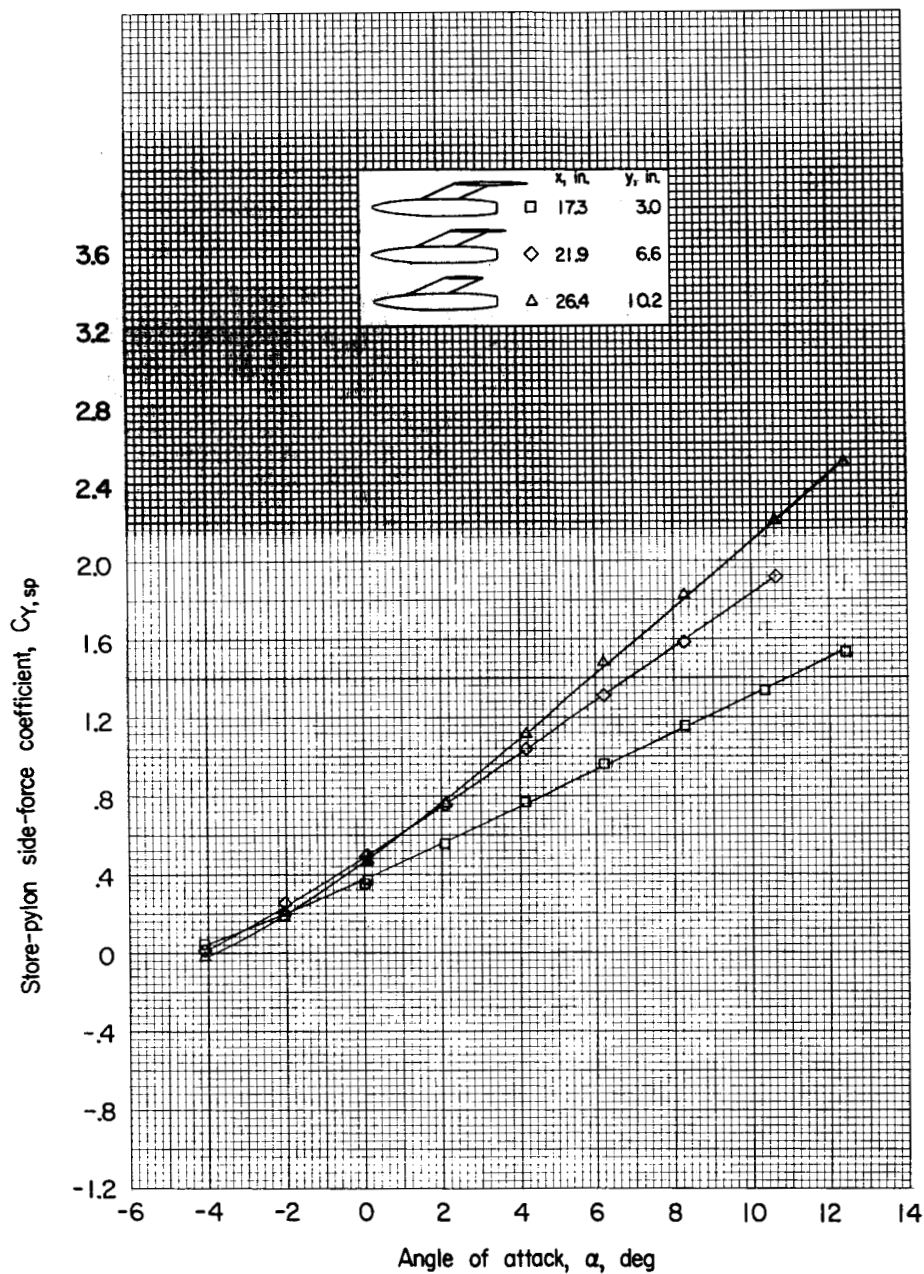
(b) Variation of $C_{m,s}$ and $C_{n,s}$ with α .

Figure 13.- Continued.



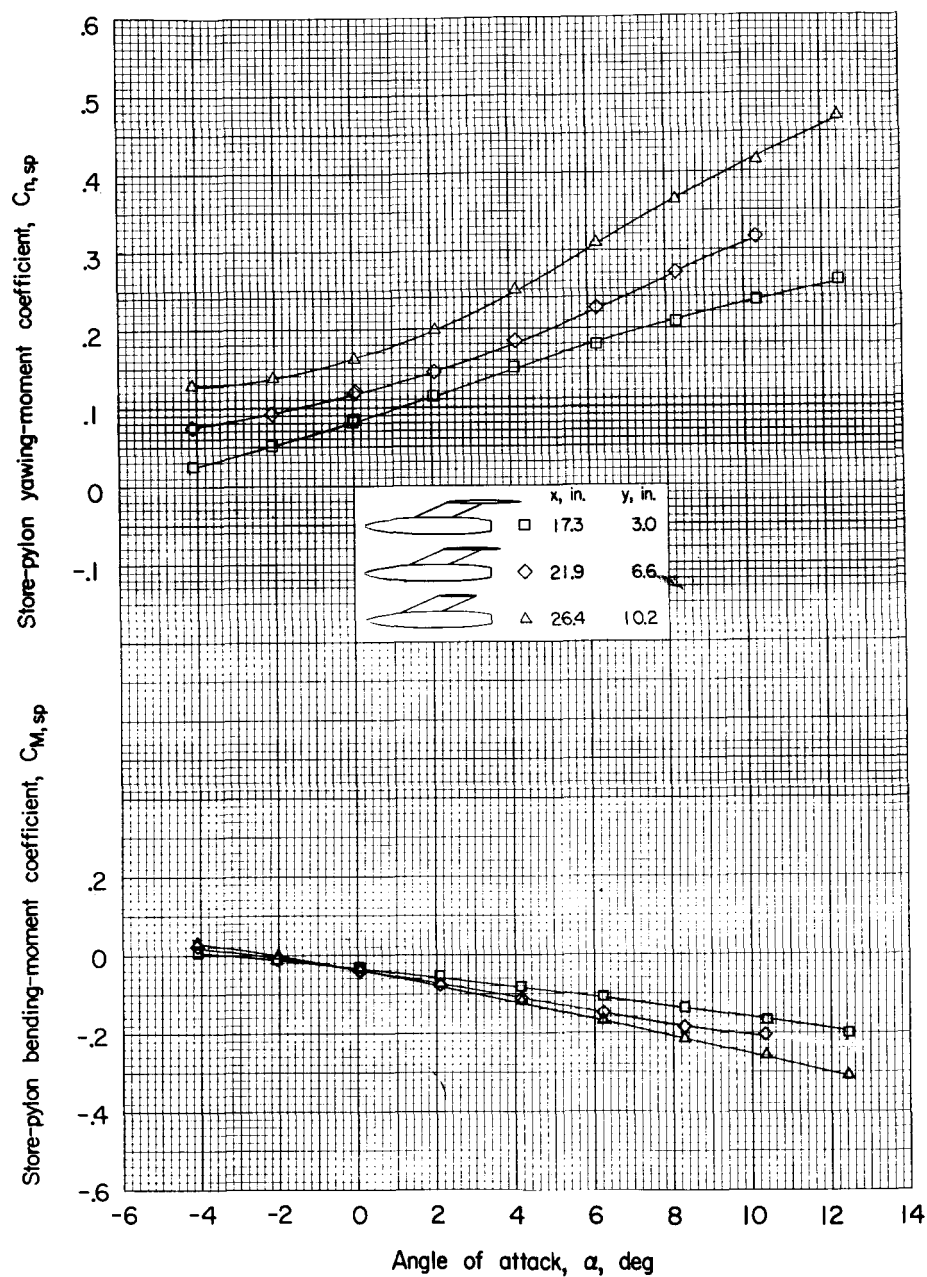
(c) Variation of $C_{Y,s}$ and $C_{n,s}'$ with α .

Figure 13.- Concluded.



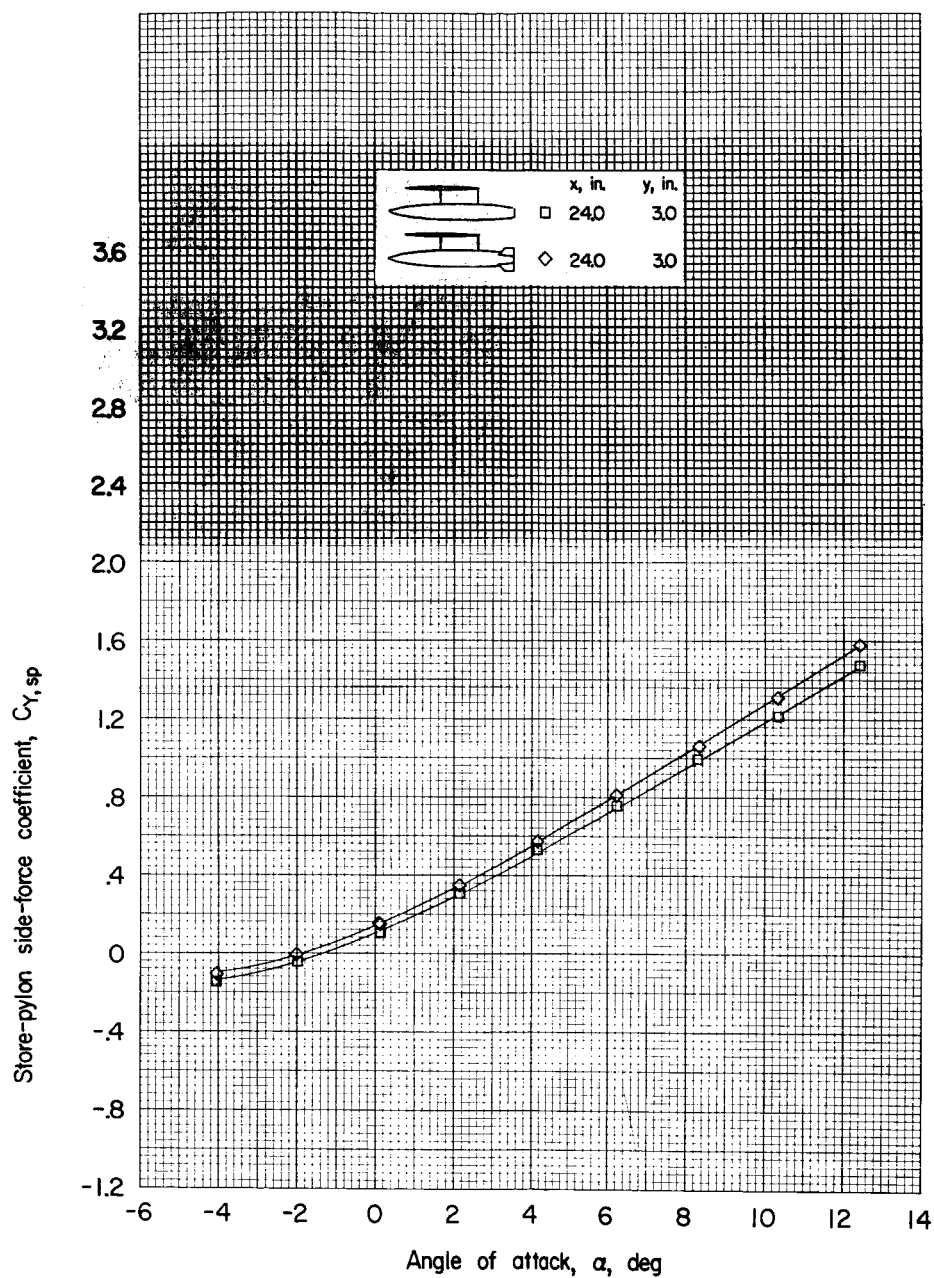
(a) Variation of $C_{Y,sp}$ with α .

Figure 14.- Aerodynamic characteristics of the store-pylon combination in the presence of the wing-fuselage combination for three spanwise store positions.



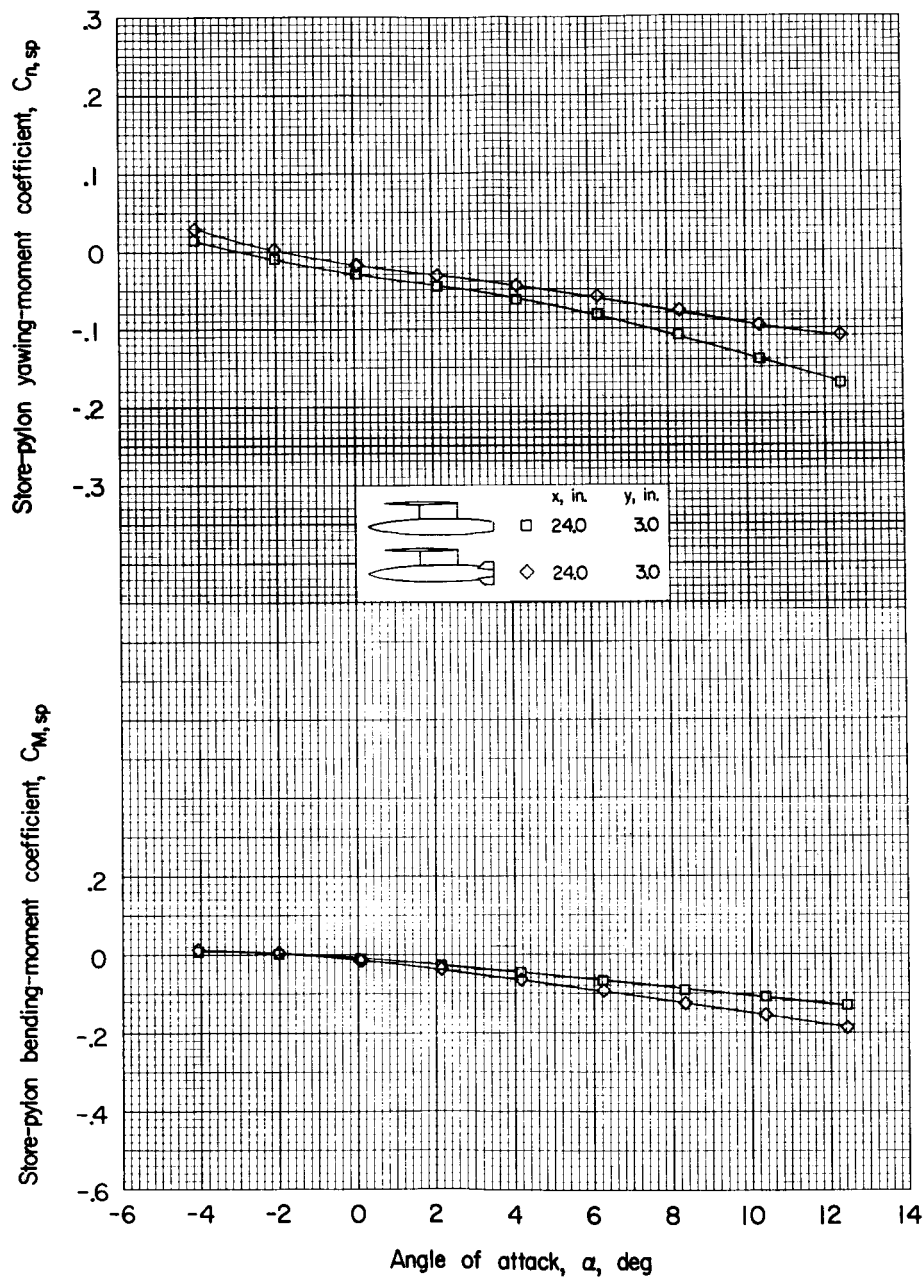
(b) Variation of $C_{n,sp}$ and $C_{M,sp}$ with α .

Figure 14.- Concluded.



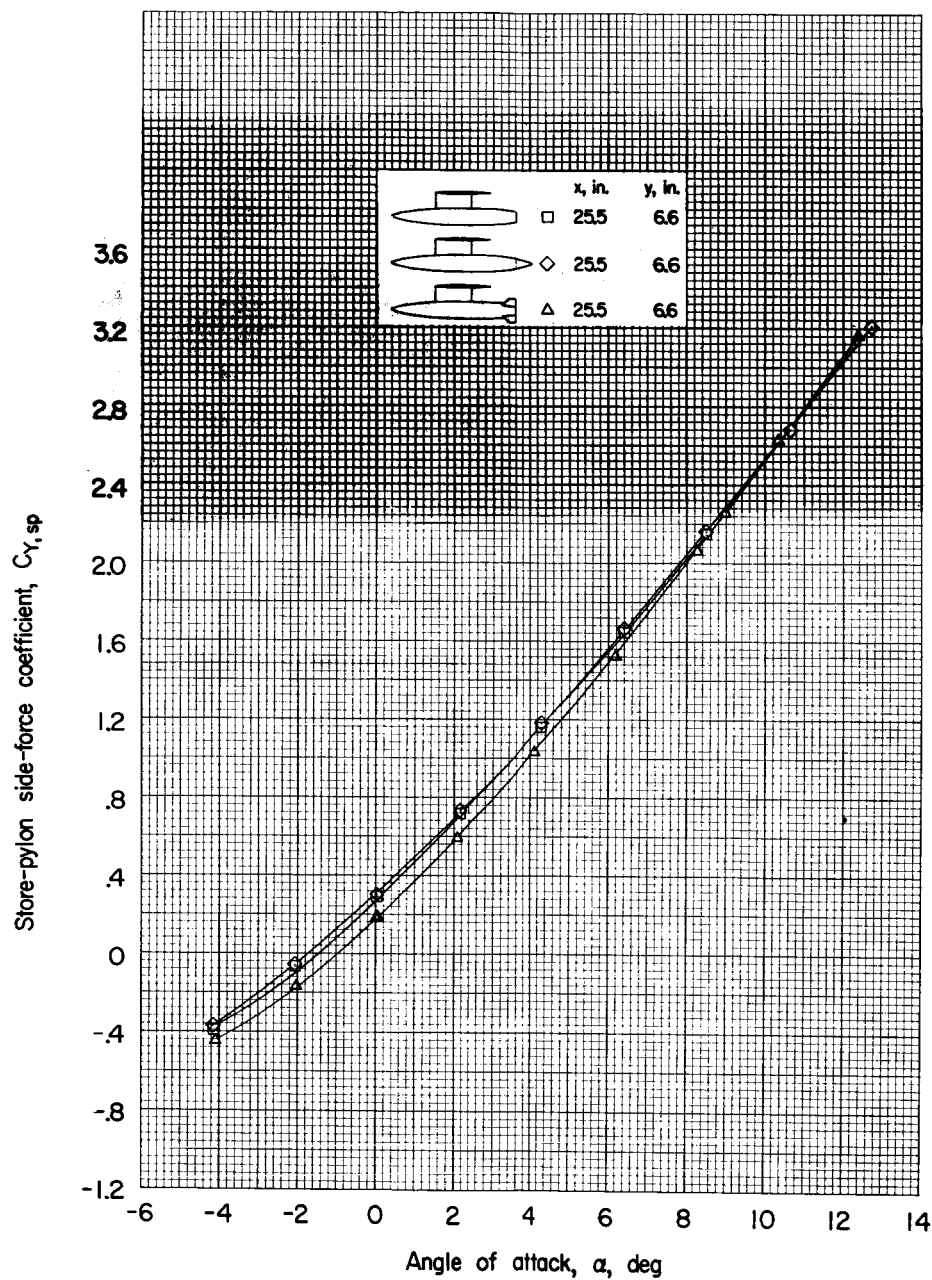
(a) Variation of $C_{Y,sp}$ with α .

Figure 15.- Effect of store fins on the aerodynamic characteristics of the store-pylon combination in the presence of the wing-fuselage combination.



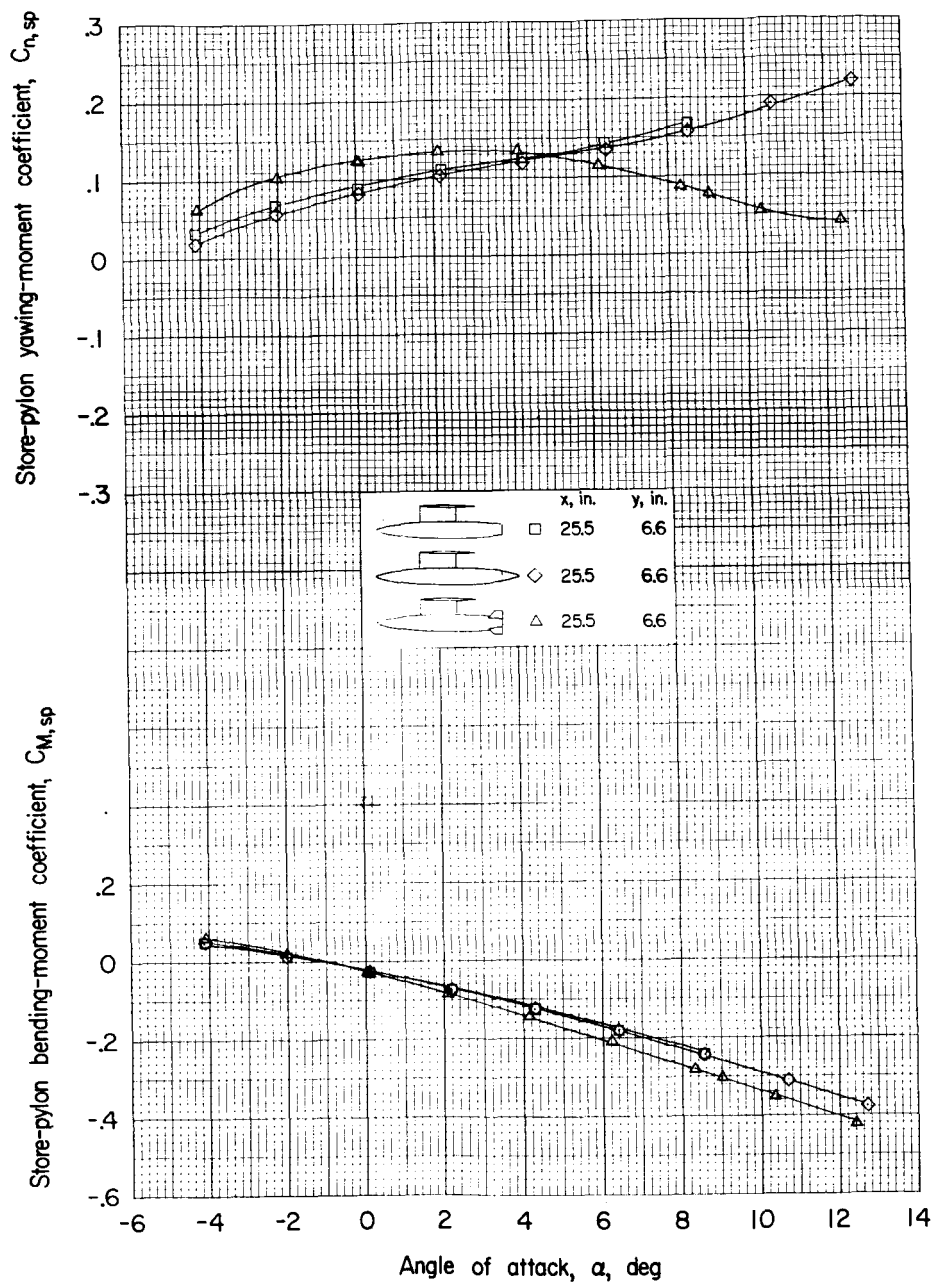
(b) Variation of $C_{n,sp}$ and $C_{M,sp}$ with α .

Figure 15.- Concluded.



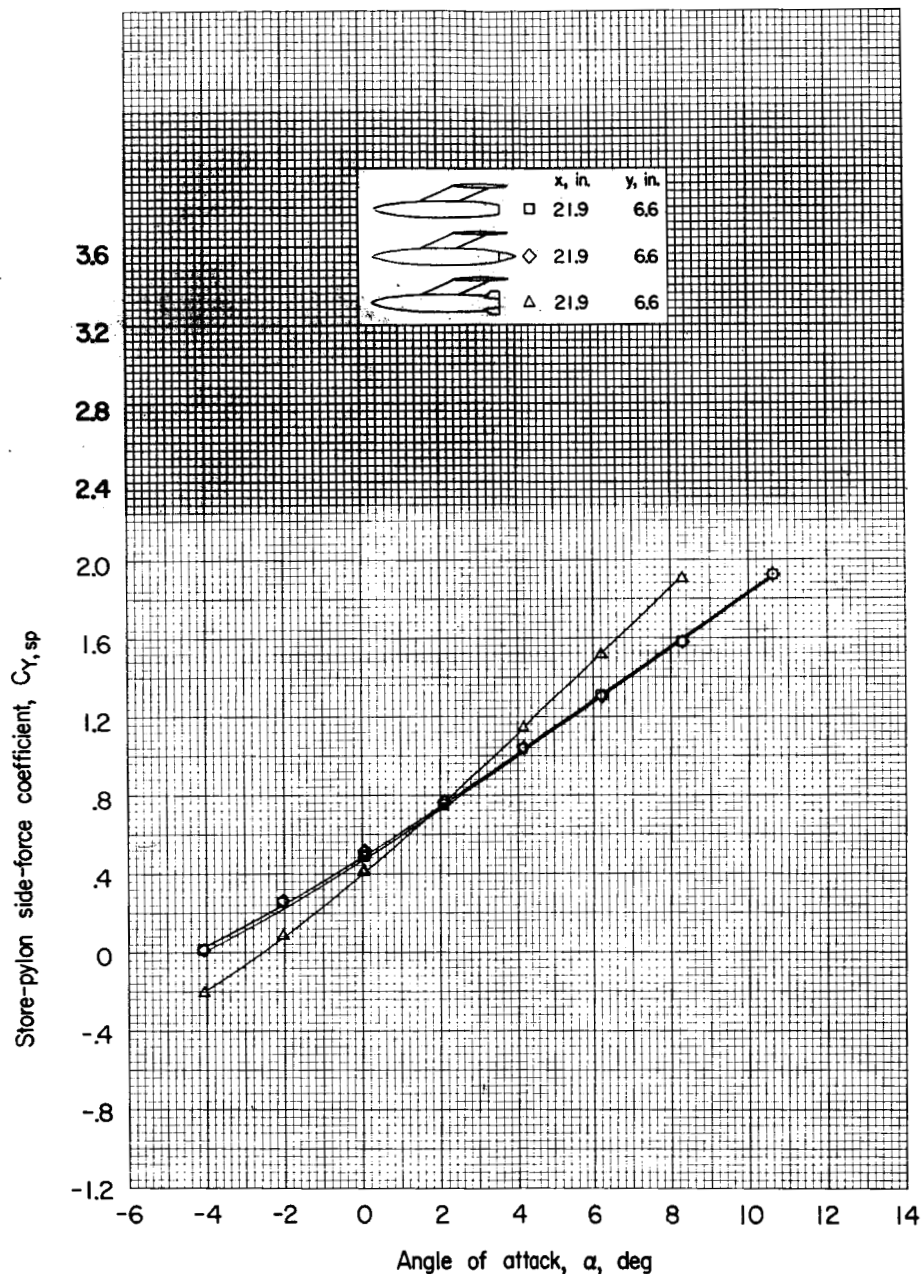
(a) Variation of $C_{Y,sp}$ with α .

Figure 16.- Effect of store fins and store tail cone on the aerodynamic characteristics of the store-pylon combination in the presence of the wing-fuselage combination.



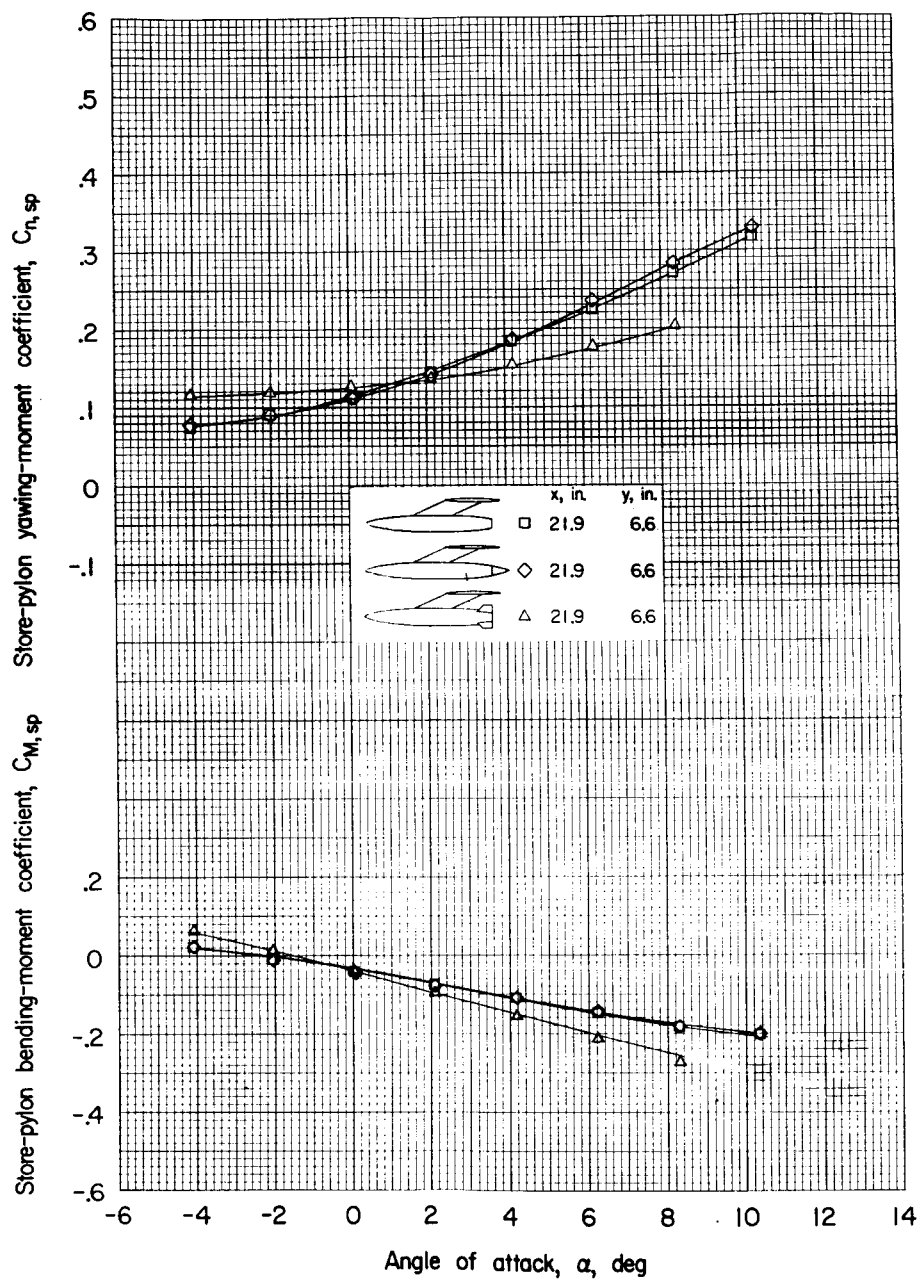
(b) Variation of $C_{n,sp}$ and $C_{M,sp}$ with α .

Figure 16.- Concluded.



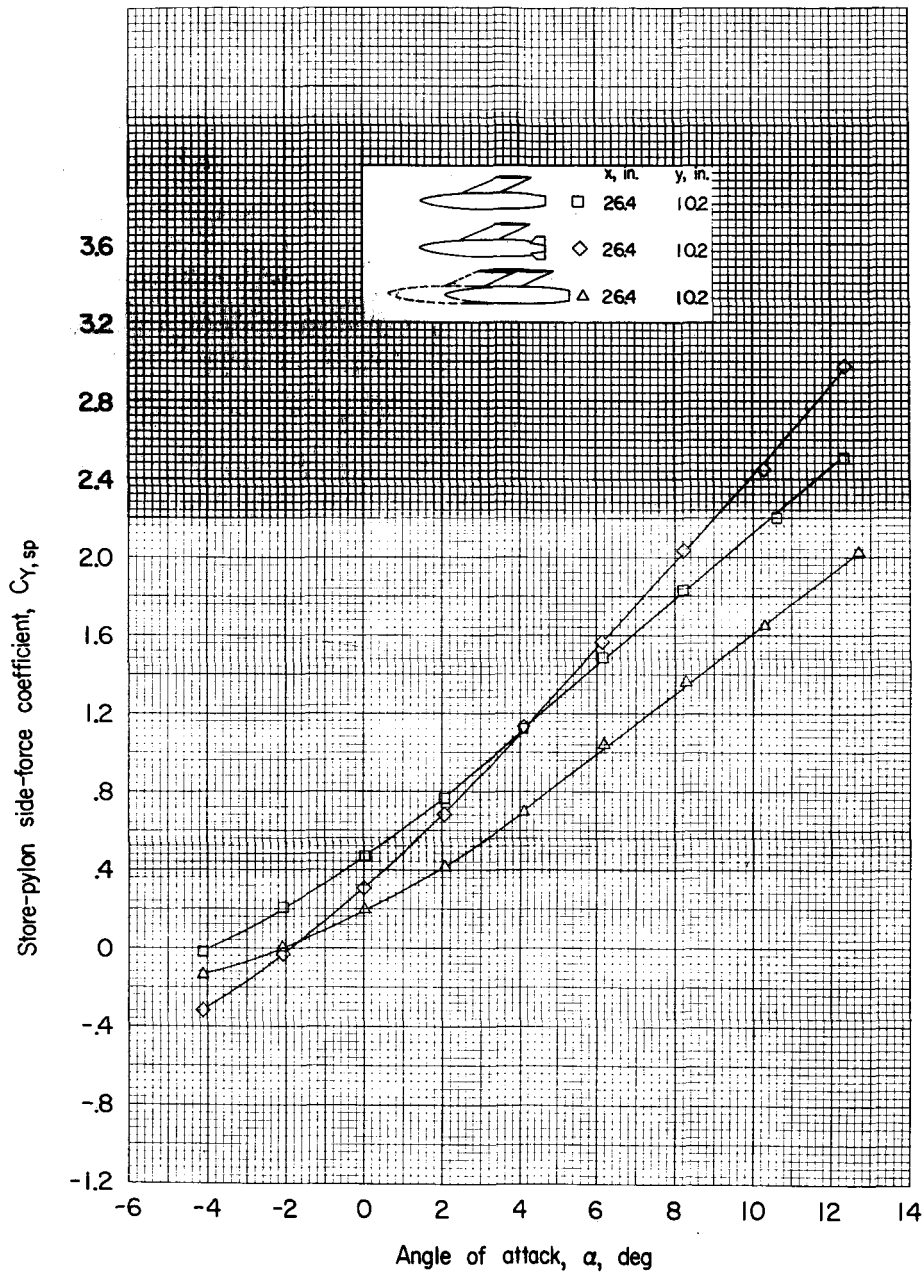
(a) Variation of $C_{Y,sp}$ with α .

Figure 17.- Effect of store fins and store tail cone on the aerodynamic characteristics of the store-pylon combination in the presence of the wing-fuselage combination.



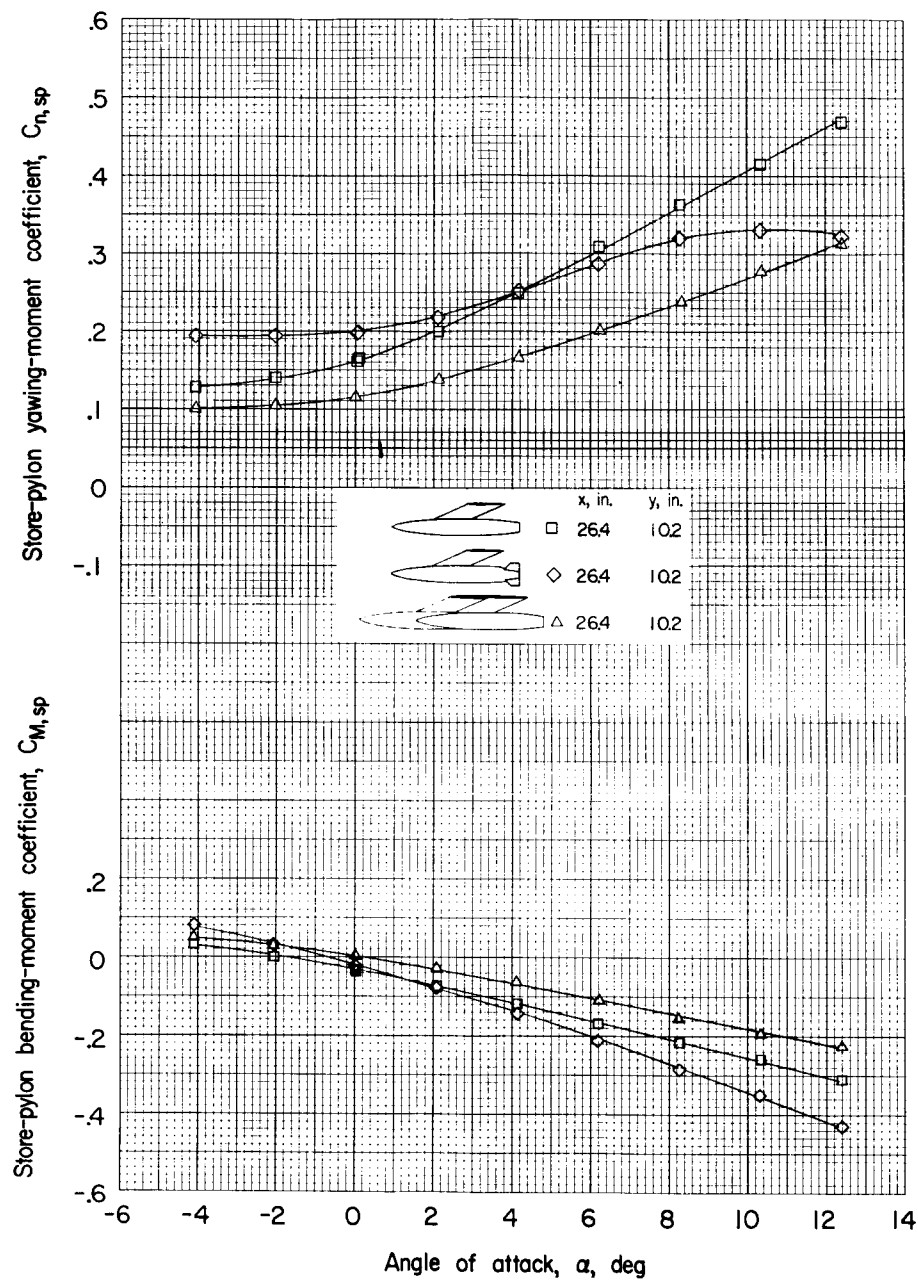
(b) Variation of $C_{n,sp}$ and $C_{M,sp}$ with α .

Figure 17.- Concluded.



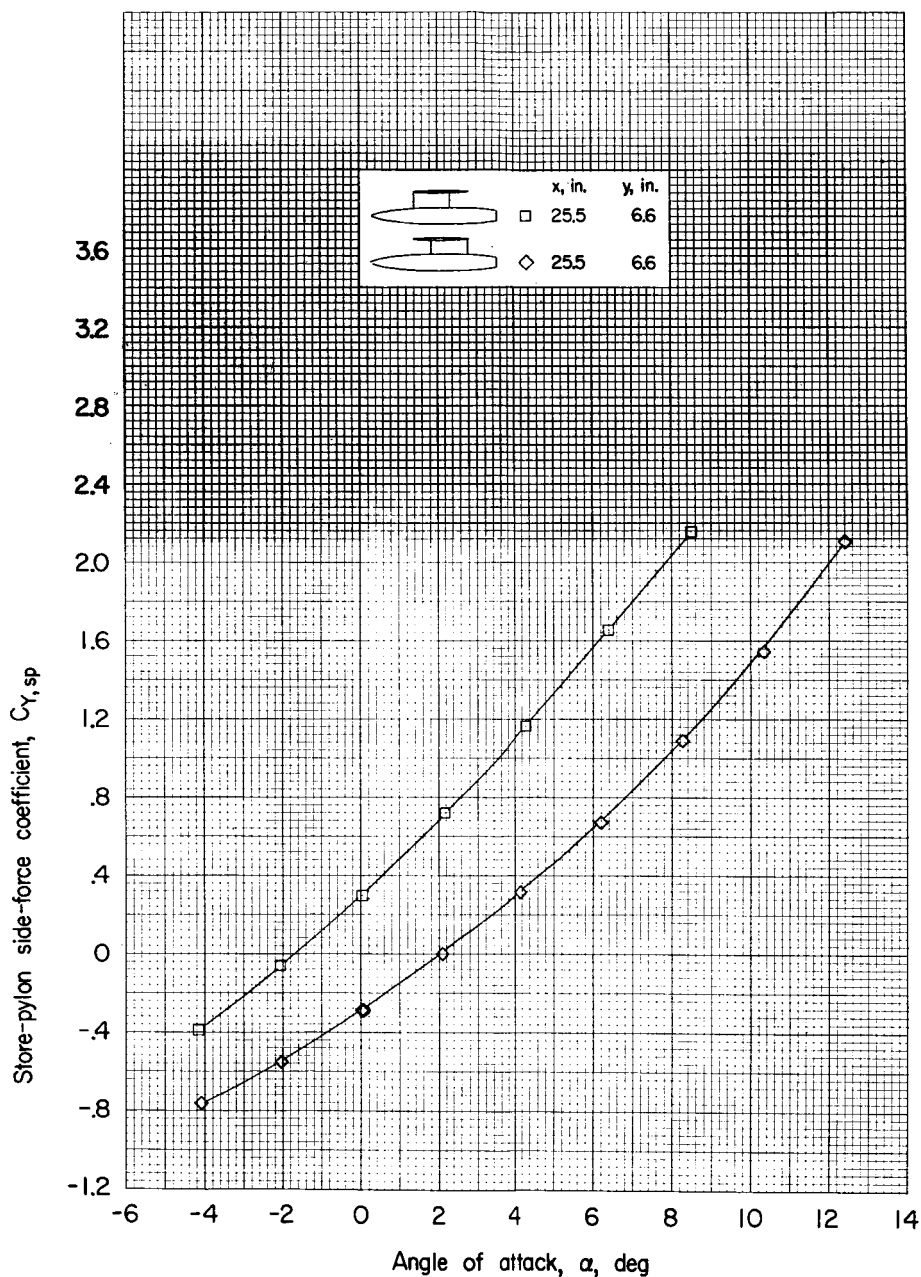
(a) Variation of $C_{Y,sp}$ with α .

Figure 18.- Effect of store fins and inboard and outboard store interference on the aerodynamic characteristics of the store-pylon combination in the presence of the wing-fuselage combination.



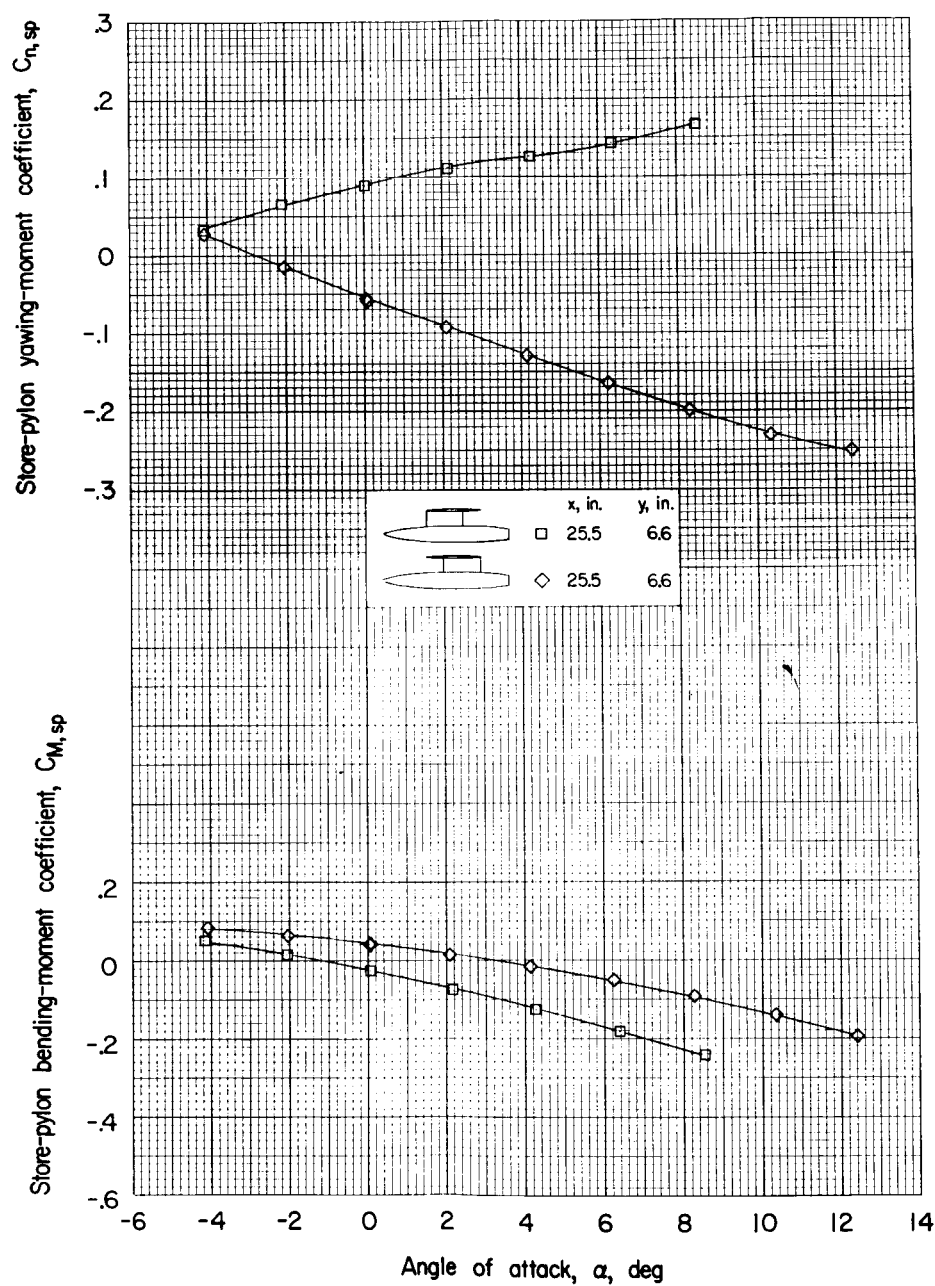
(b) Variation of $C_{n,sp}$ and $C_{M,sp}$ with α .

Figure 18.- Concluded.



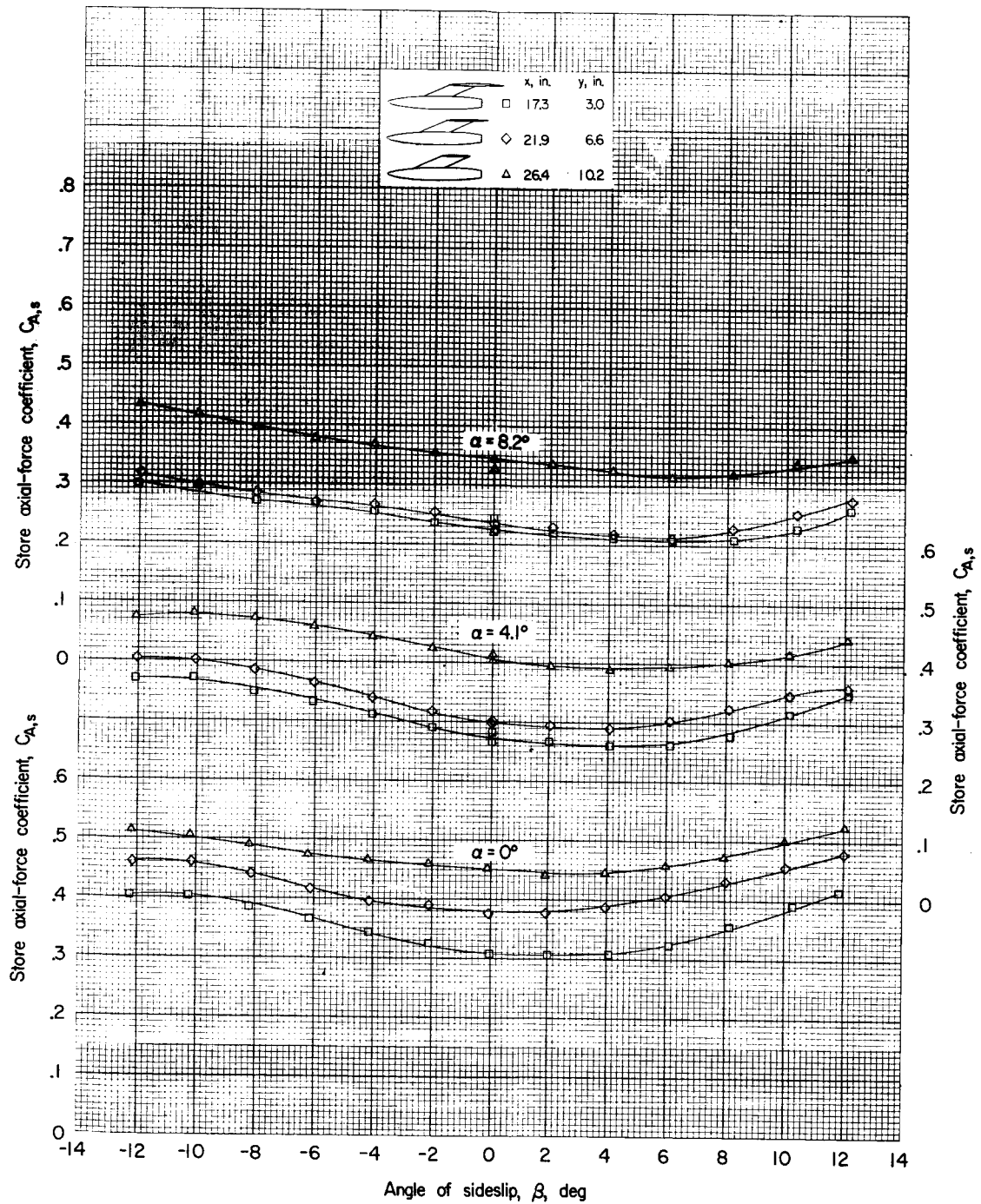
(a) Variation of $C_{Y,sp}$ with α .

Figure 19.- Effect of pylon location on the aerodynamic characteristics of the store-pylon combination in the presence of the wing-fuselage combination.



(b) Variation of $C_{n,sp}$ and $C_{M,sp}$ with α .

Figure 19.- Concluded.



(a) Variation of $C_{A,s}$ with β .

Figure 20.- Aerodynamic characteristics of the store in the presence of the wing-fuselage combination for three spanwise store positions.

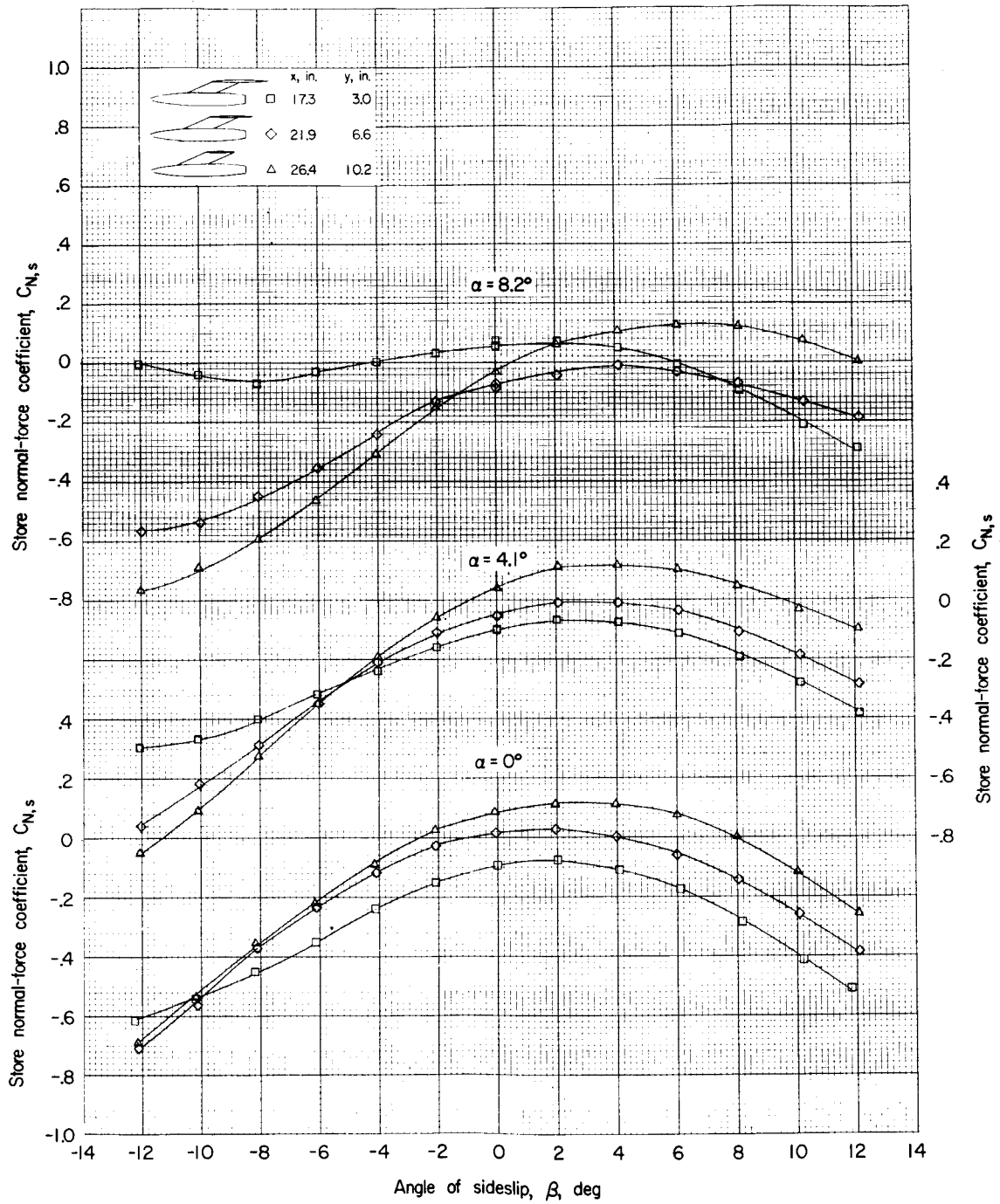
(b) Variation of $C_{N,s}$ with β .

Figure 20.- Continued.

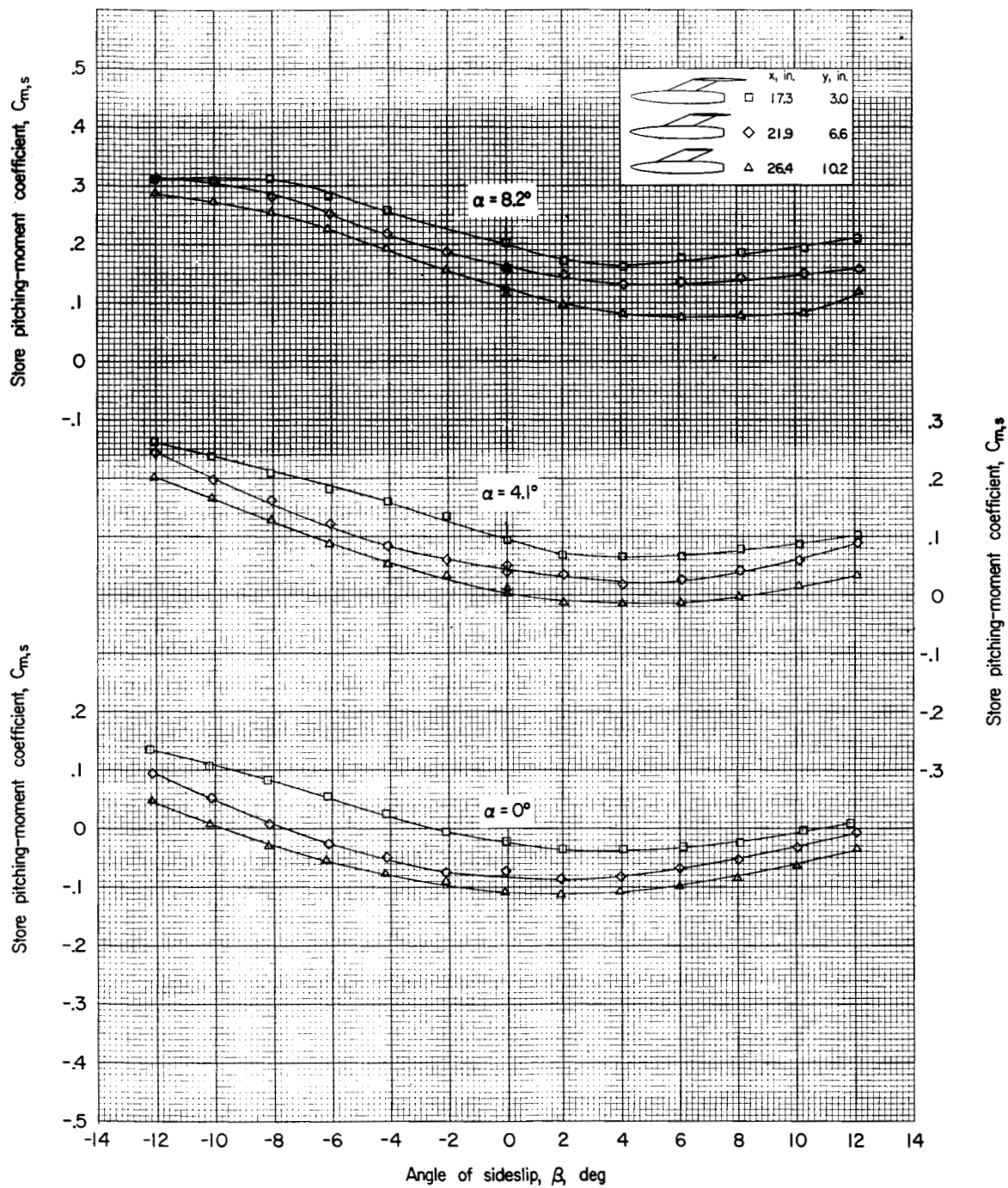
(c) Variation of $C_{m,s}$ with β .

Figure 20.- Continued.

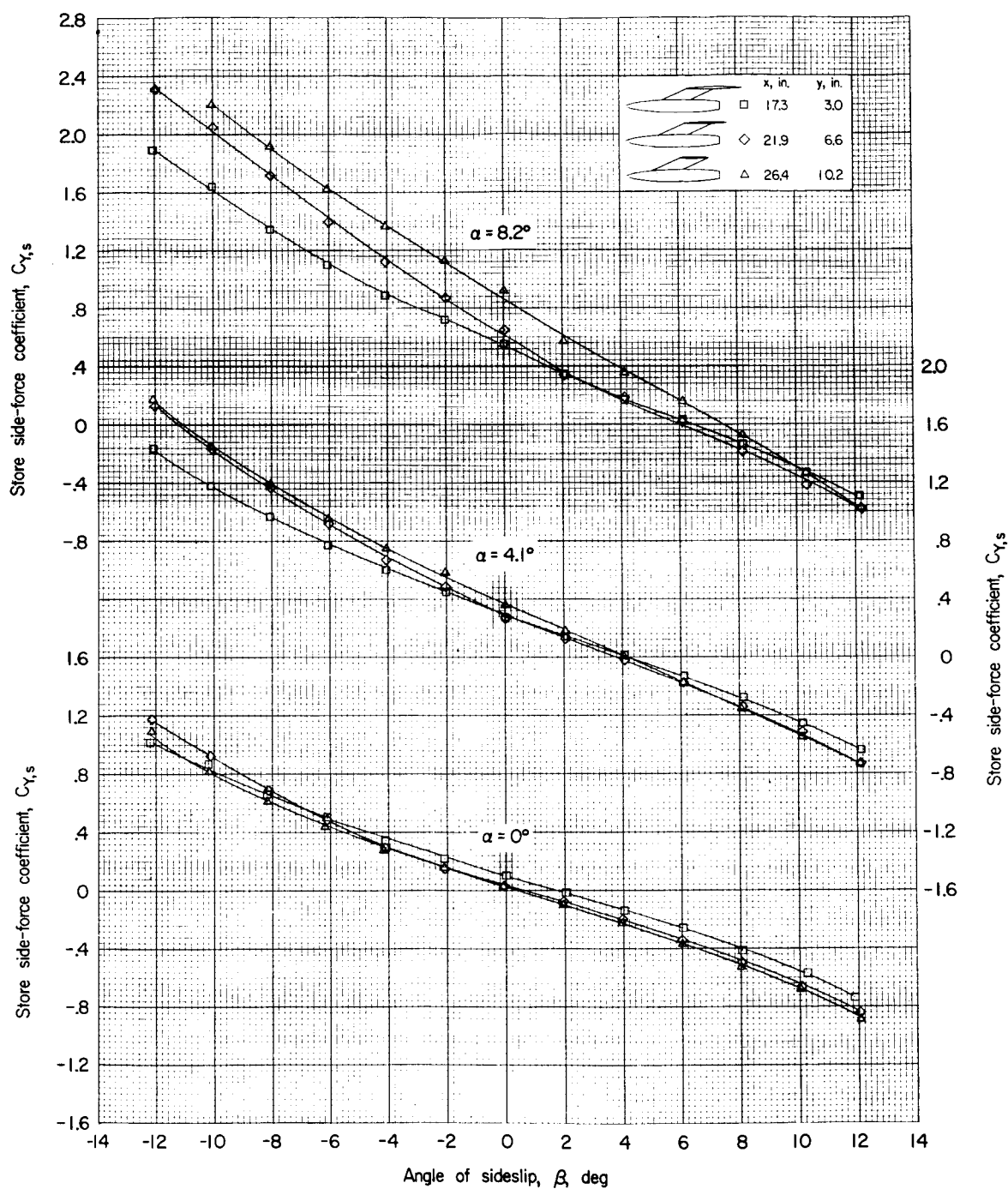
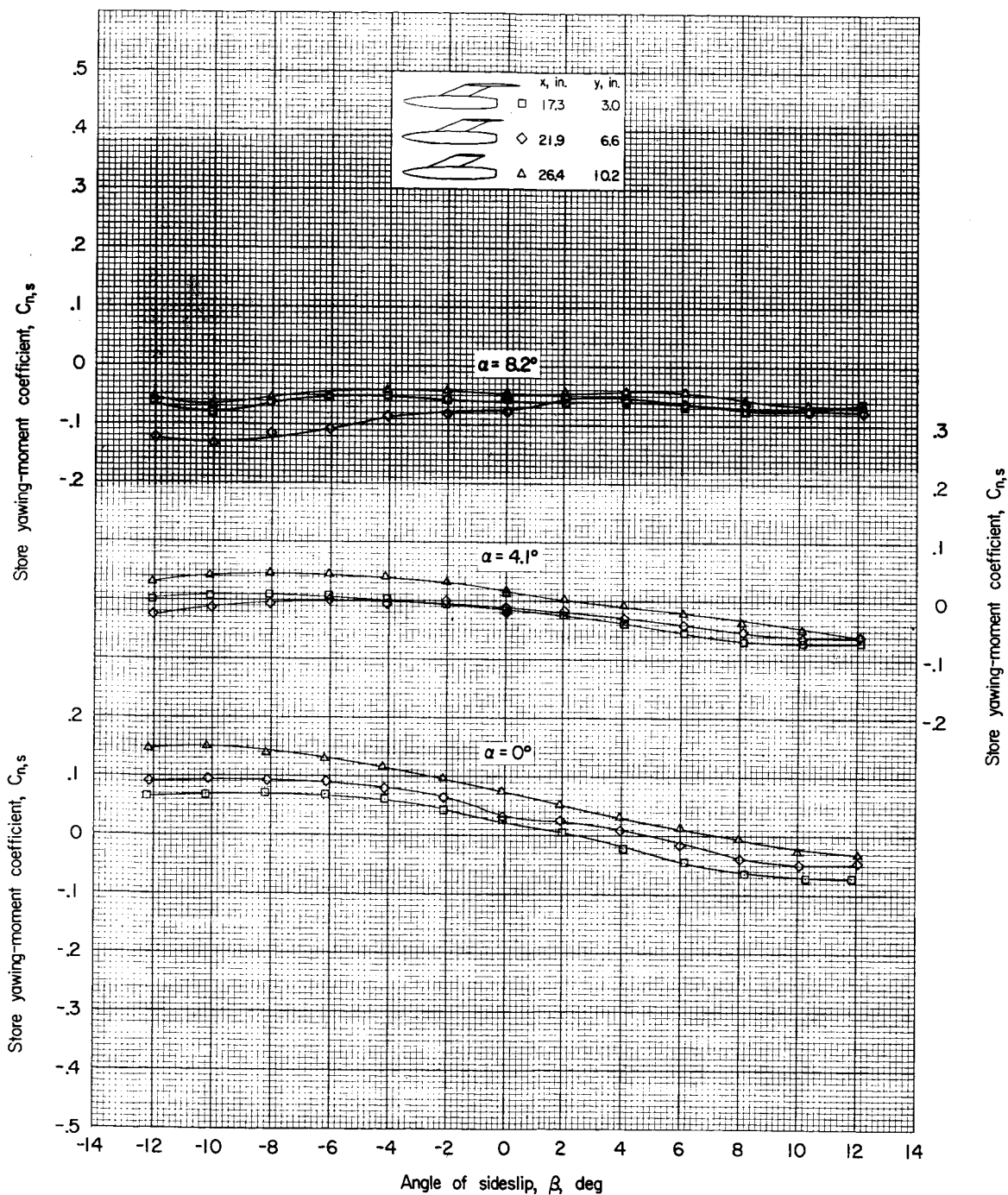
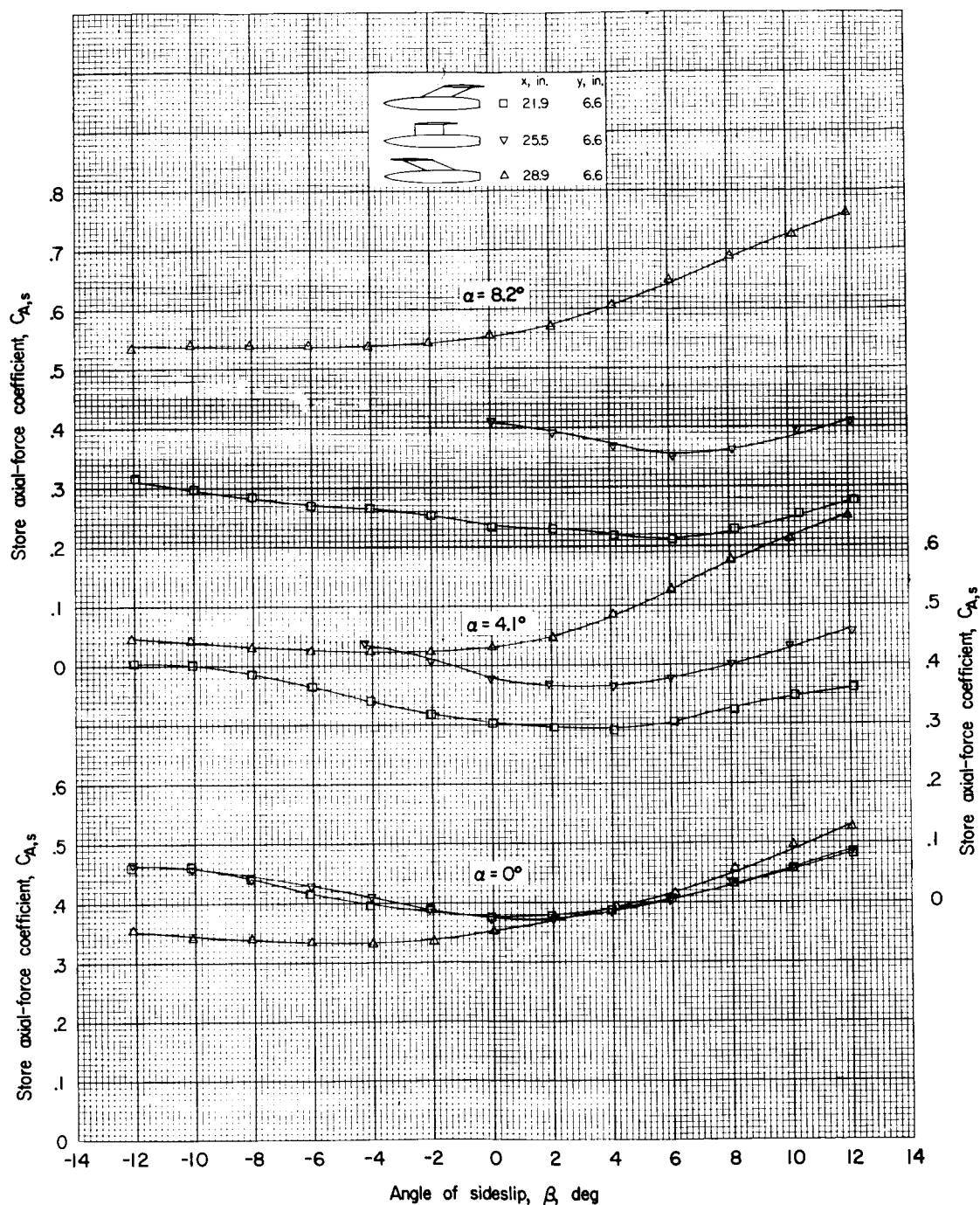
(d) Variation of $C_{Y,s}$ with β .

Figure 20.- Continued.



(e) Variation of $C_{n,s}$ with β .

Figure 20.- Concluded.



(a) Variation of $C_{A,s}$ with β .

Figure 21.- Aerodynamic characteristics of the store in the presence of the wing-fuselage combination for three chordwise store positions.

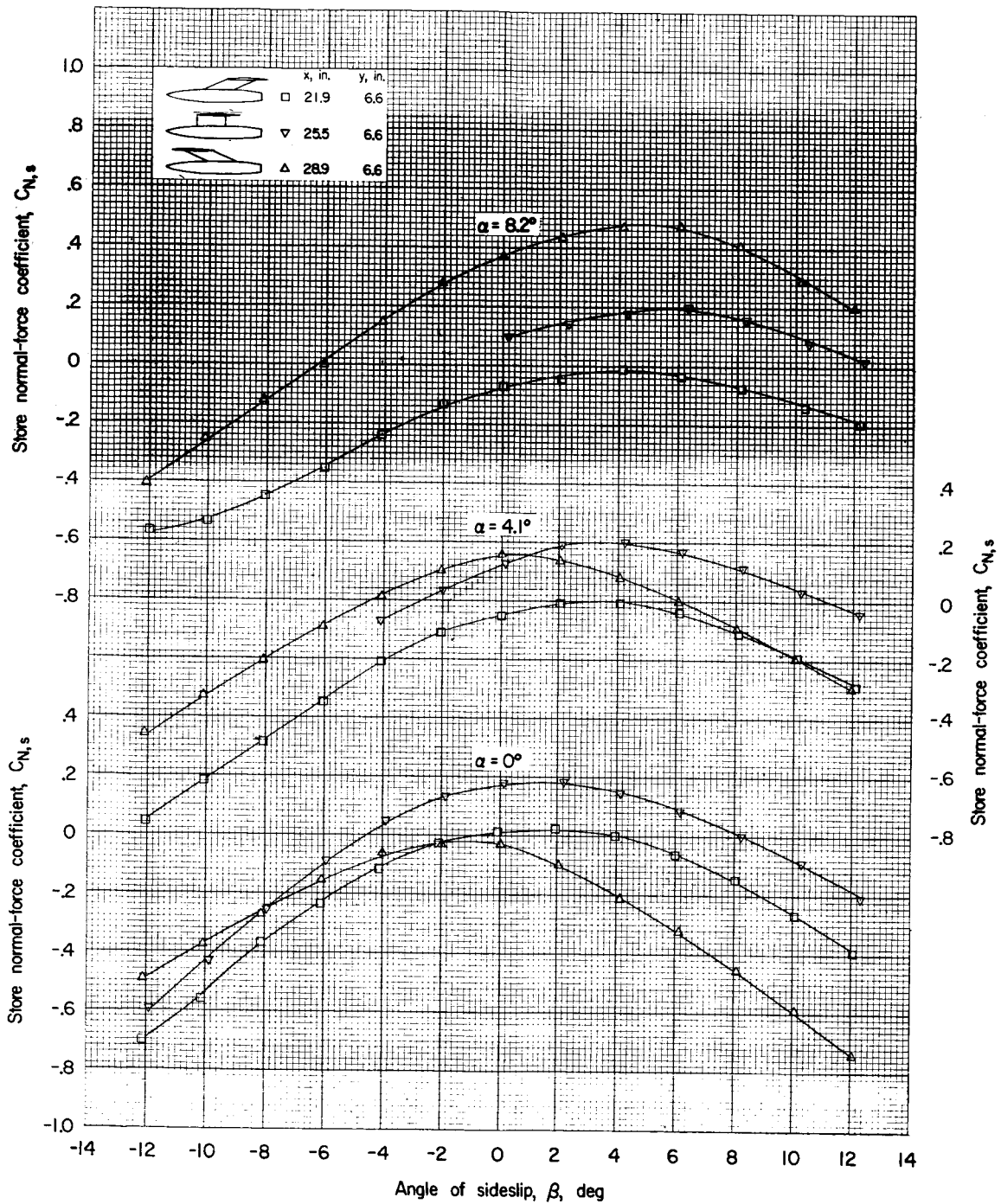
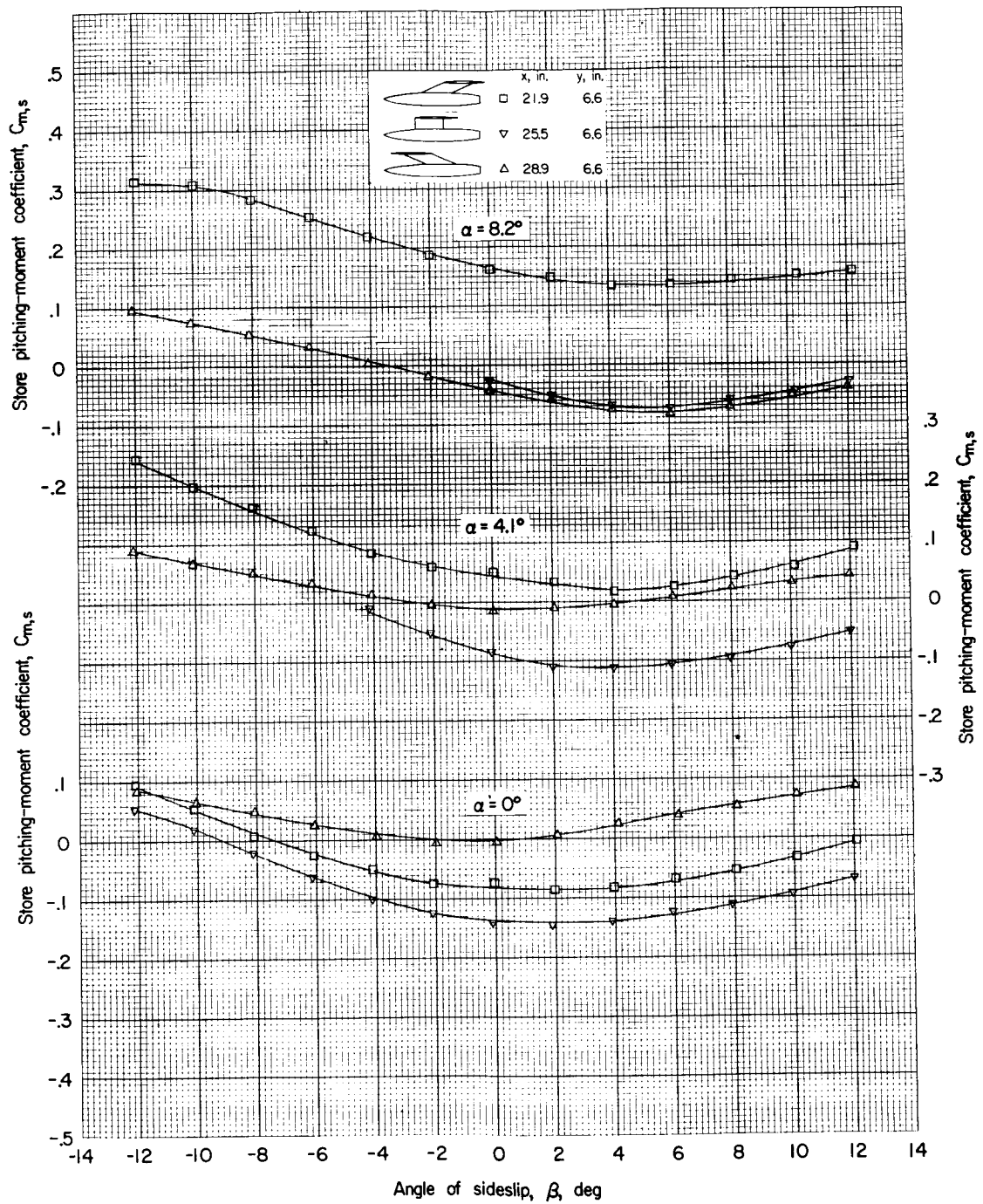
(b) Variation of $C_{N,s}$ with β .

Figure 21.- Continued.



(c) Variation of $C_{m,s}$ with β .

Figure 21.- Continued.

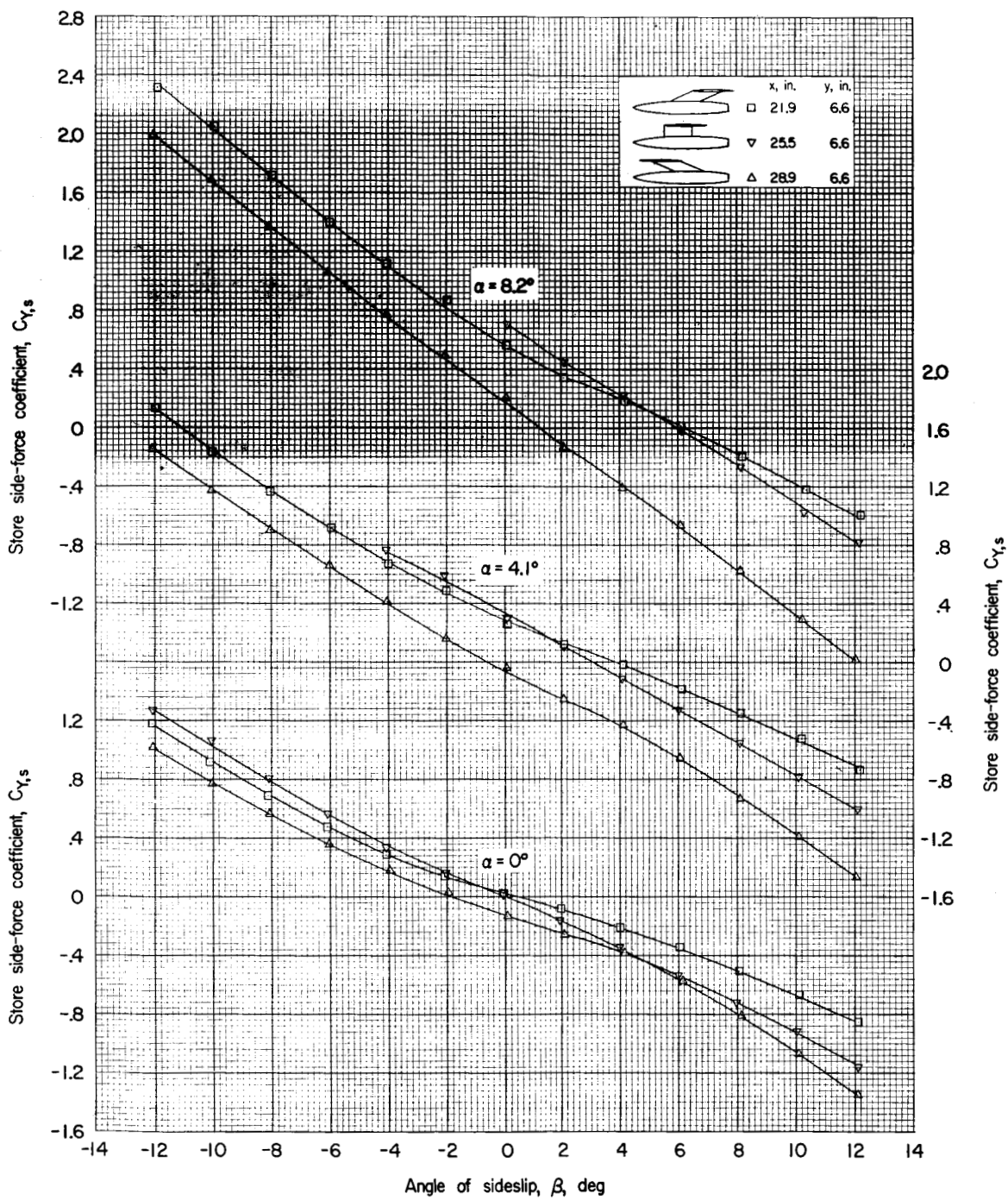
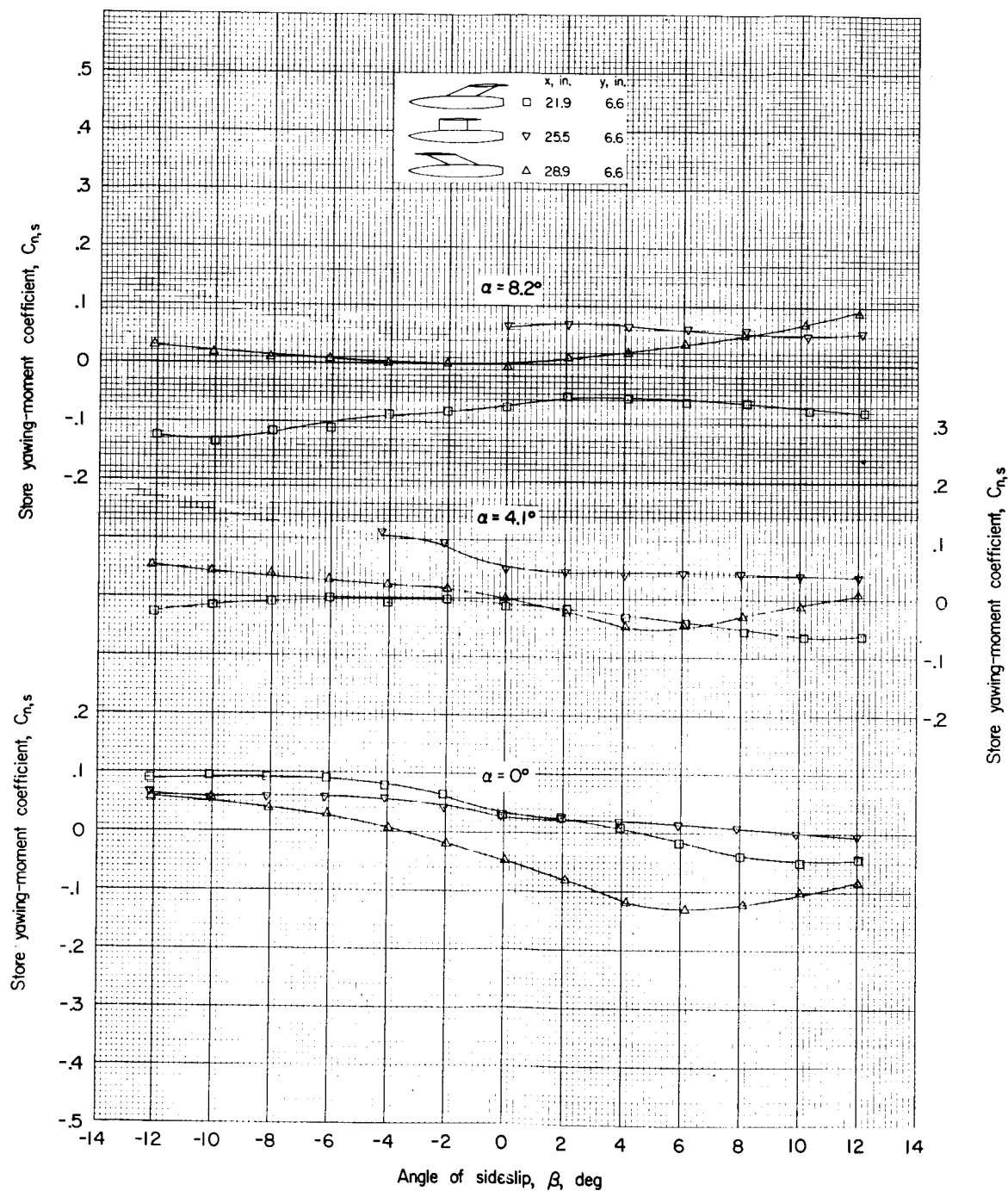
(d) Variation of $C_{Y,s}$ with β .

Figure 21.- Continued.



(e) Variation of $C_{n,s}$ with β .

Figure 21.- Concluded.

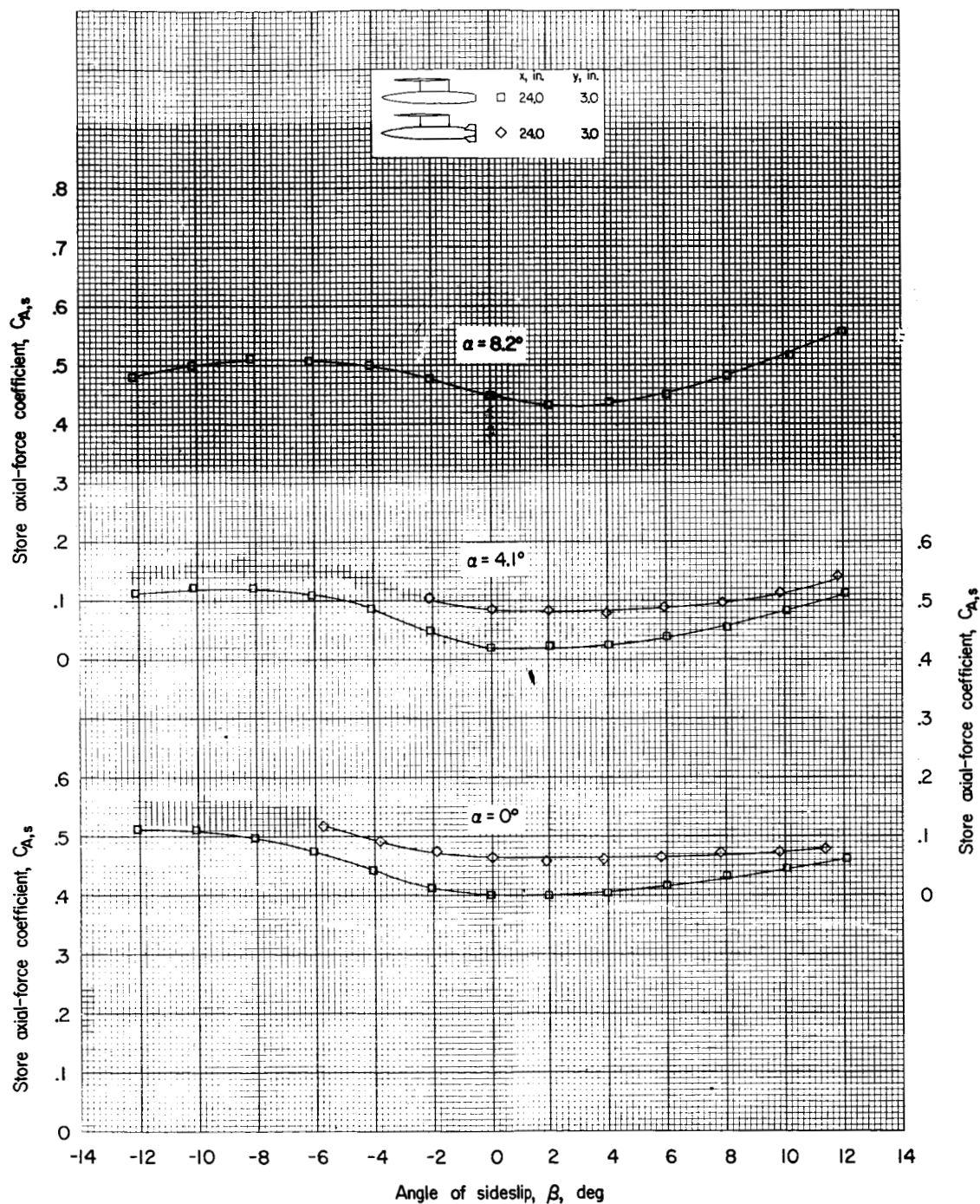
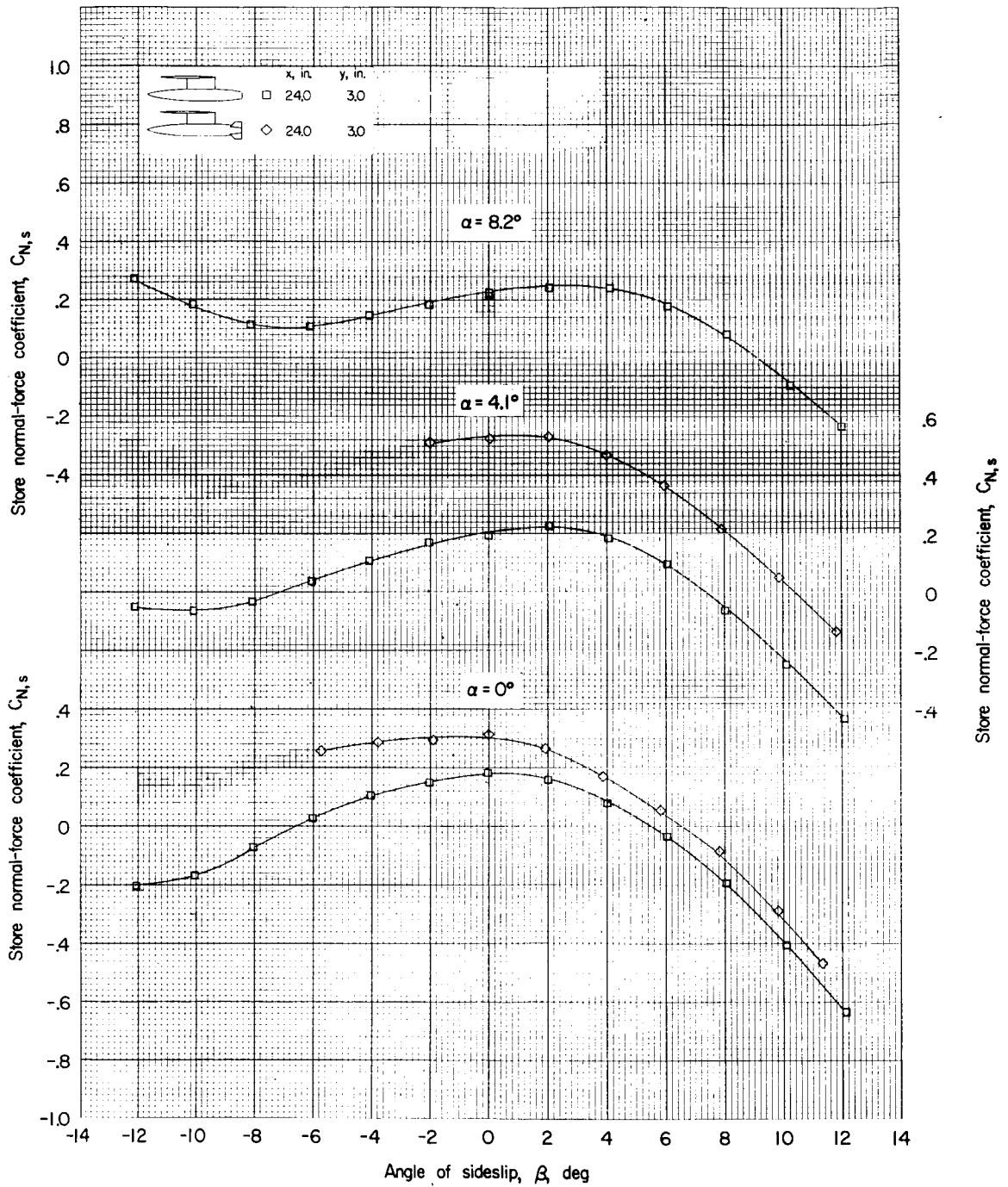
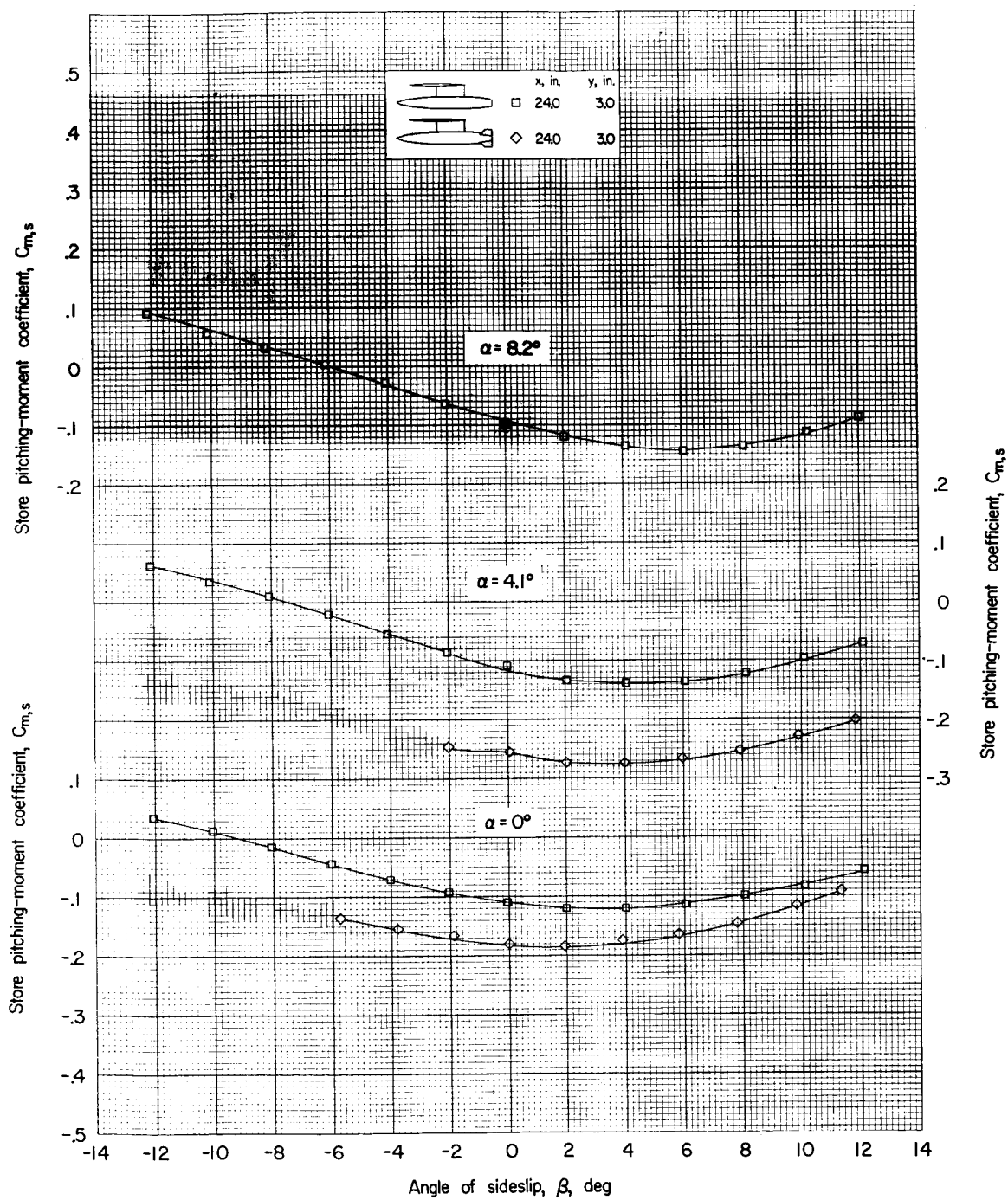
(a) Variation of $C_{A,s}$ with β .

Figure 22.- Effect of store fins on the aerodynamic characteristics of the store in the presence of the wing-fuselage combination.



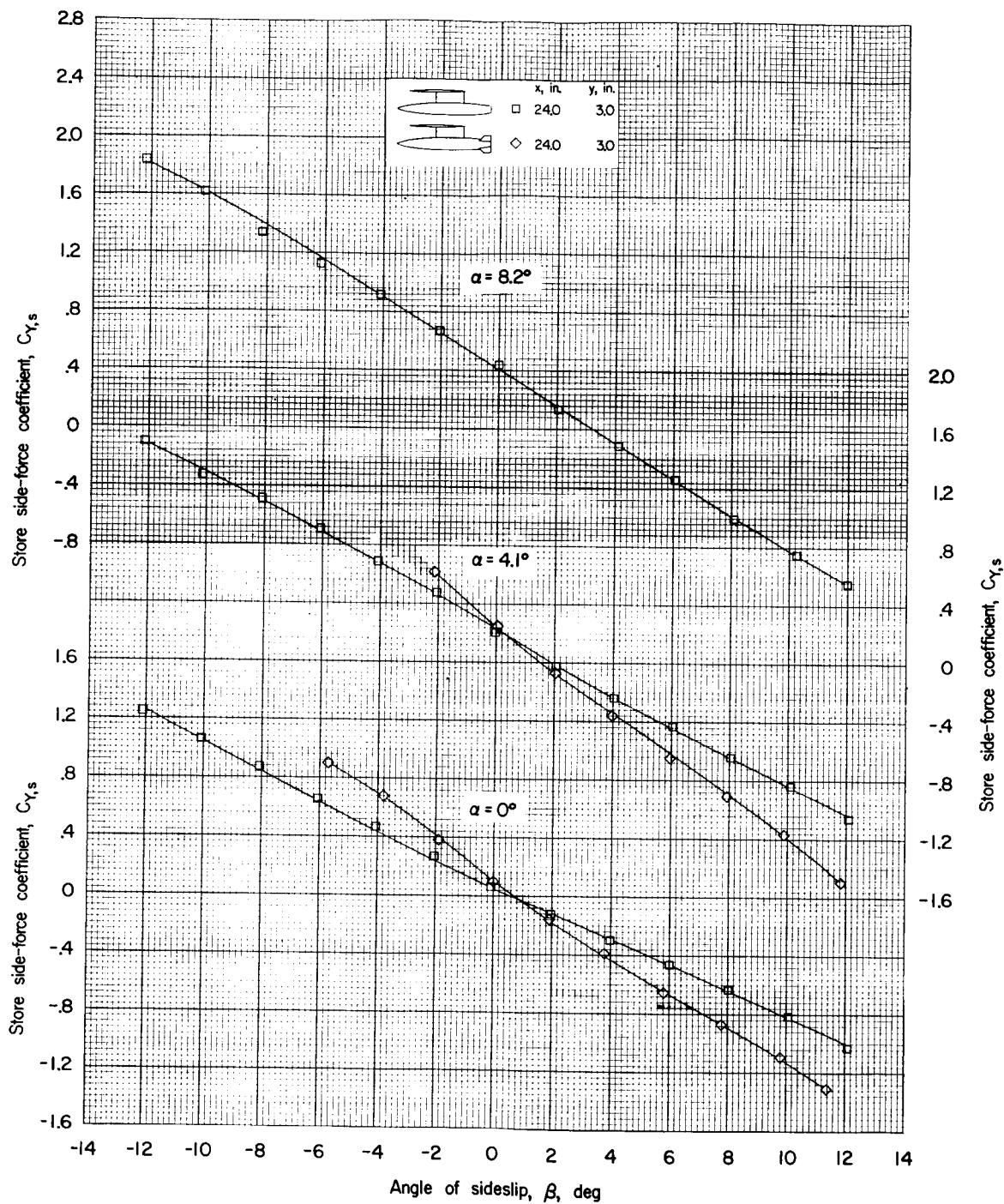
(b) Variation of $C_{N,s}$ with β .

Figure 22.- Continued.



(c) Variation of $C_{m,s}$ with β .

Figure 22.- Continued.



(d) Variation of $C_{Y,s}$ with β .

Figure 22.- Continued.

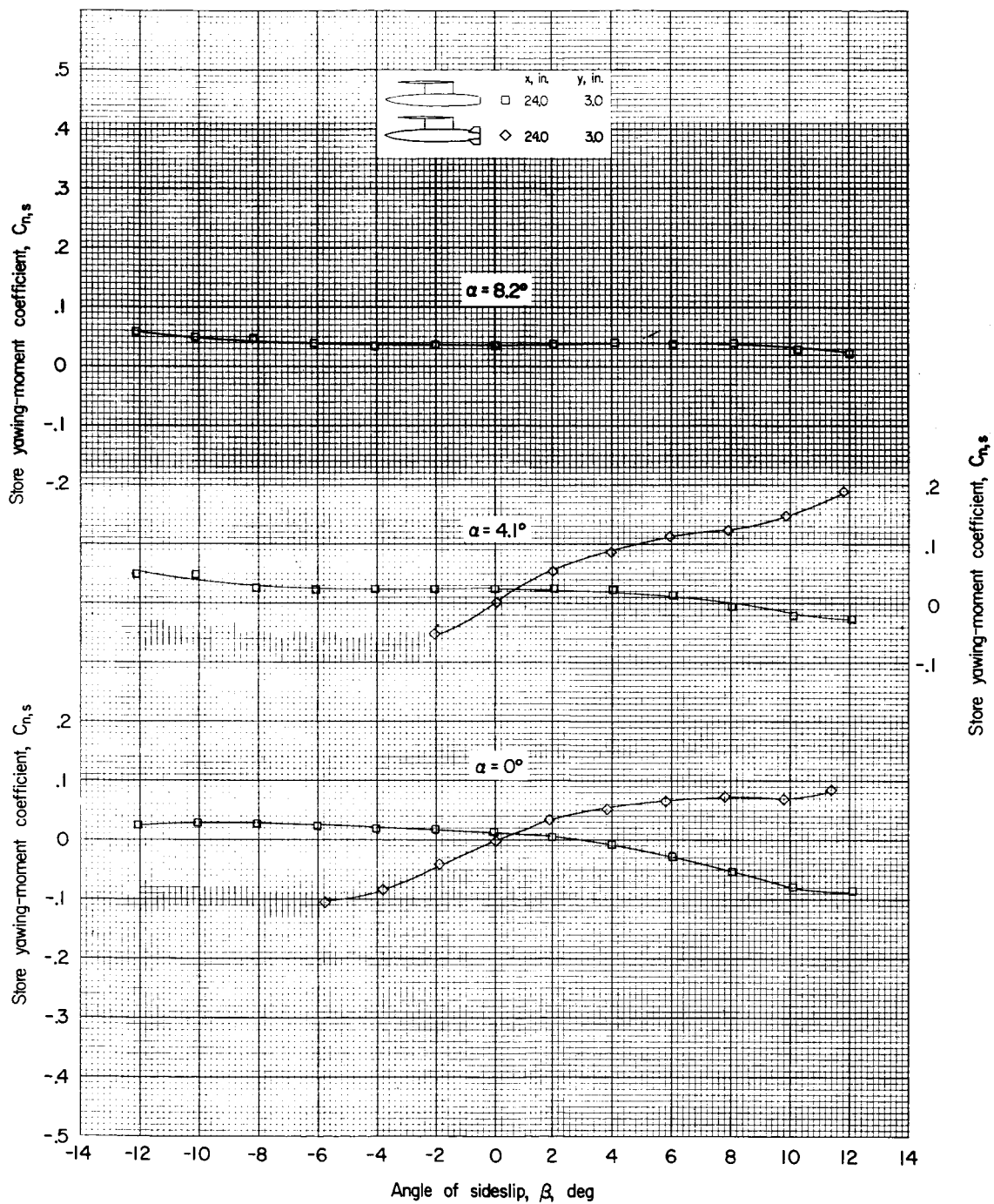
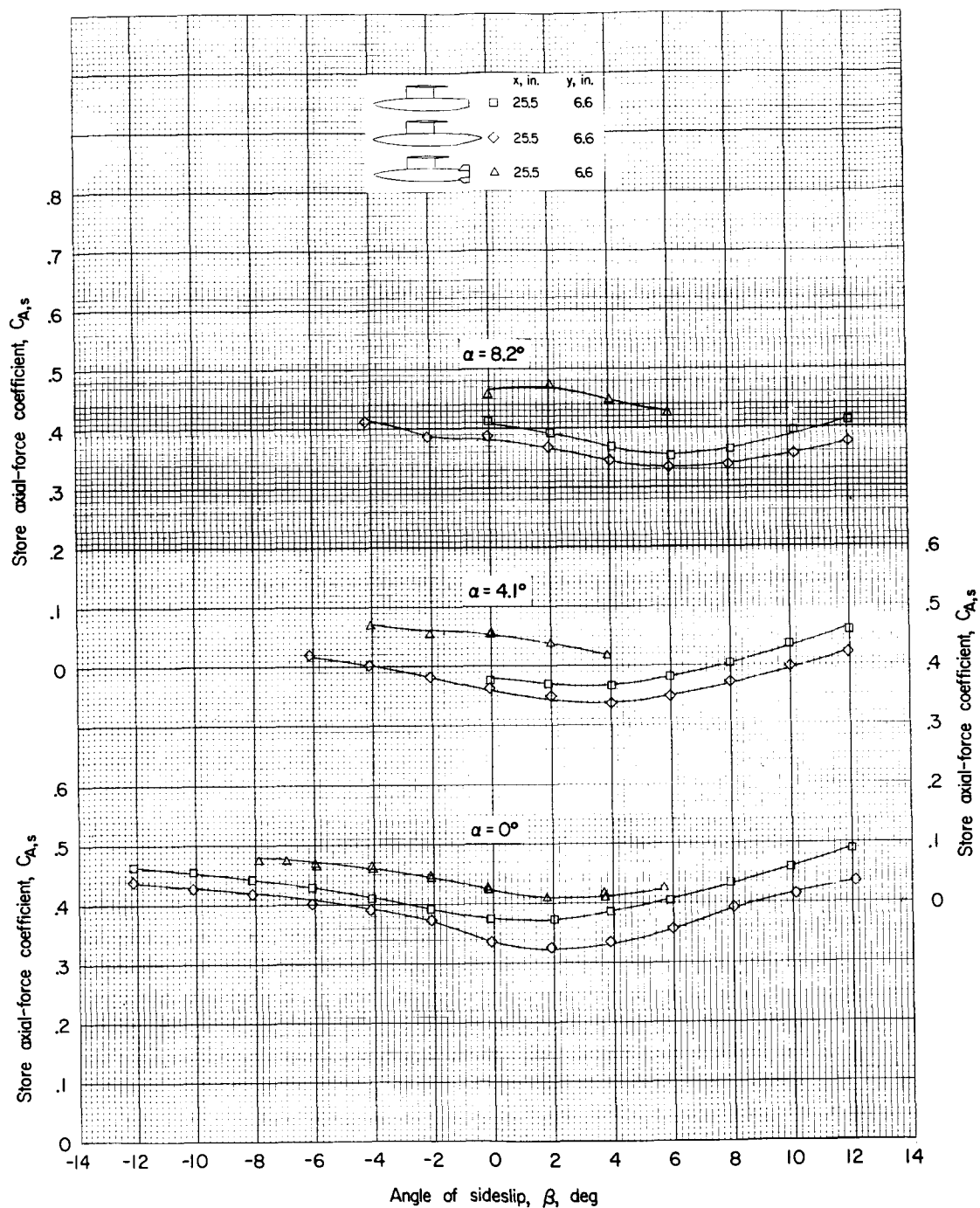
(e) Variation of $C_{n,s}$ with β .

Figure 22.- Concluded.



(a) Variation of $C_{A,s}$ with β .

Figure 23.- Effect of store fins and store tail cone on the aerodynamic characteristics of the store in the presence of the wing-fuselage combination.

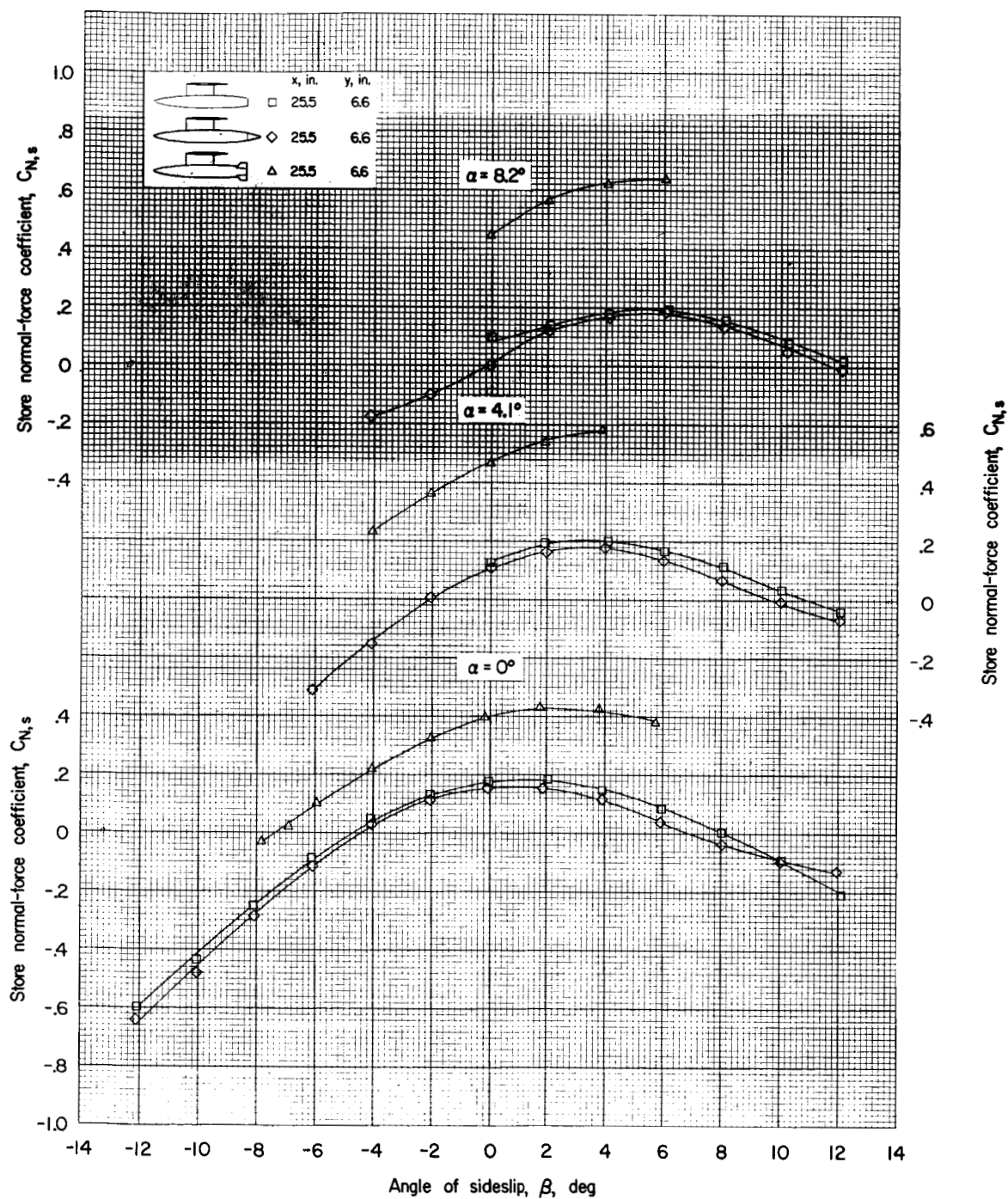
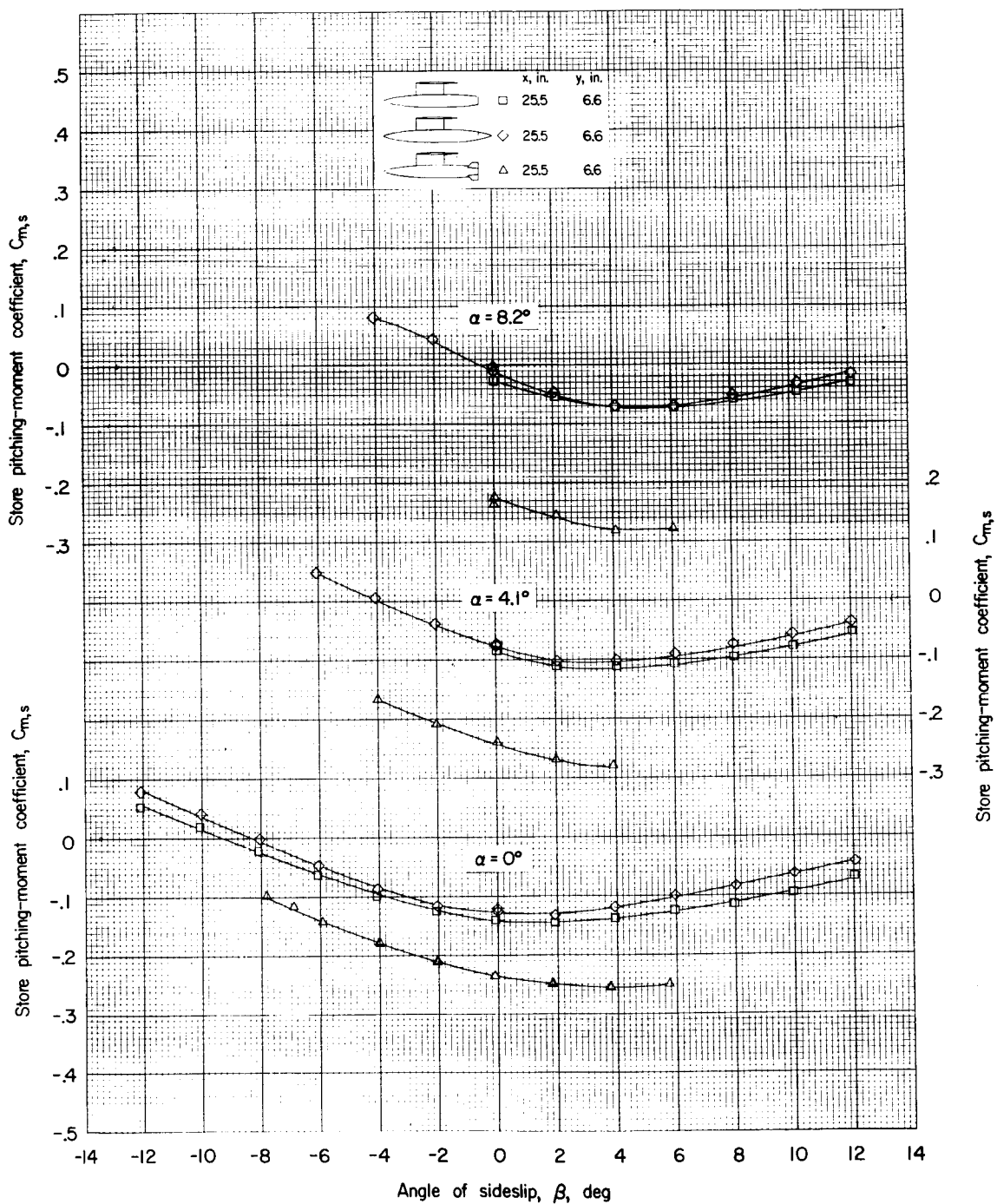
(b) Variation of $C_{N,s}$ with β .

Figure 23.- Continued.



(c) Variation of $C_{m,s}$ with β .

Figure 23.- Continued.

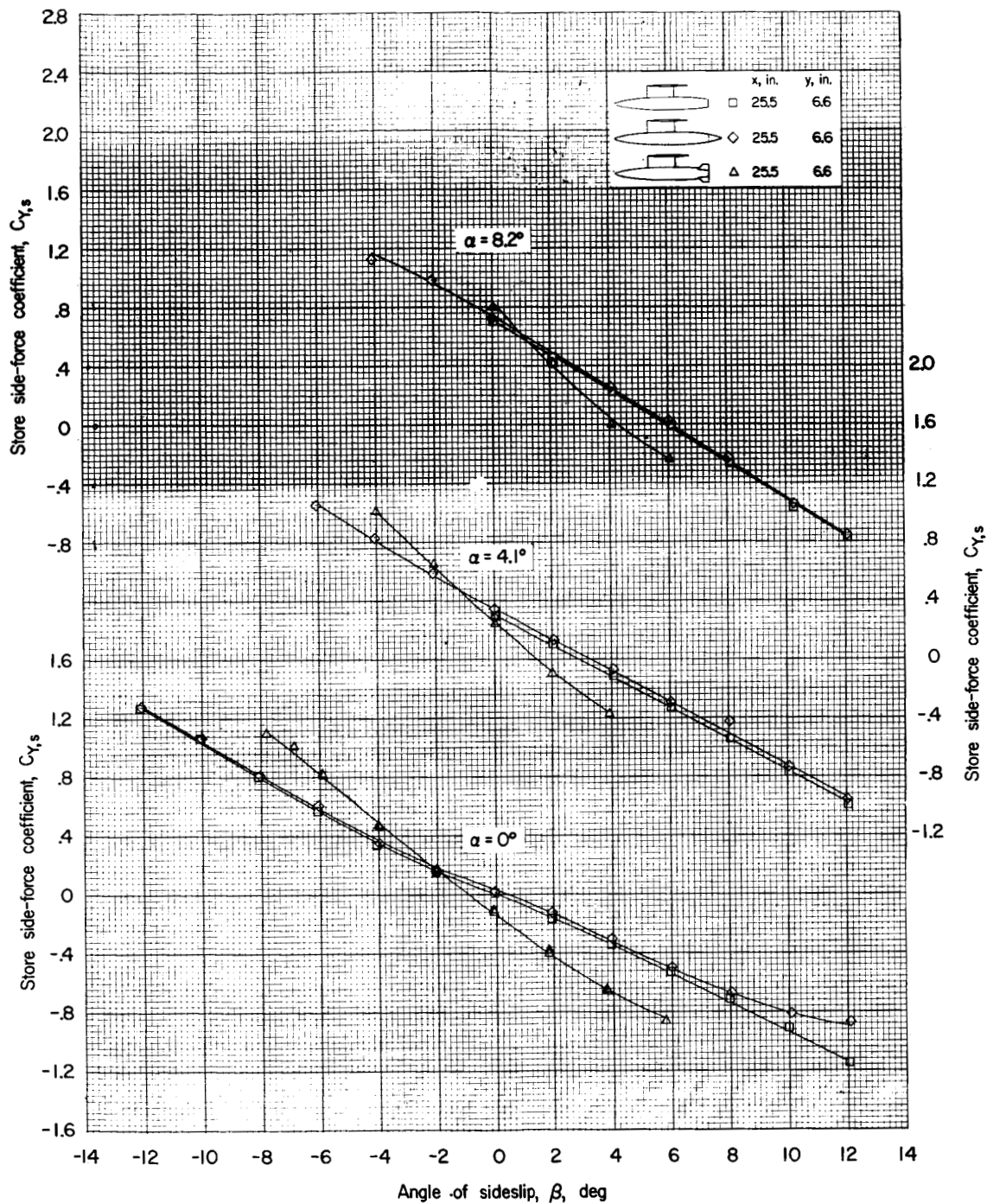
(d) Variation of $C_{Y,s}$ with β .

Figure 23.- Continued.

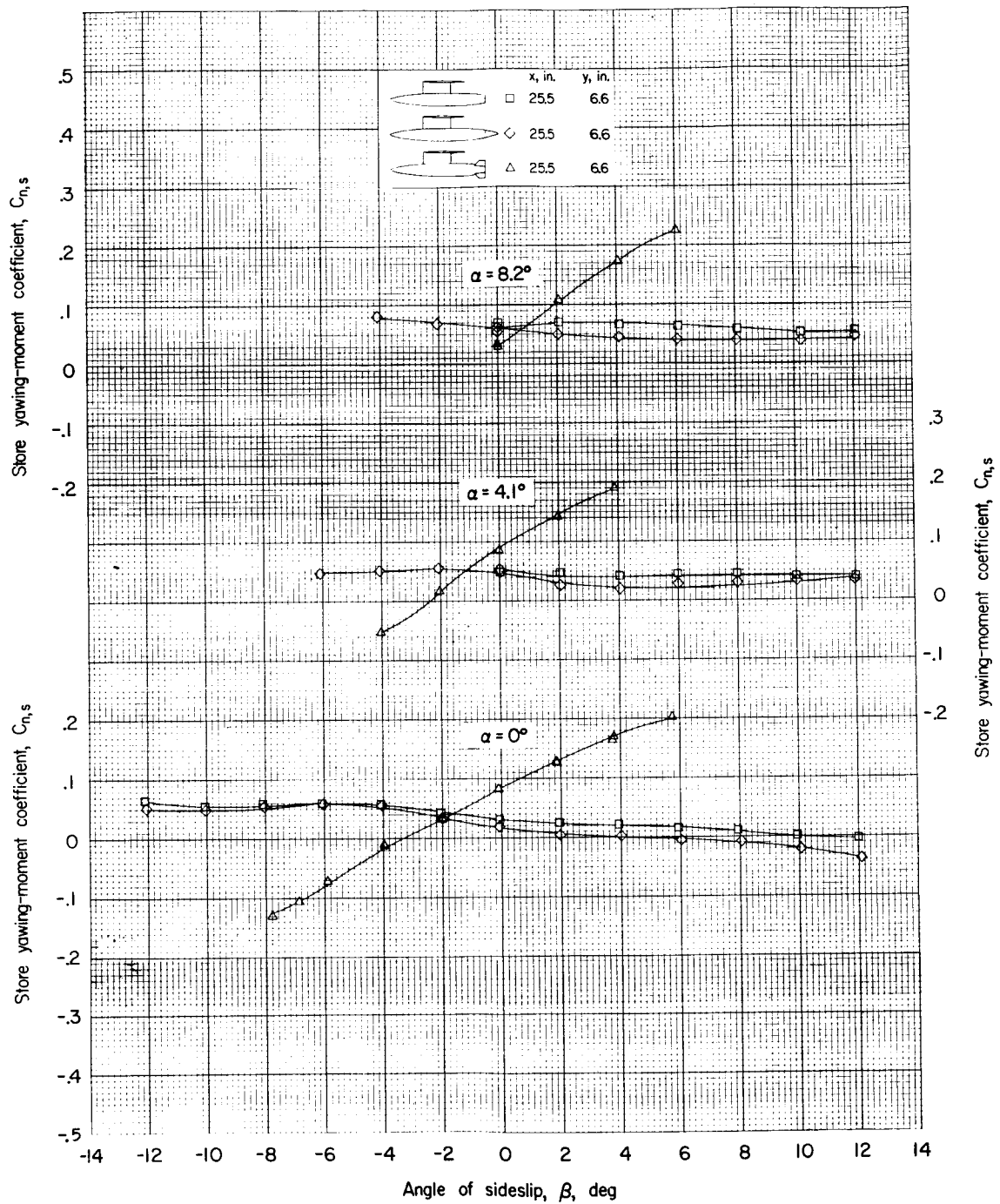
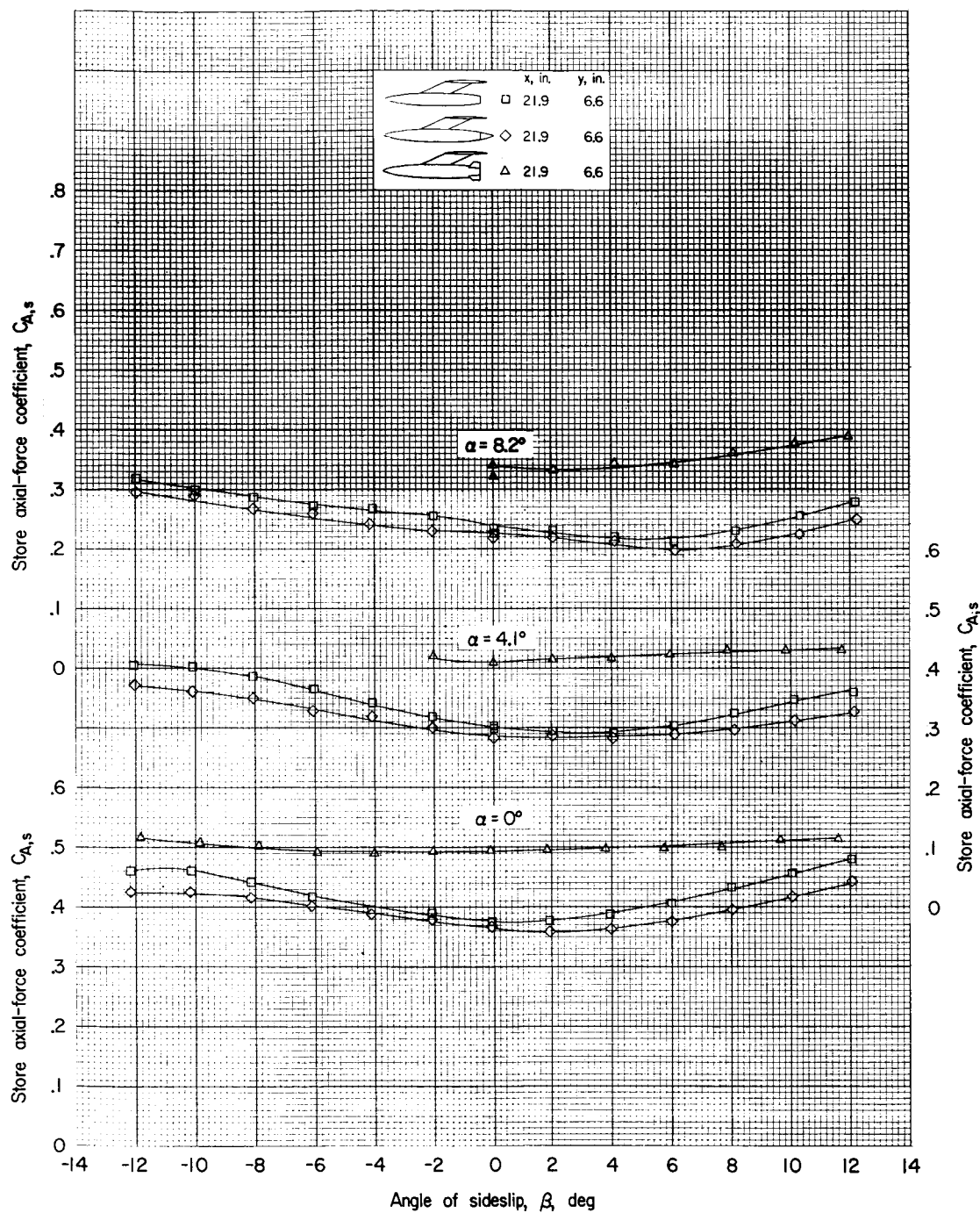
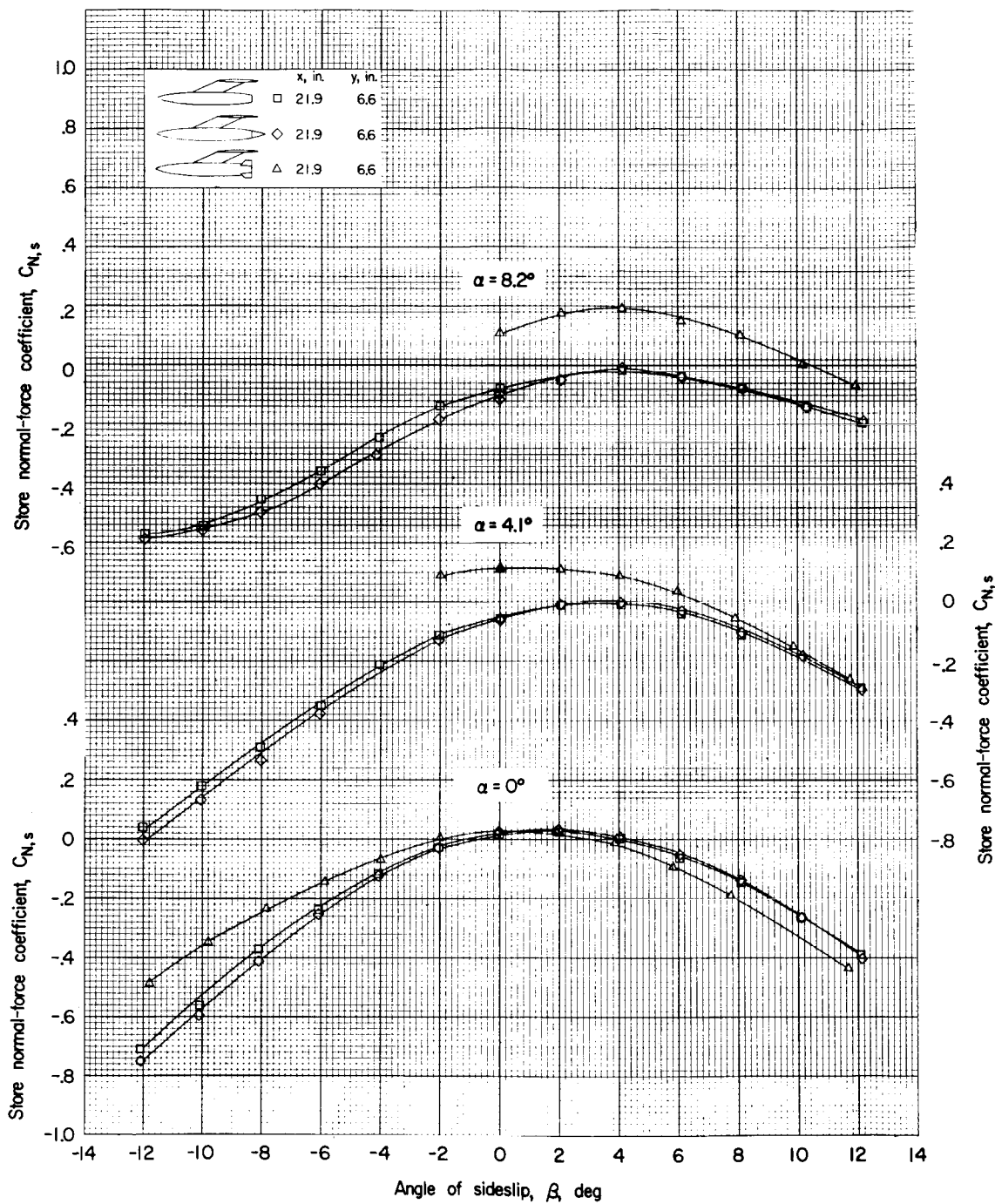
(e) Variation of $C_{n,s}$ with β .

Figure 23.- Concluded.



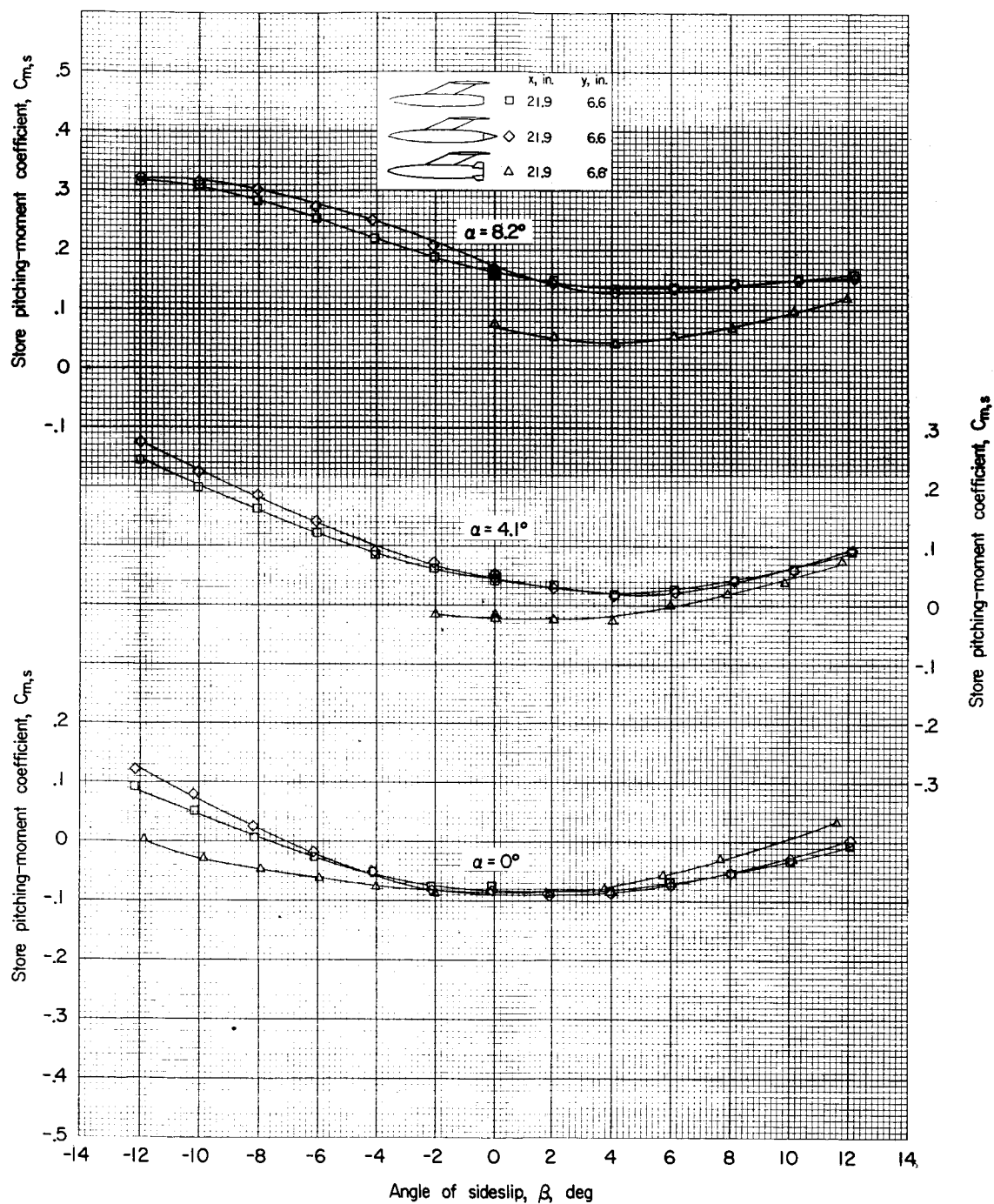
(a) Variation of $C_{A,s}$ with β .

Figure 24.- Effect of store fins and store tail cone on the aerodynamic characteristics of the store in the presence of the wing-fuselage combination.



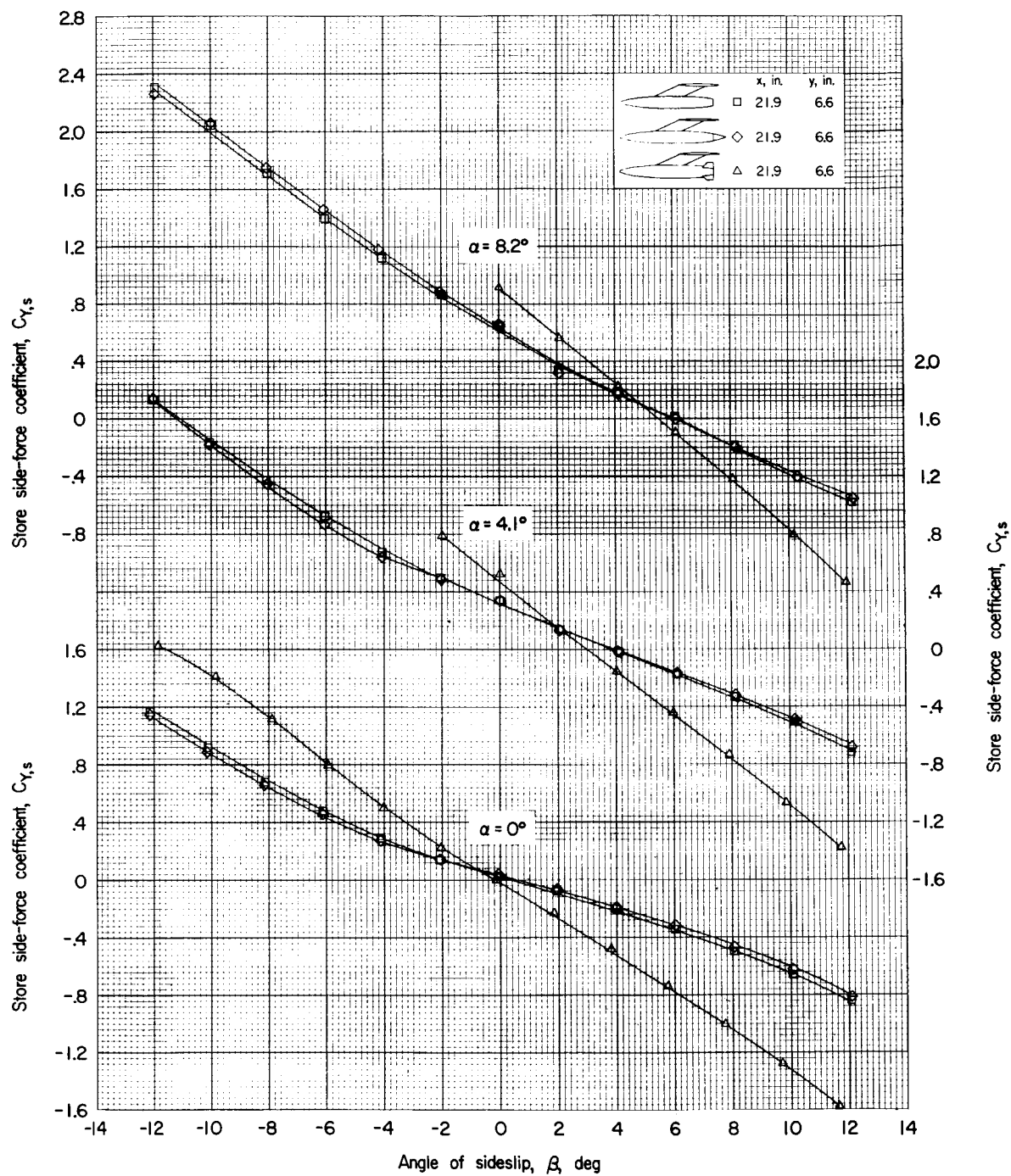
(b) Variation of $C_{N,s}$ with β .

Figure 24.- Continued.



(c) Variation of $C_{m,s}$ with β .

Figure 24.- Continued.



(d) Variation of $C_{Y,s}$ with β .

Figure 24.- Continued.

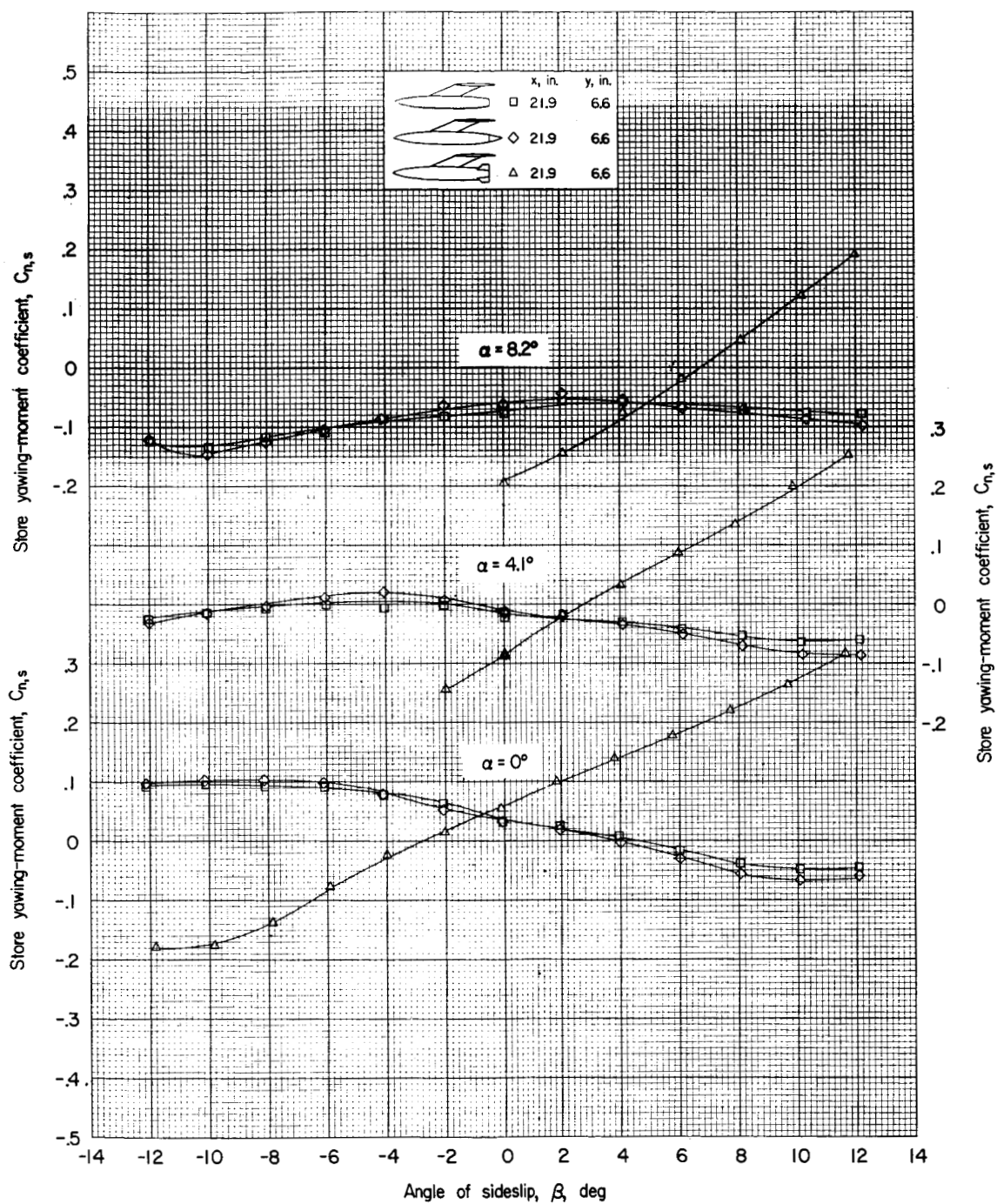
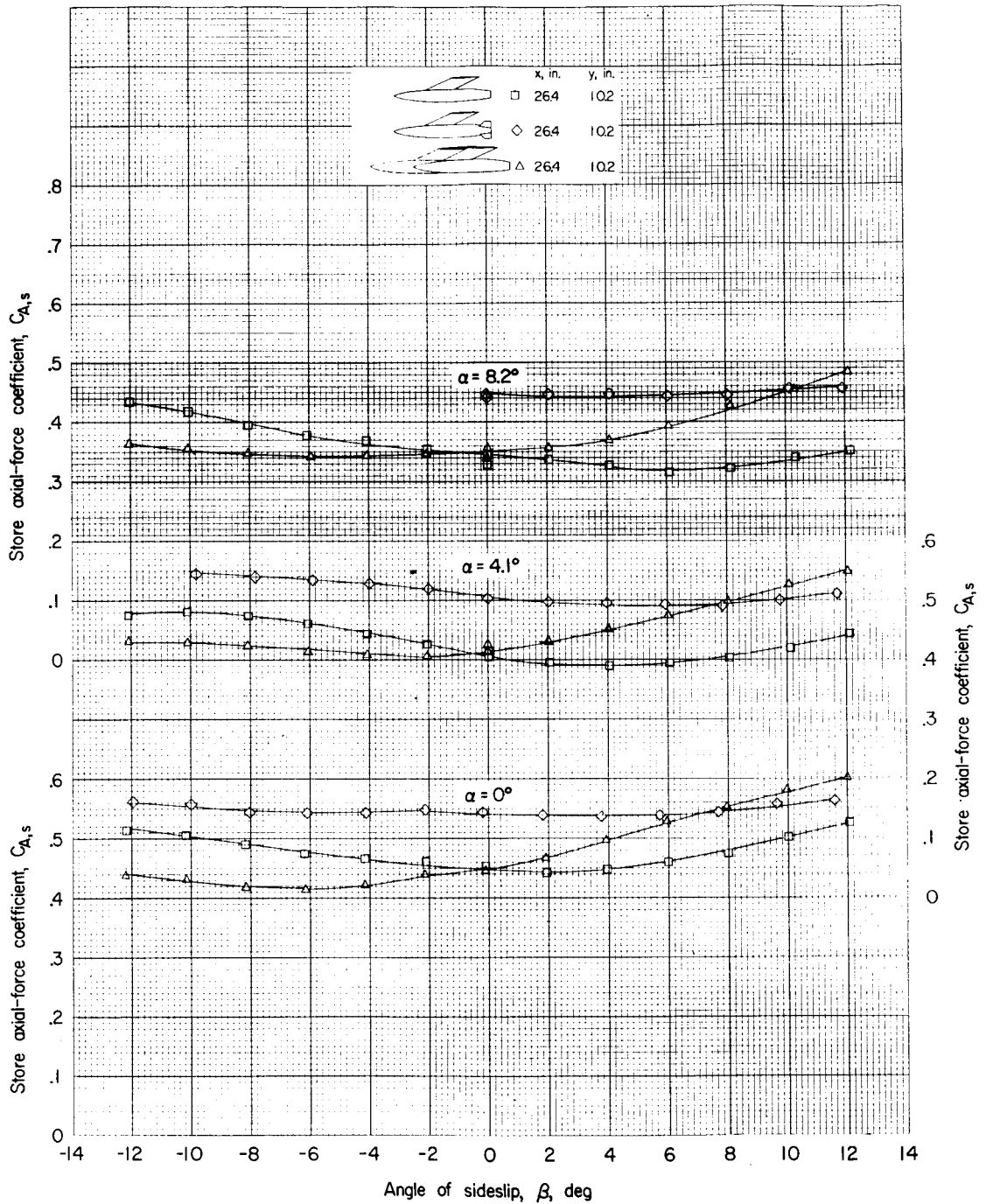
(e) Variation of $C_{n,s}$ with β .

Figure 24.- Concluded.



(a) Variation of $C_{A,s}$ with β .

Figure 25.- Effect of store fins and inboard and outboard store interference on the aerodynamic characteristics of the store in the presence of the wing-fuselage combination.

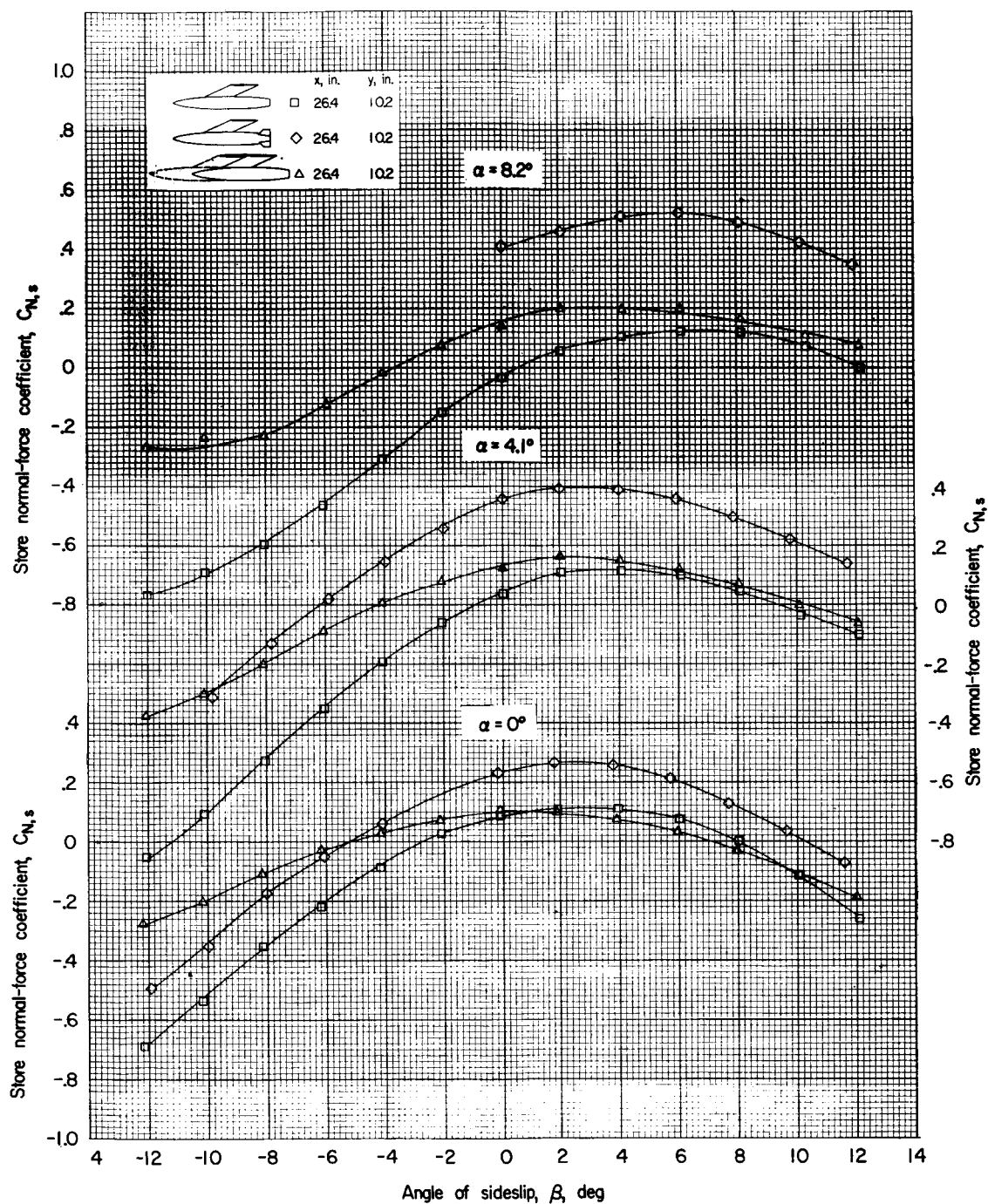
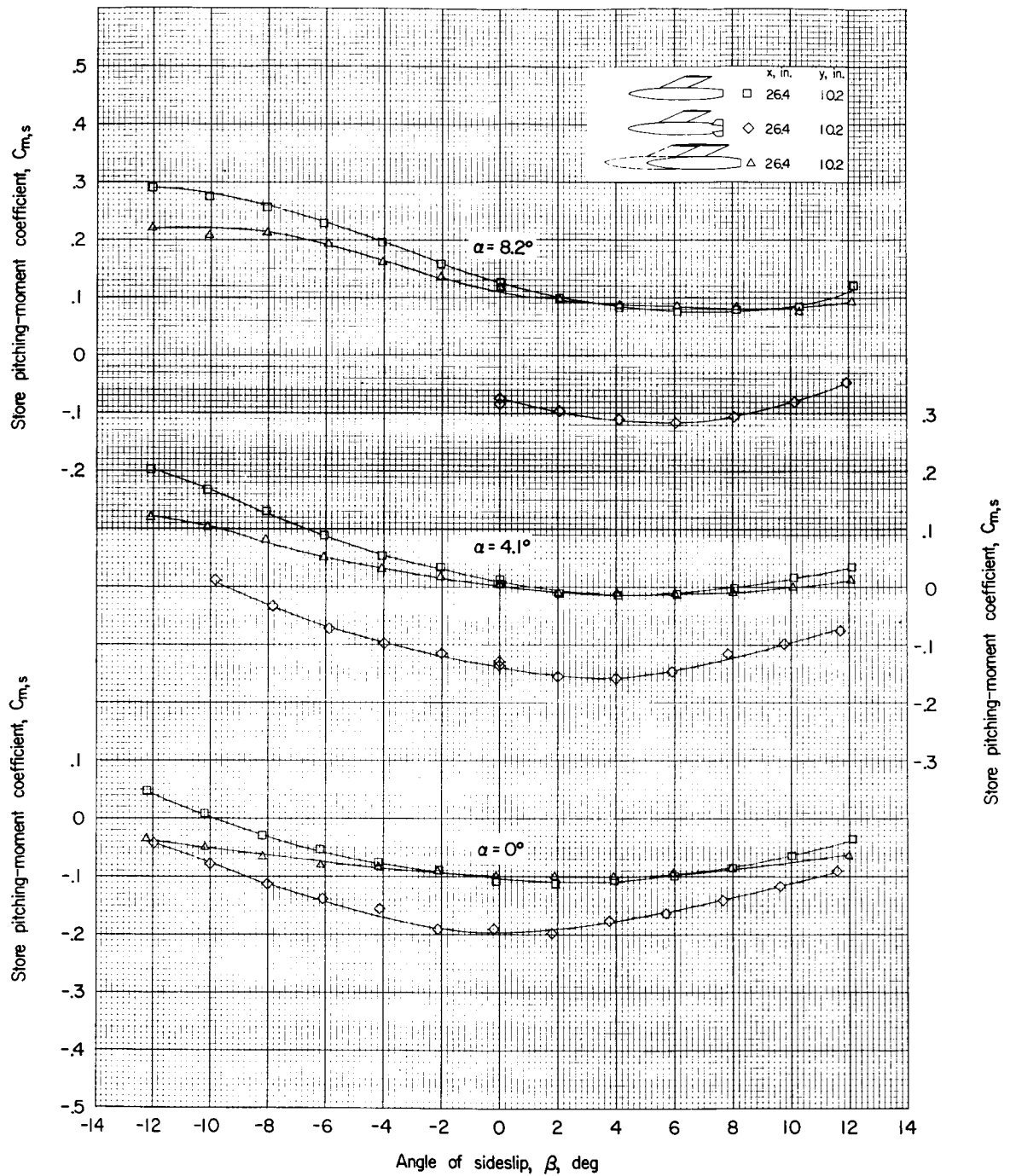
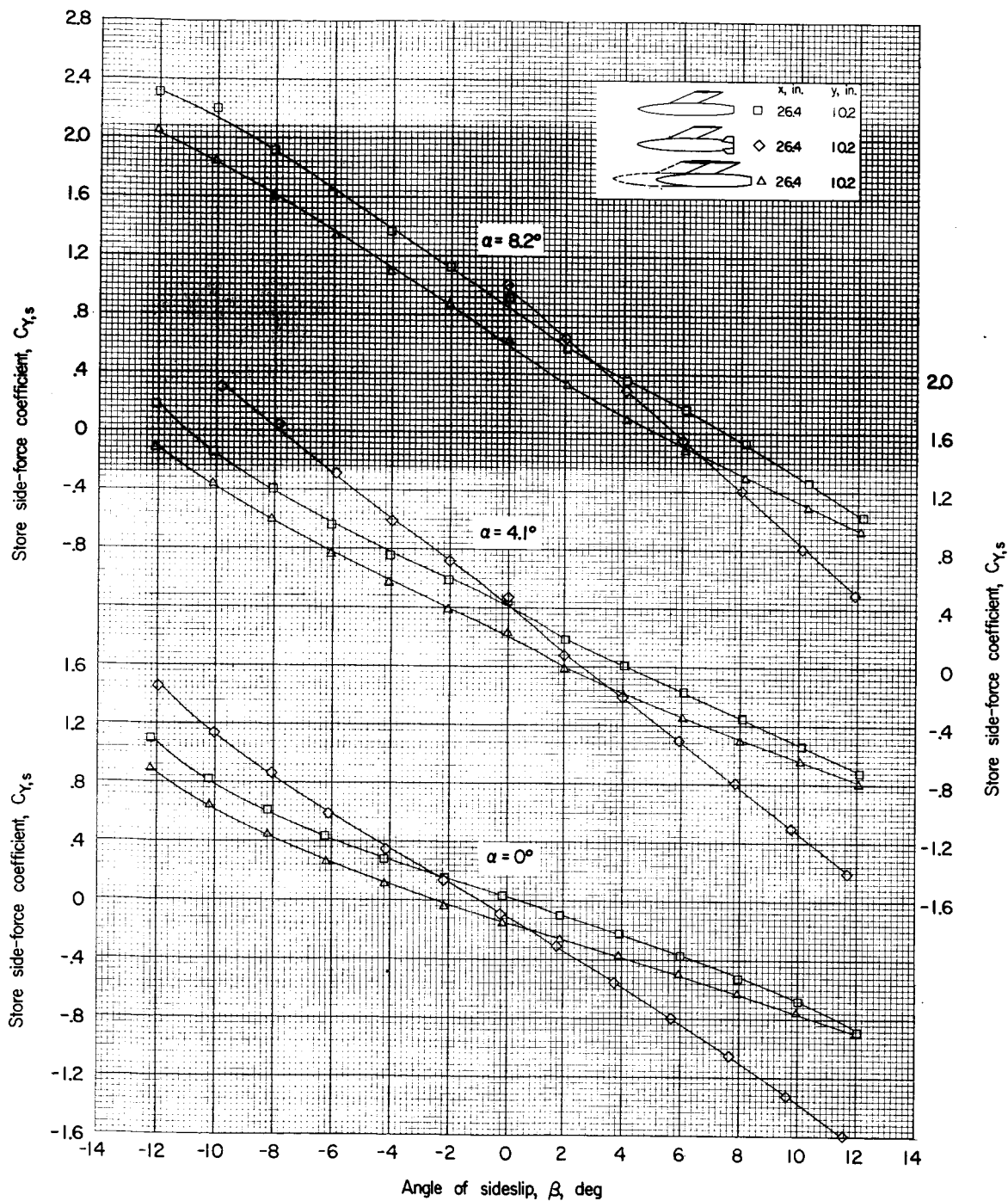
(b) Variation of $C_{N,s}$ with β .

Figure 25.- Continued.



(c) Variation of $C_{m,s}$ with β .

Figure 25.- Continued.



(d) Variation of $C_{Y,s}$ with β .

Figure 25.- Continued.

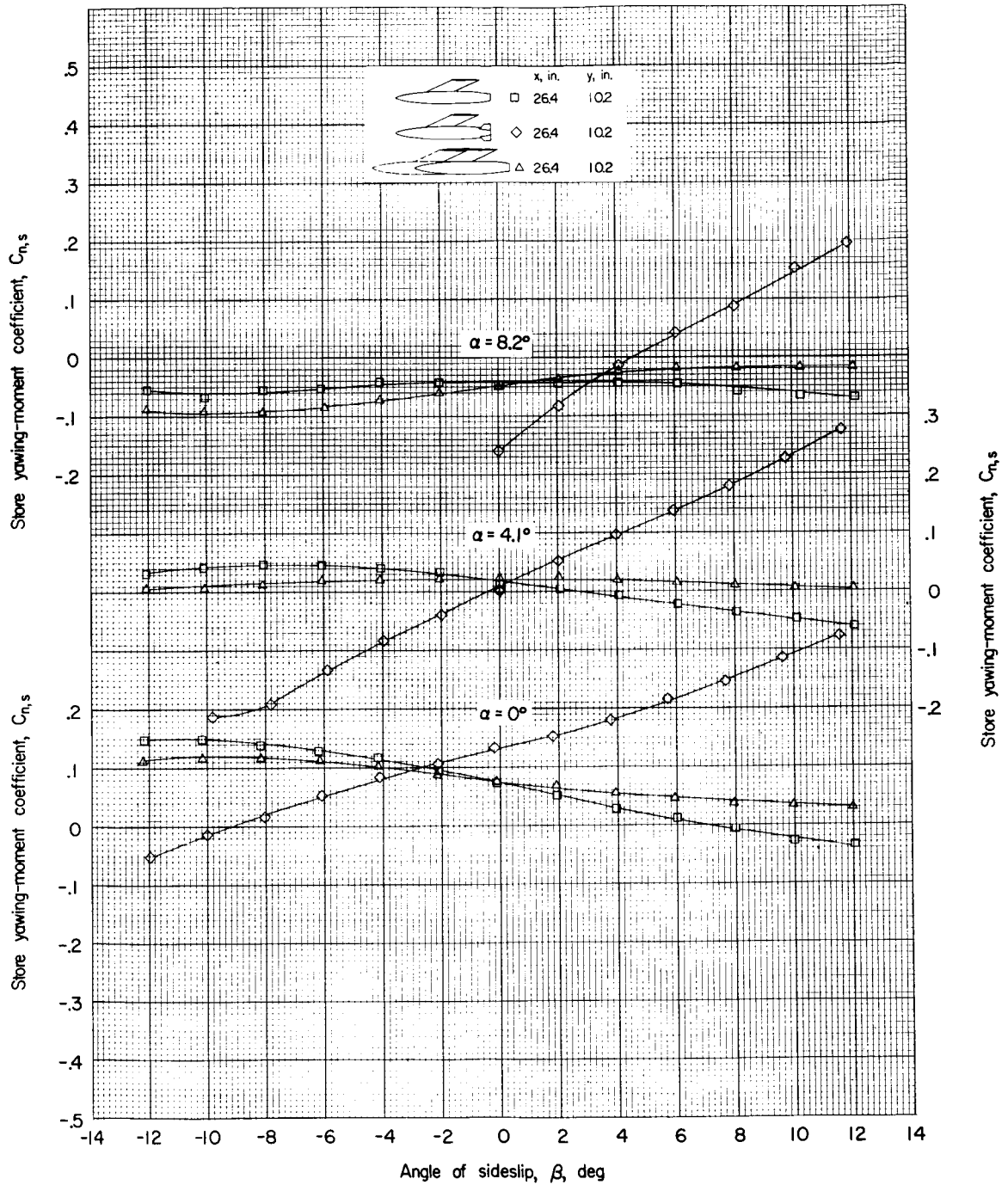
(e) Variation of $C_{n,s}$ with β .

Figure 25.- Concluded.

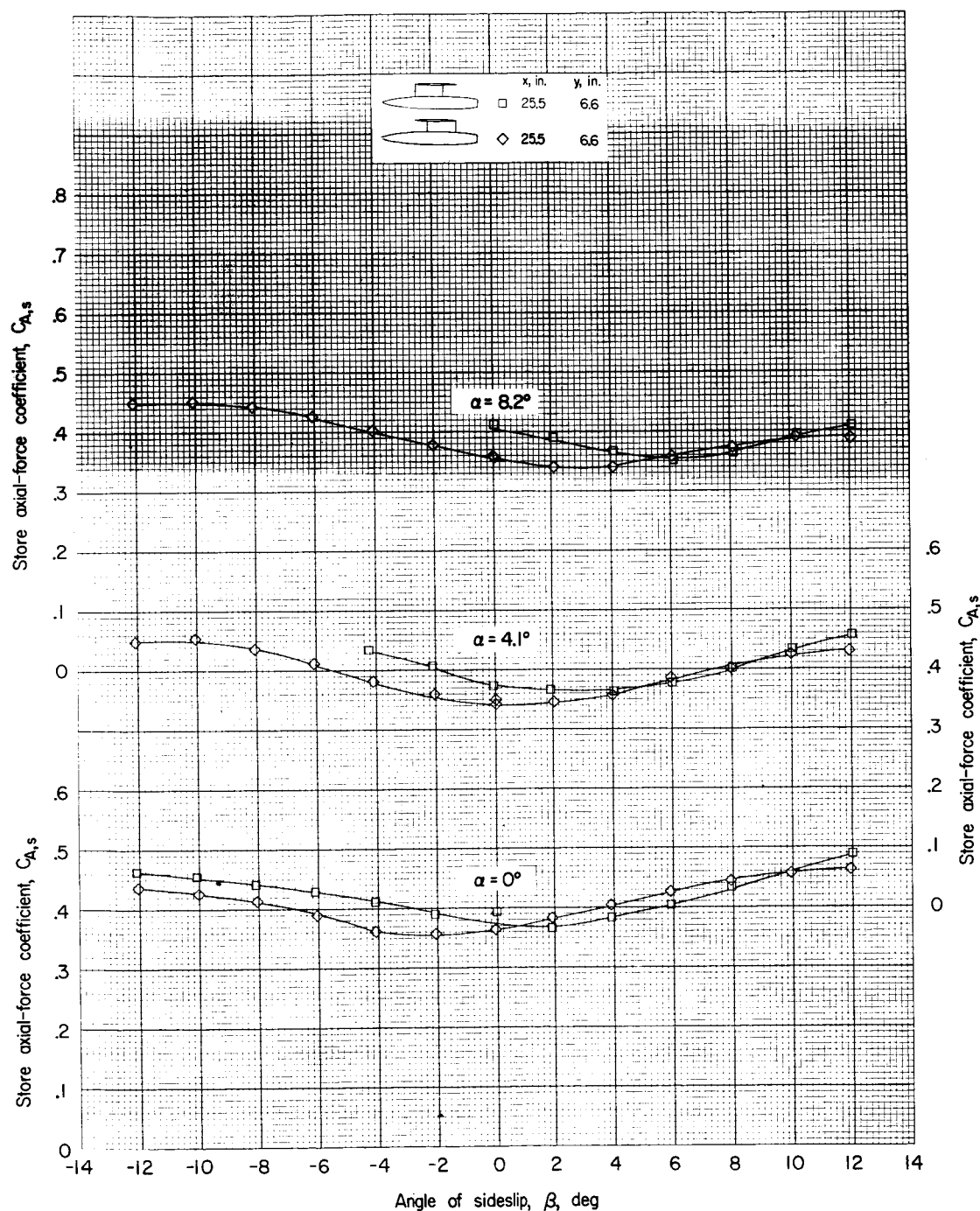
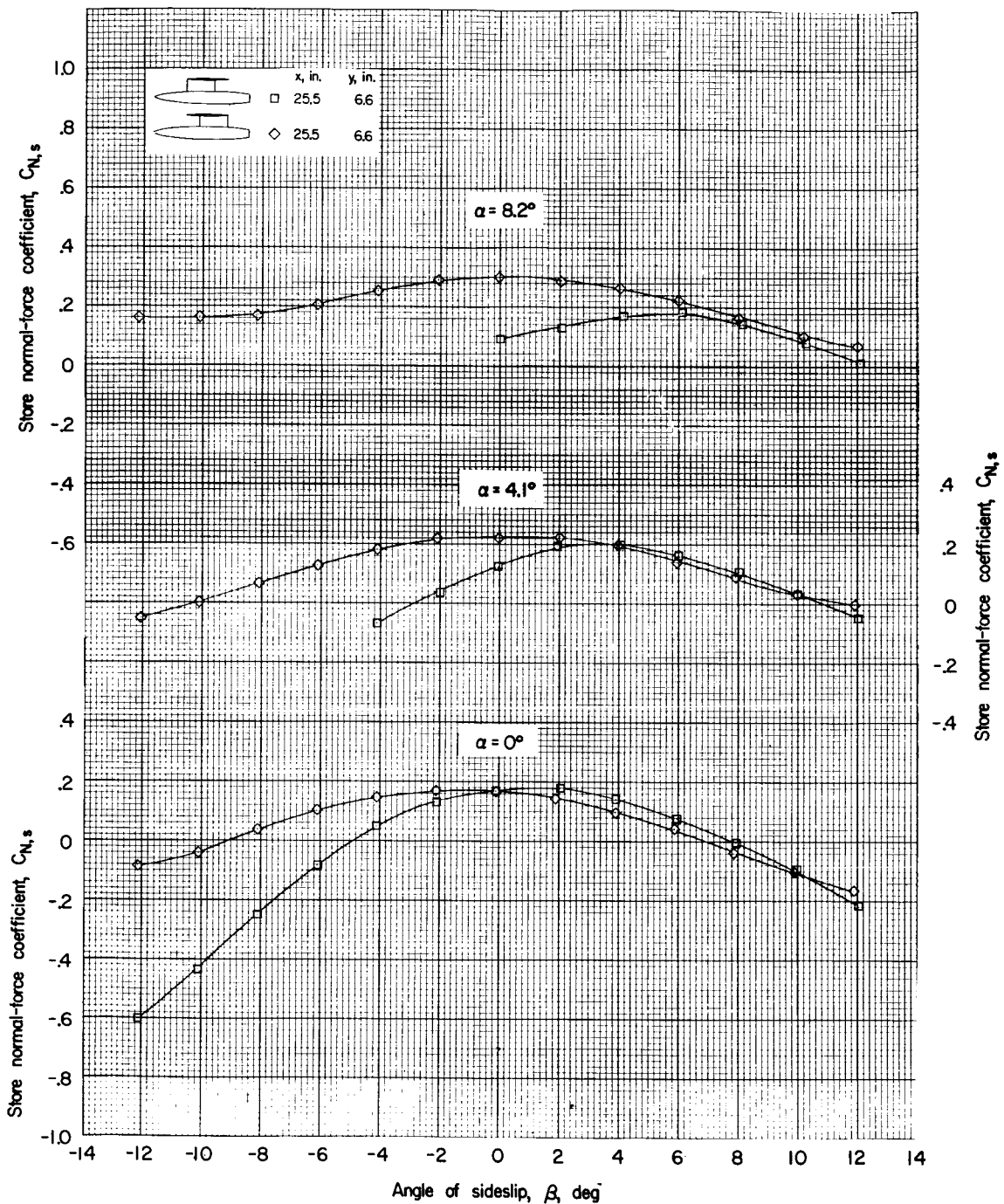
(a) Variation of $C_{A,s}$ with β .

Figure 26.- Effect of pylon location on the aerodynamic characteristics of the store in the presence of the wing-fuselage combination.



(b) Variation of $C_{N,s}$ with β .

Figure 26.- Continued.

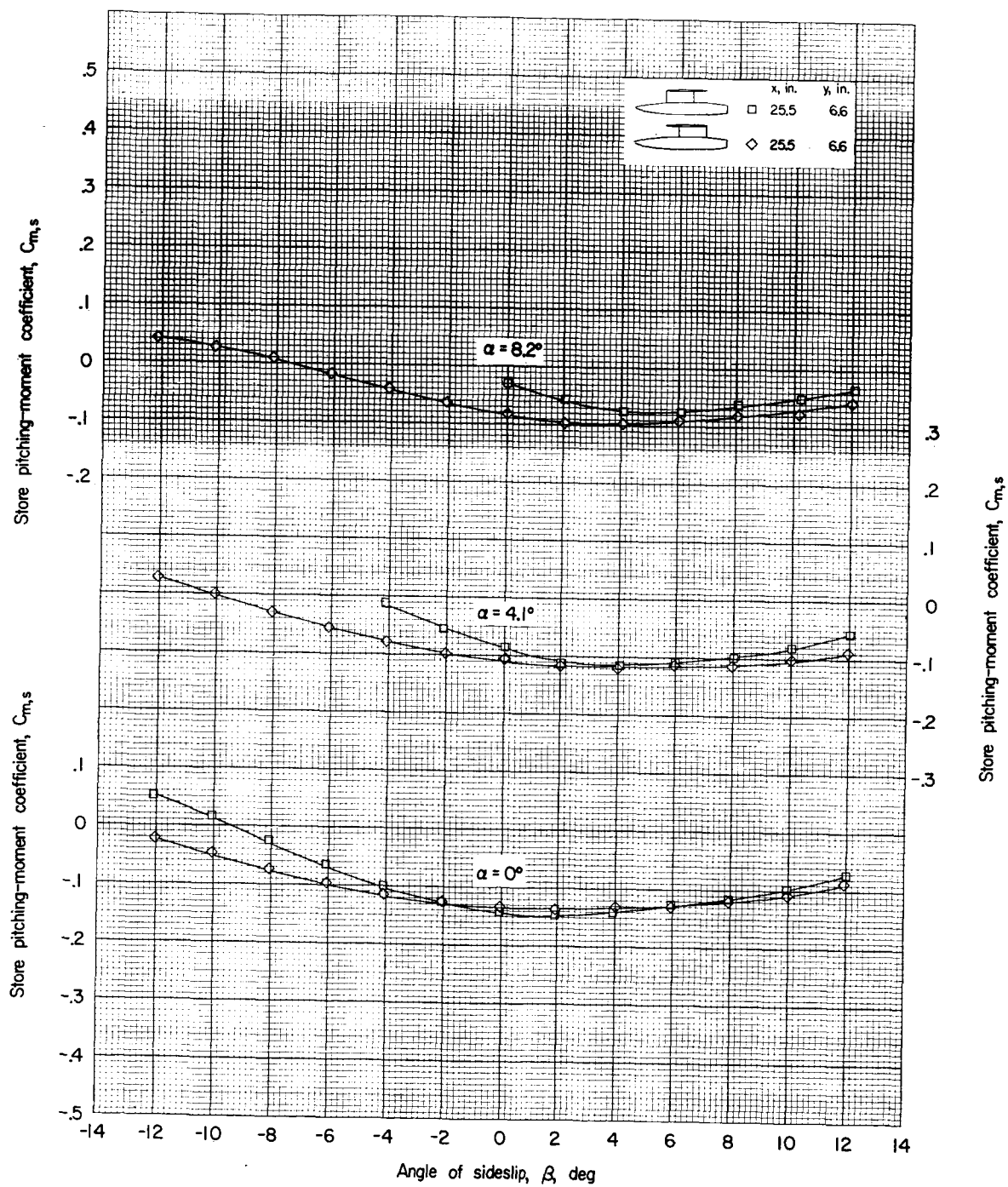
(c) Variation of $C_{m,s}$ with β .

Figure 26.- Continued.

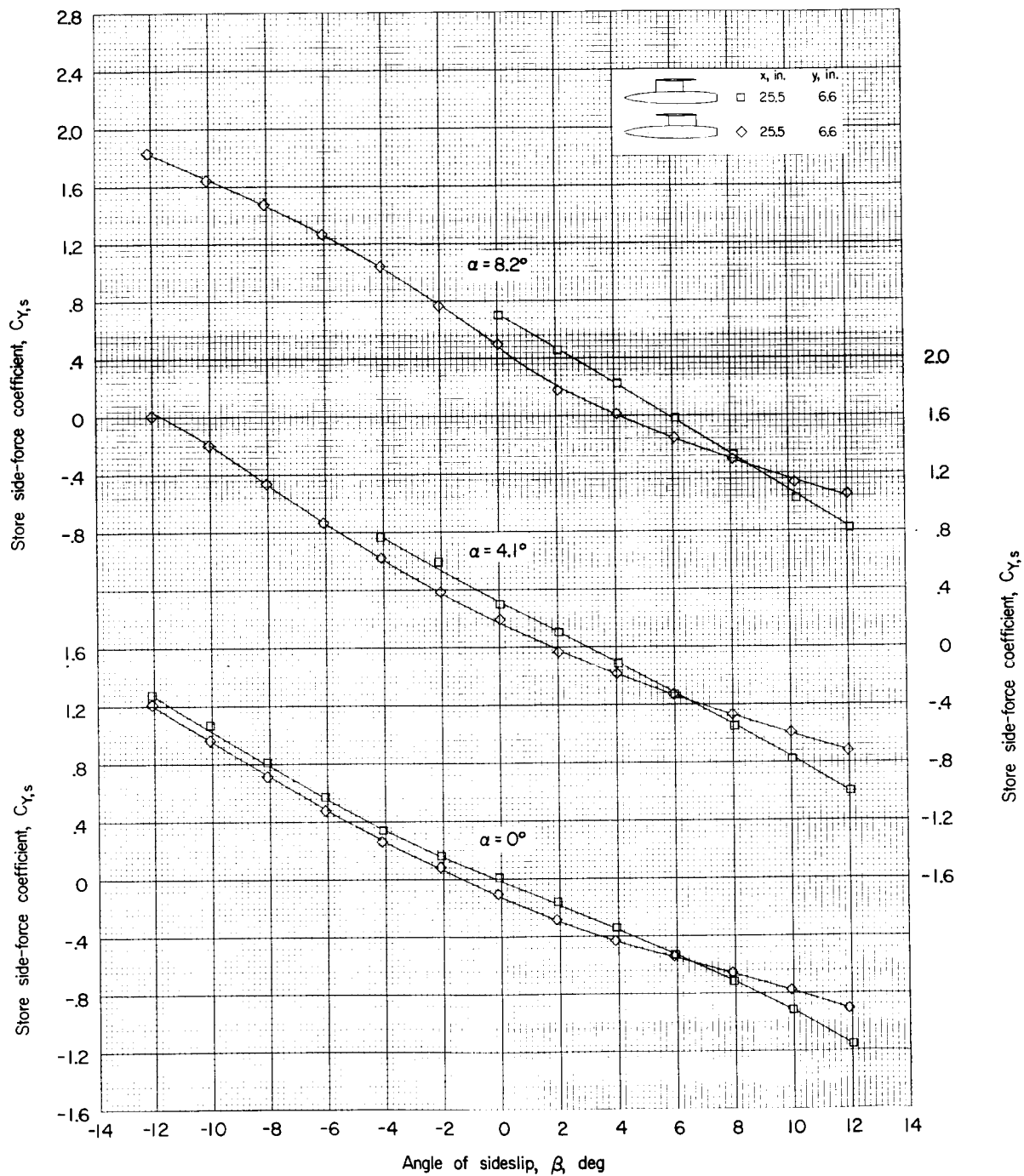
(d) Variation of $C_{Y,s}$ with β .

Figure 26.- Continued.

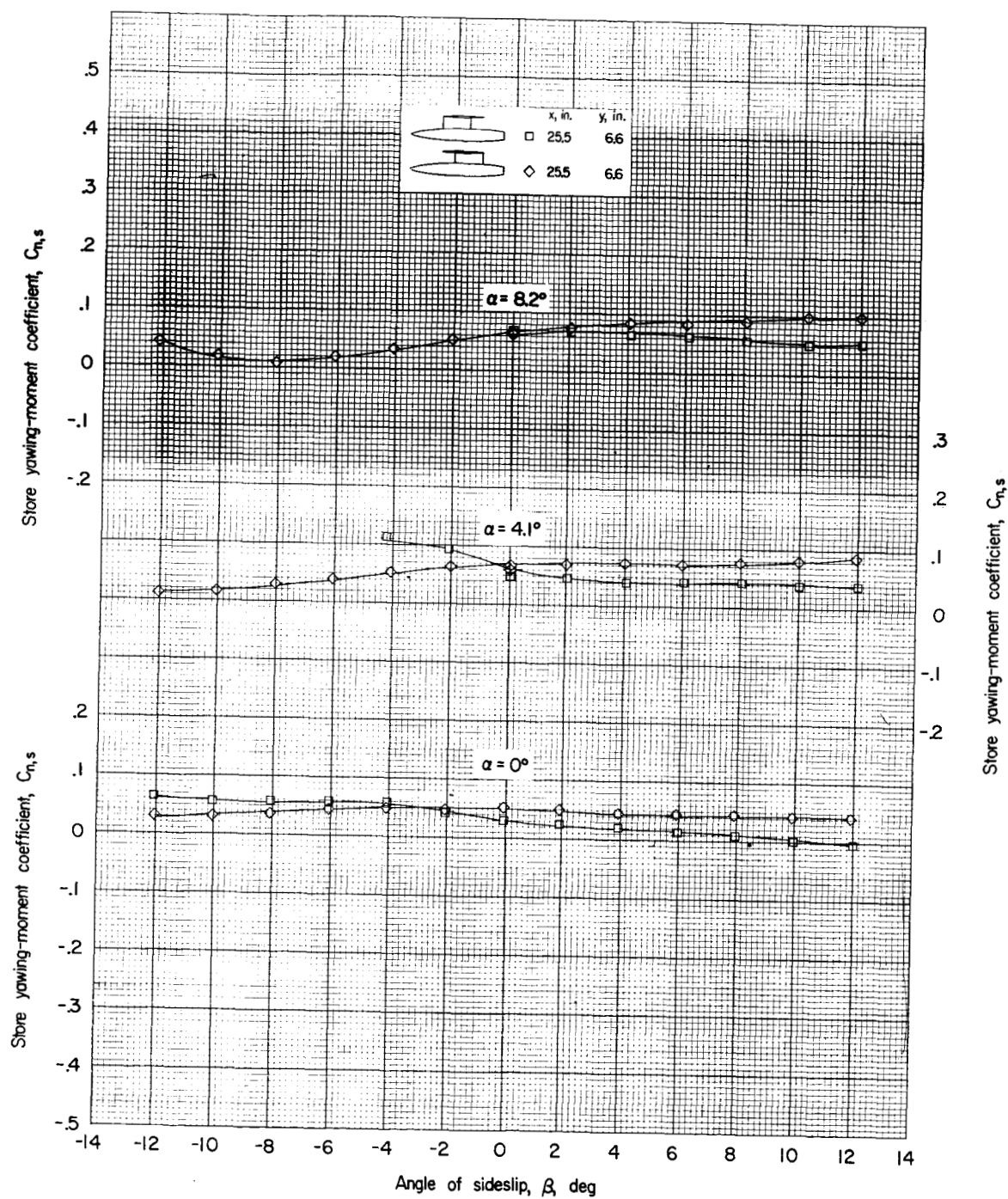
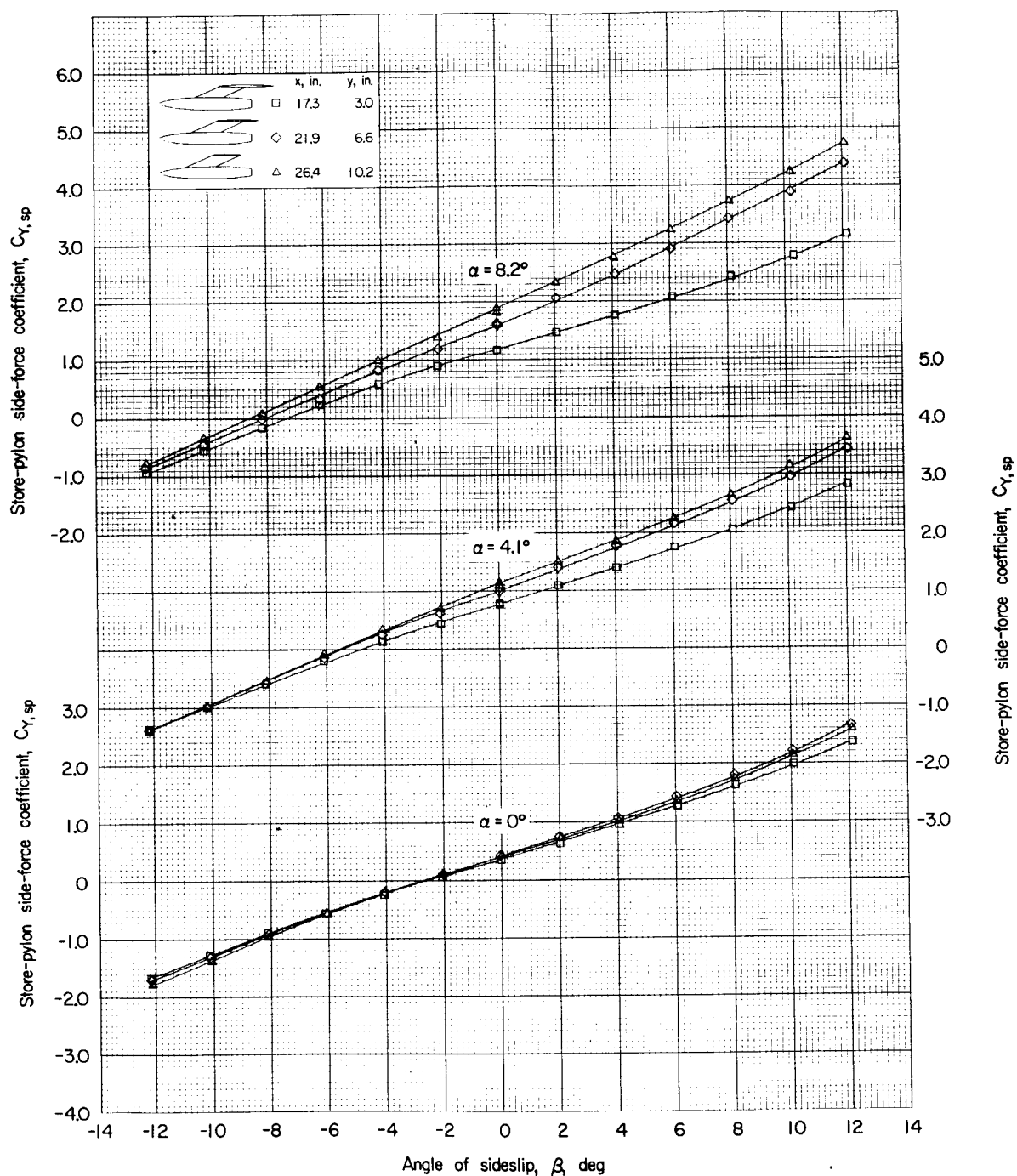
(e) Variation of $C_{n,s}$ with β .

Figure 26.- Concluded.



(a) Variation of $C_{Y,sp}$ with β .

Figure 27.- Aerodynamic characteristics of the store-pylon combination in the presence of the wing-fuselage combination for three spanwise store positions.

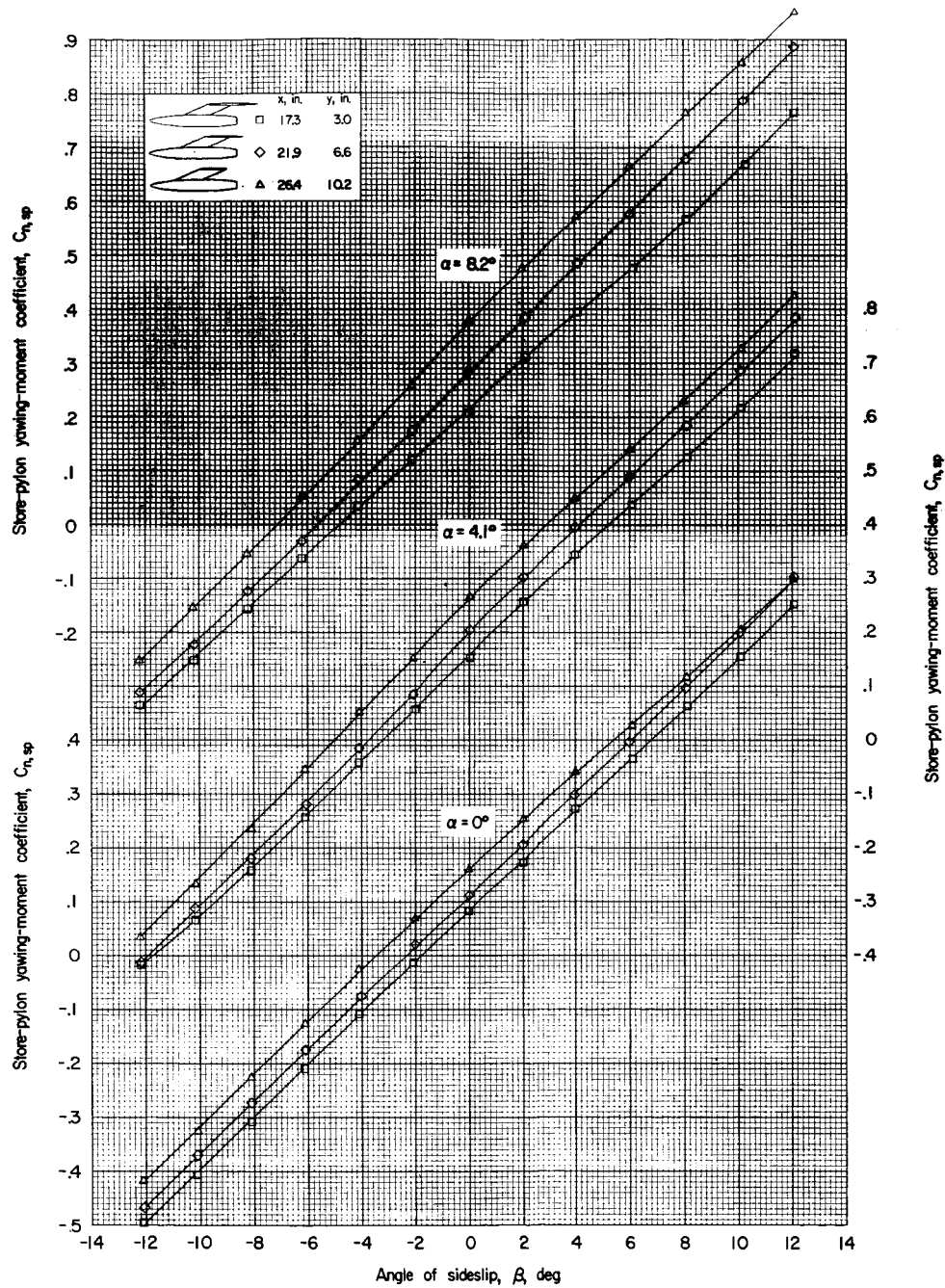
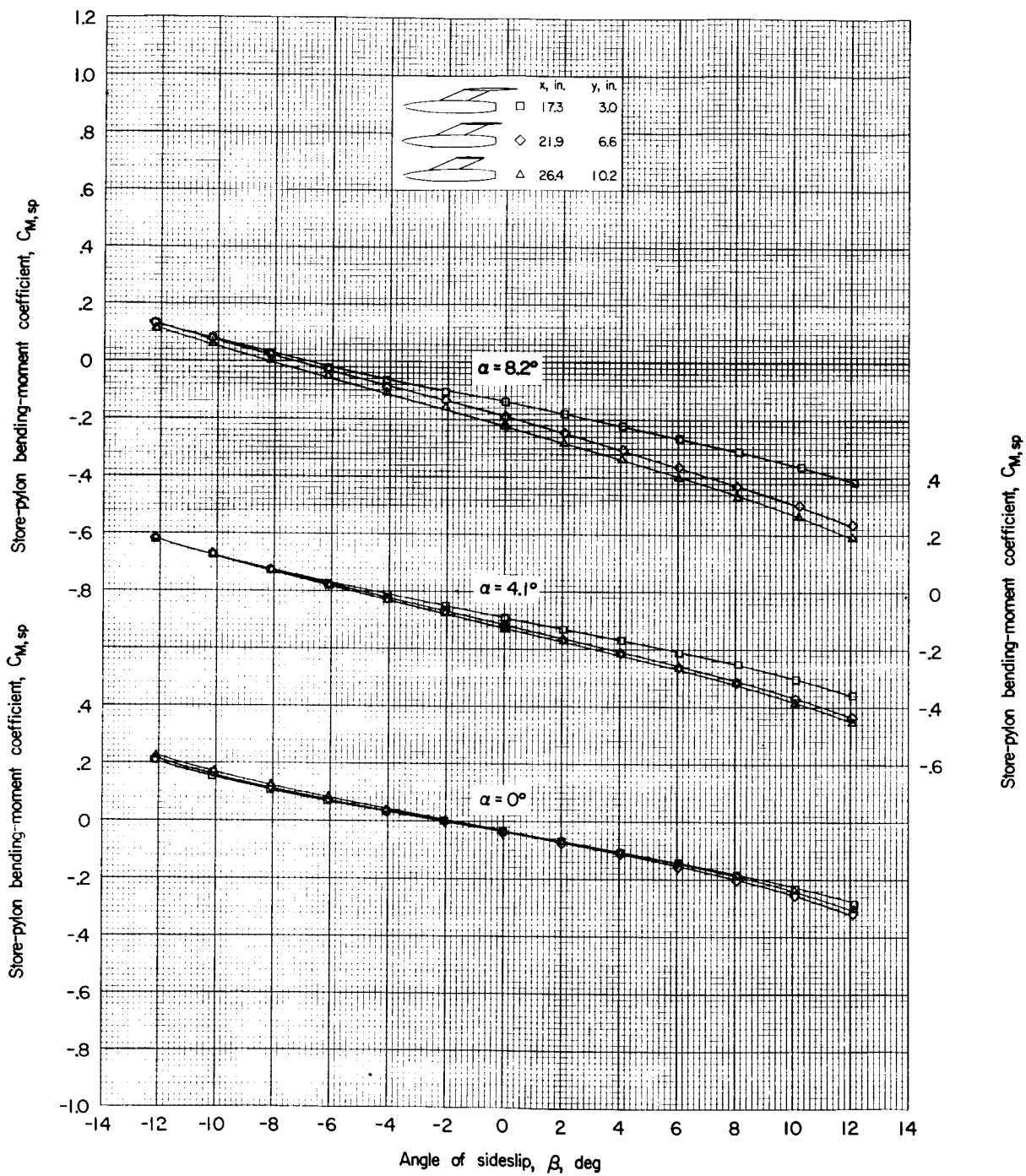
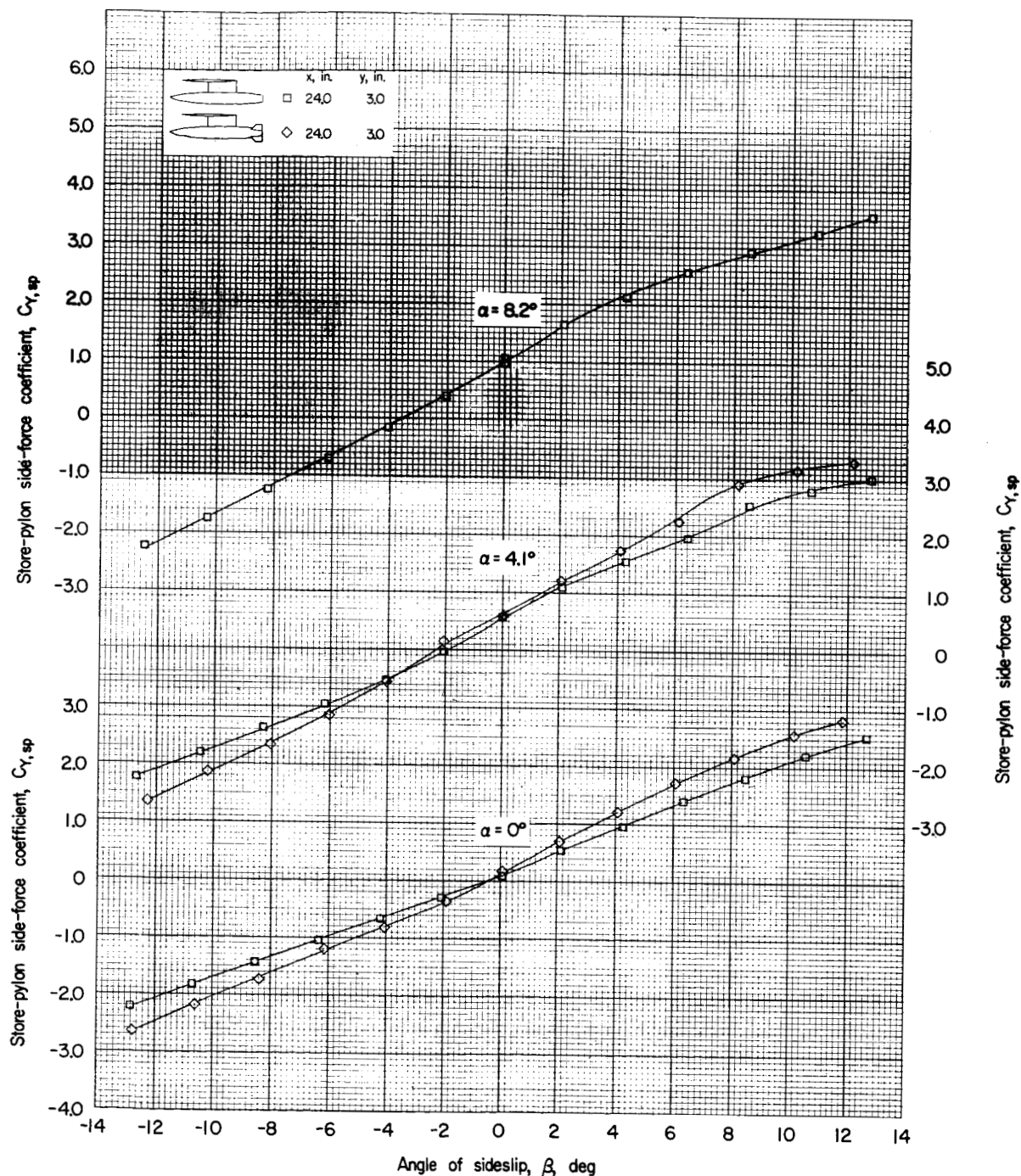
(b) Variation of $C_{n,sp}$ with β .

Figure 27.- Continued.



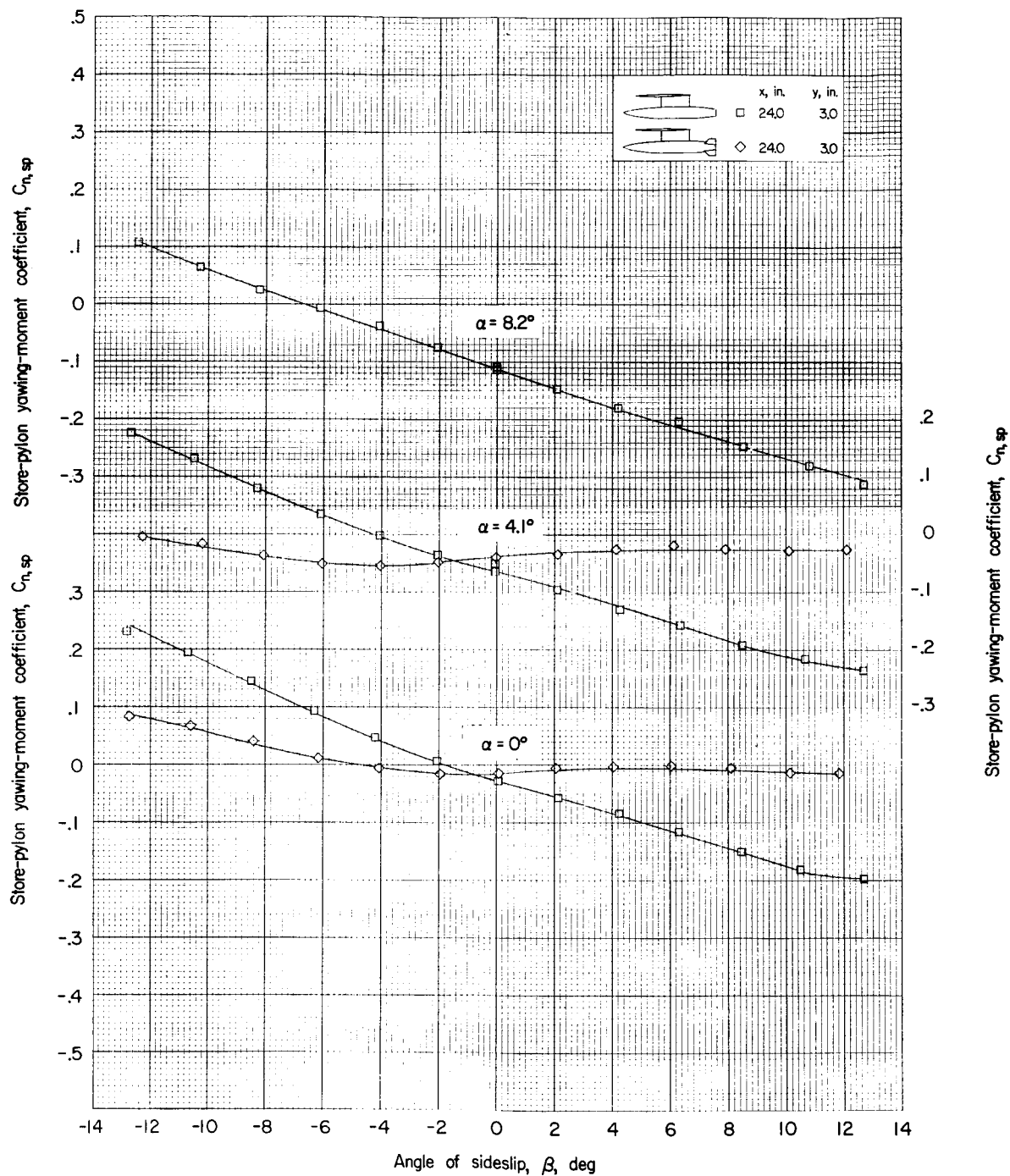
(c) Variation of $C_{M,sp}$ with β .

Figure 27.- Concluded.



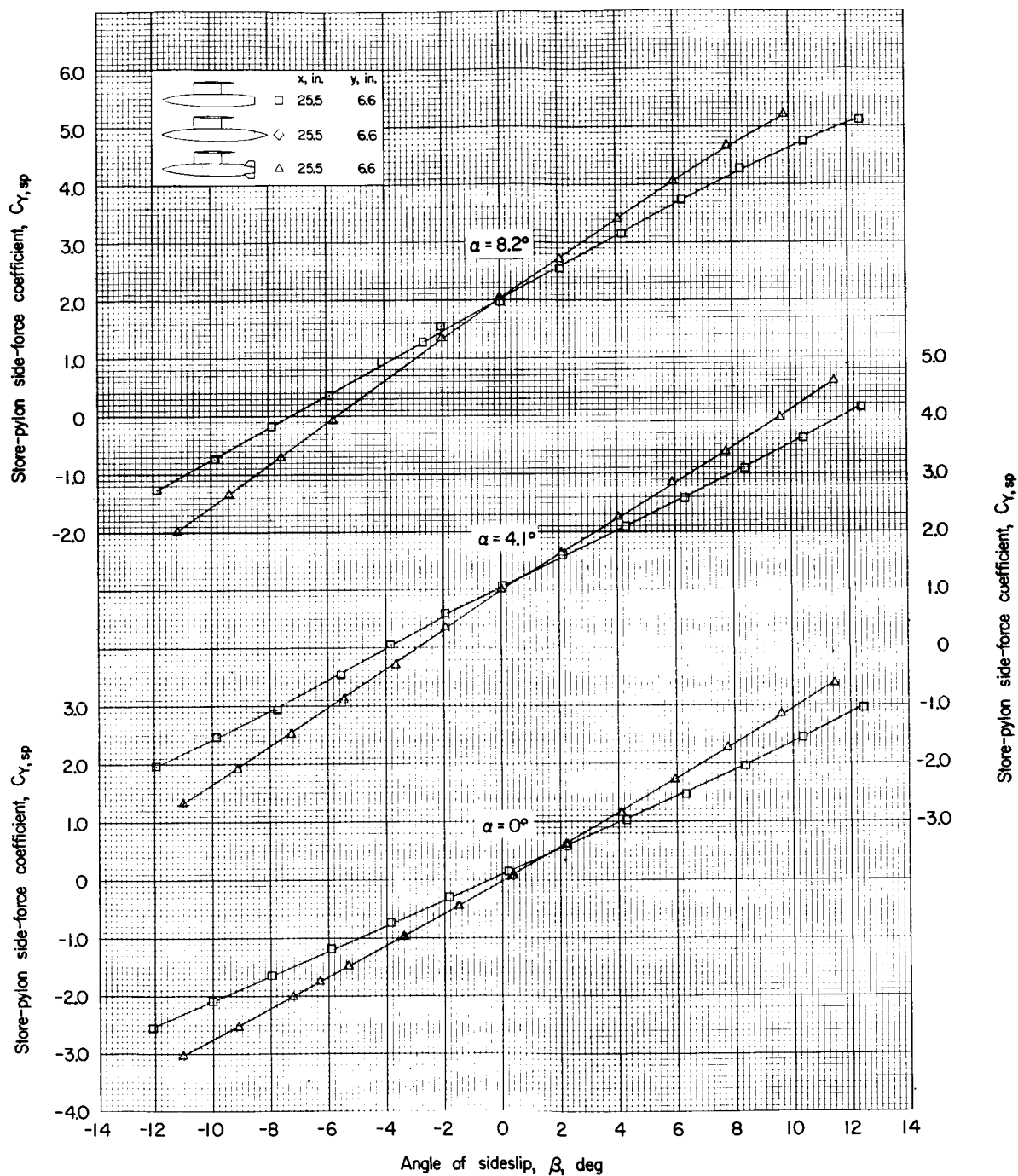
(a) Variation of $C_{Y,sp}$ with β .

Figure 28.- Effect of store fins on the aerodynamic characteristics of the store-pylon combination in the presence of the wing-fuselage combination.



(b) Variation of $C_{n,sp}$ with β .

Figure 28.- Continued.



(a) Variation of $C_{Y,sp}$ with β .

Figure 29.- Effect of store fins and store tail cone on the aerodynamic characteristics of the store-pylon combination in the presence of the wing-fuselage combination.

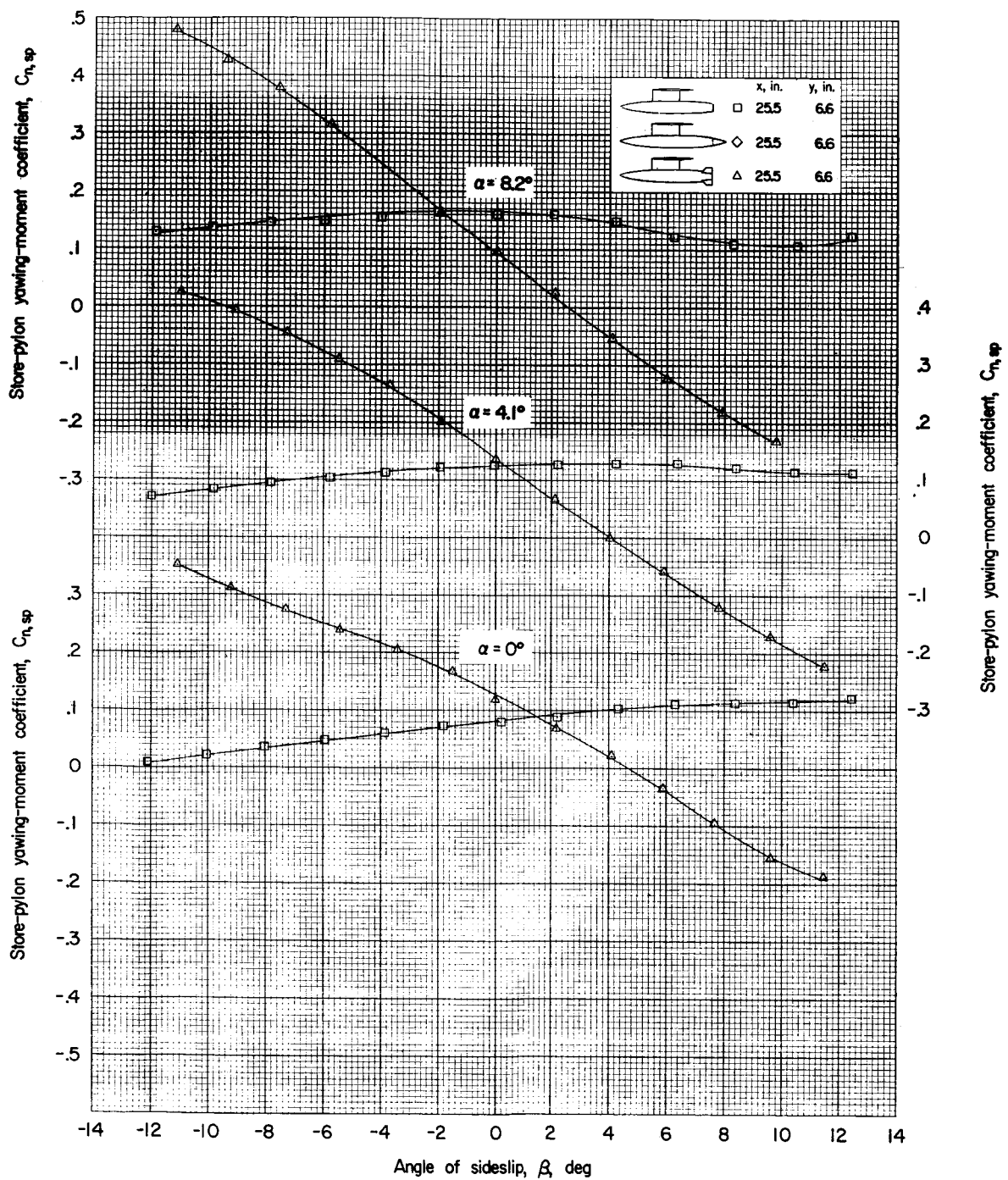
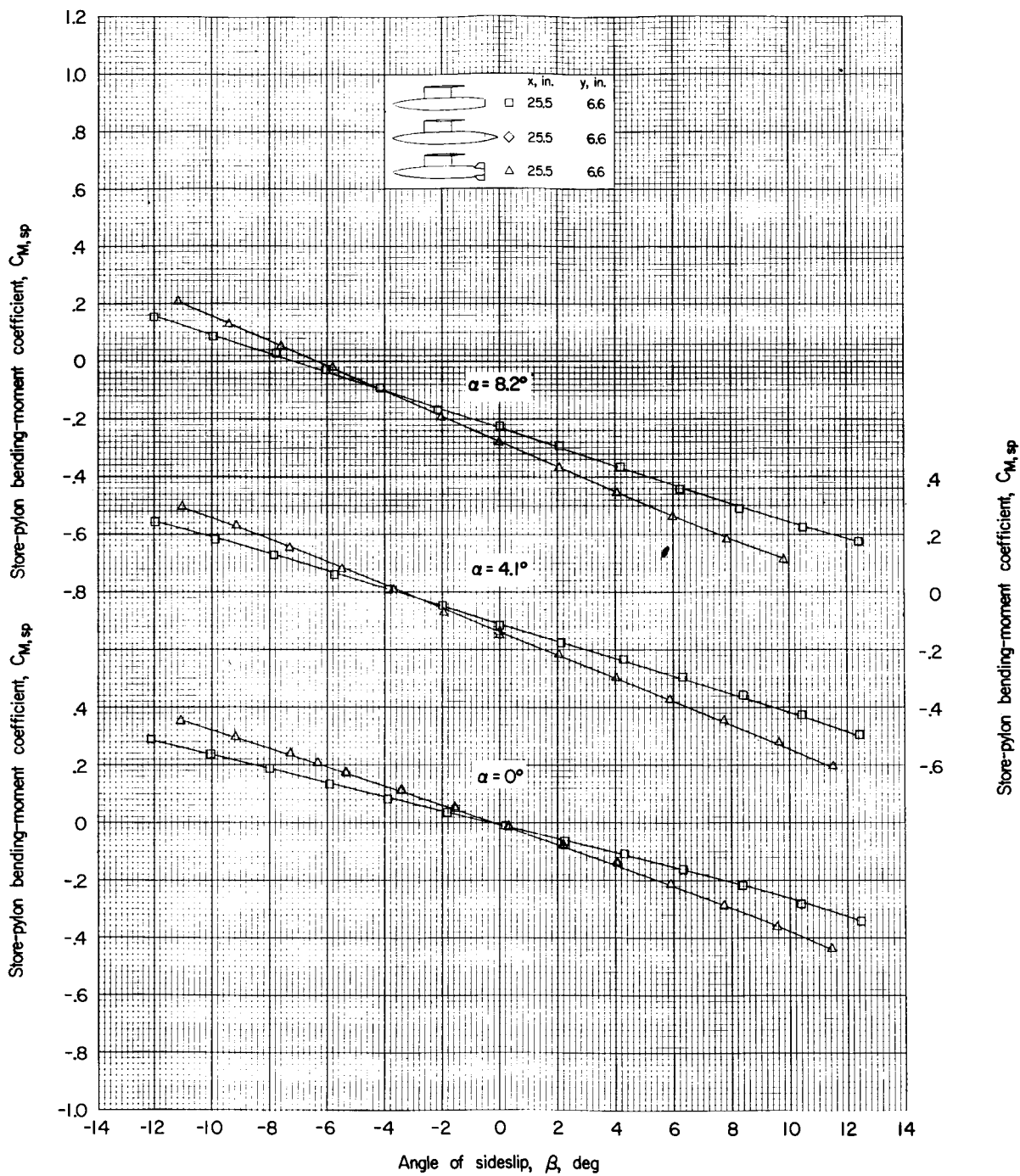
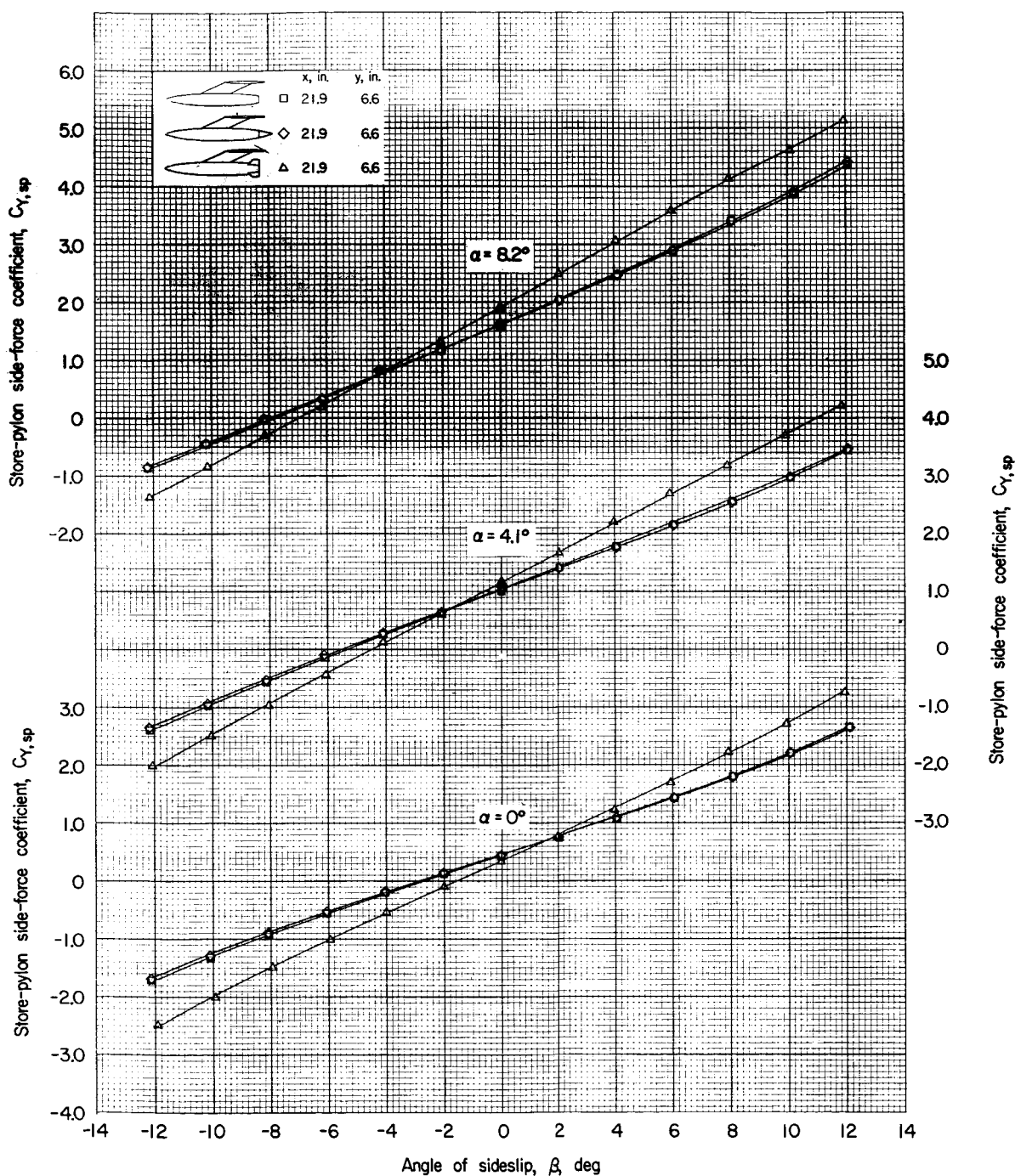


Figure 29.- Continued.



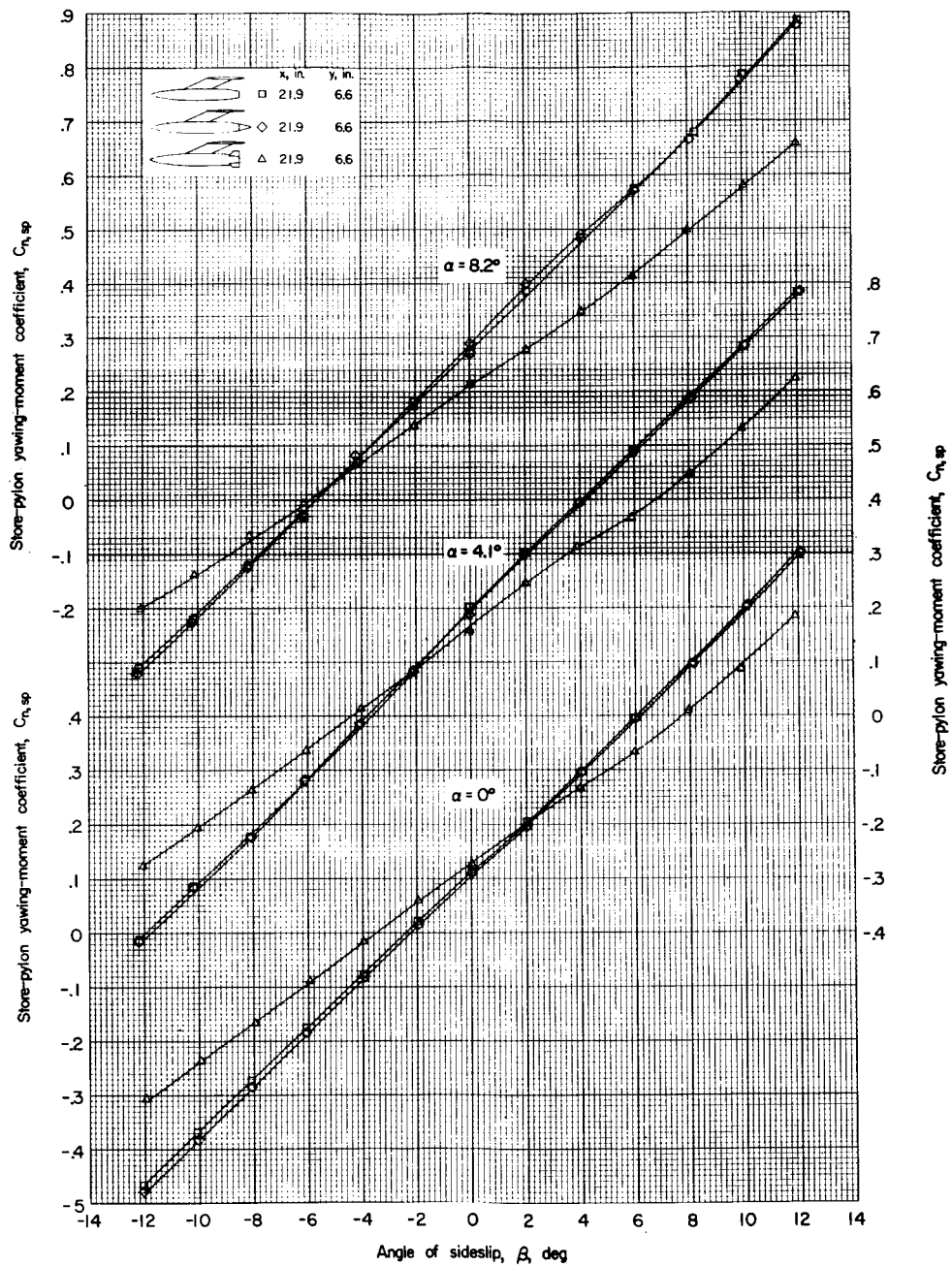
(c) Variation of $C_{M,sp}$ with β .

Figure 29.- Concluded.



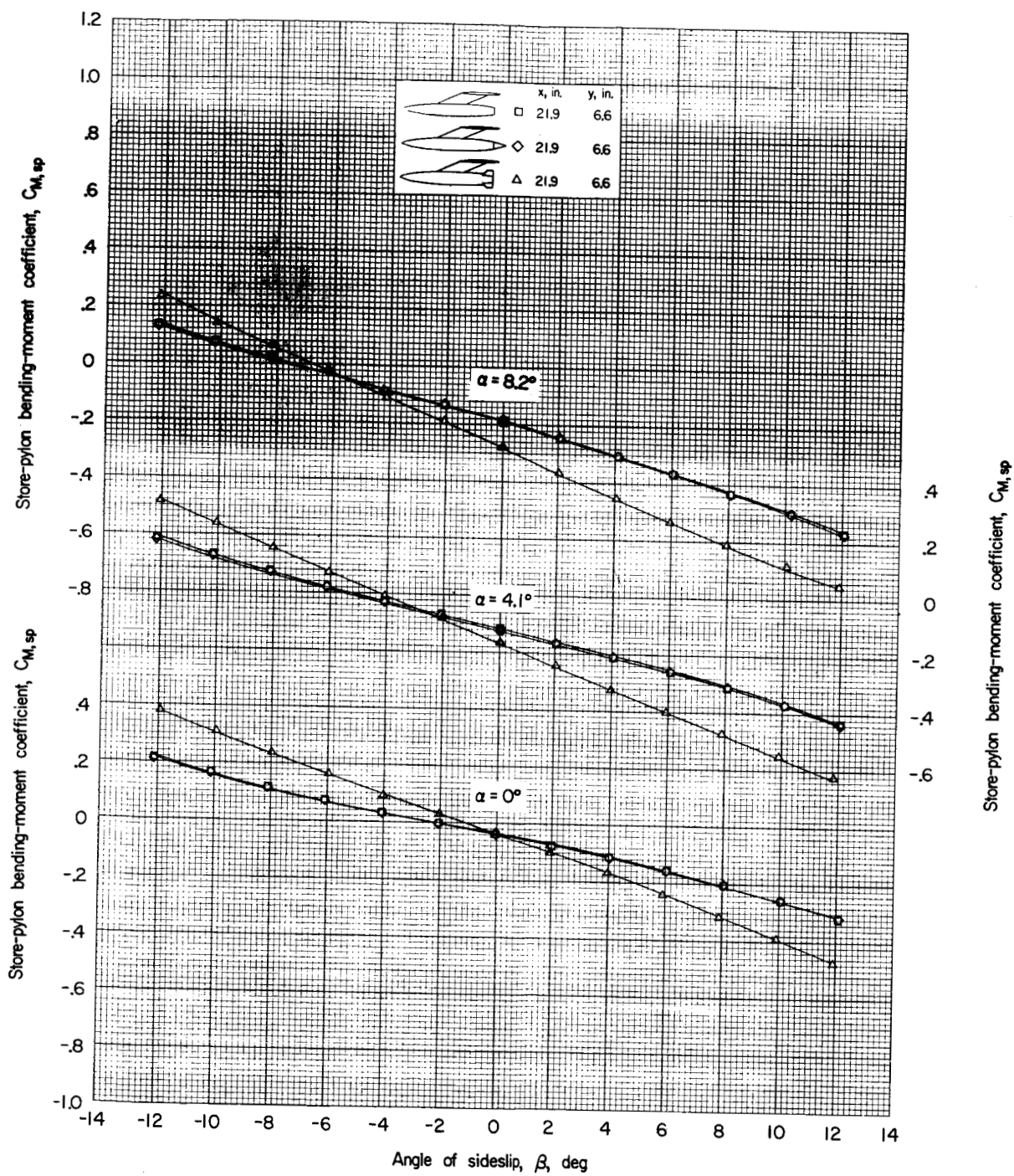
(a) Variation of $C_{Y,sp}$ with β .

Figure 30.- Effect of store fins and store tail cone on the aerodynamic characteristics of the store-pylon combination in the presence of the wing-fuselage combination.

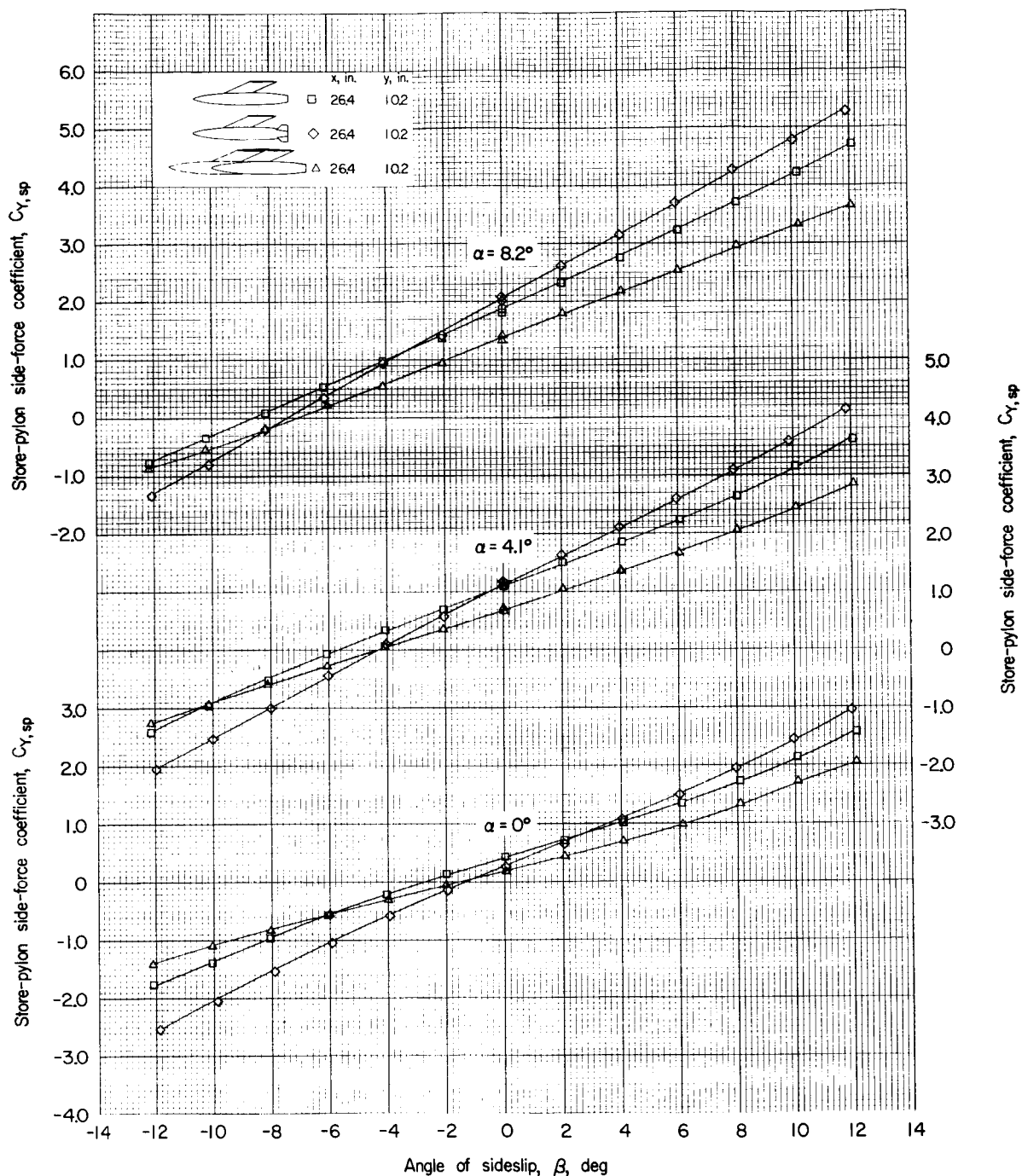


(b) Variation of $C_{n,sp}$ with β .

Figure 30.- Continued.

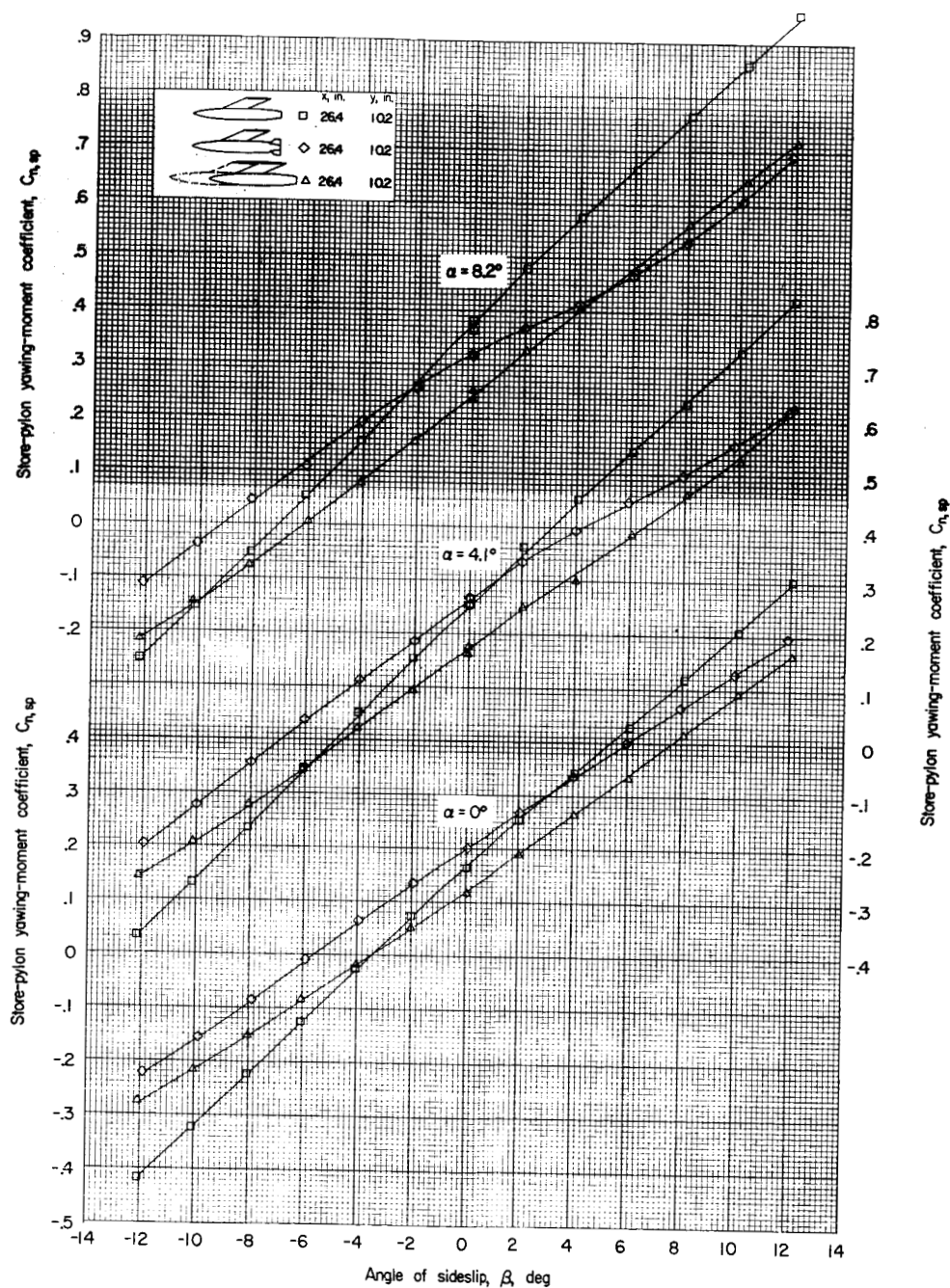


(c) Variation of $C_{M,sp}$ with β .

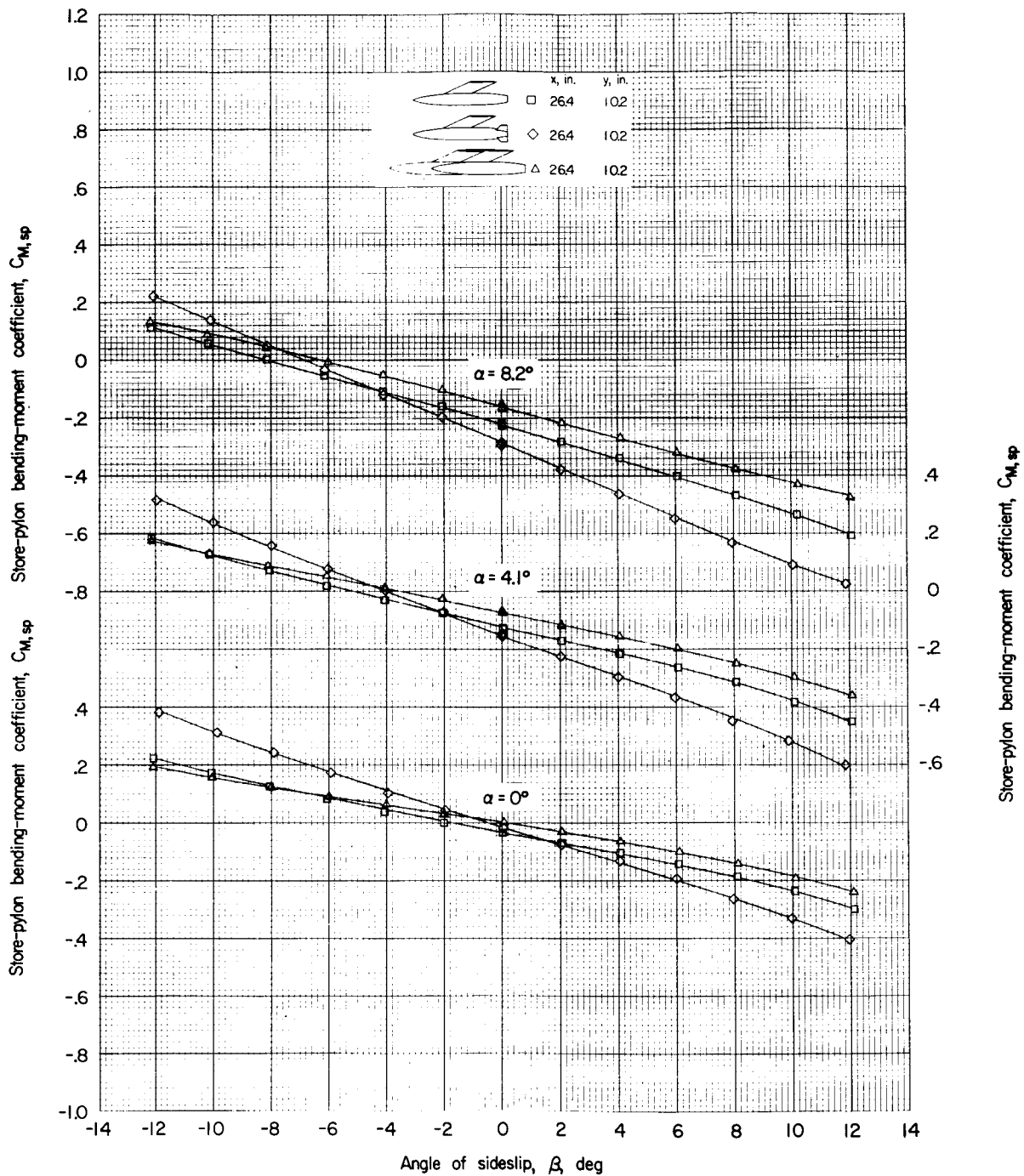


(a) Variation of $C_{Y,sp}$ with β .

Figure 31.- Effect of store fins and inboard and outboard store interference on the aerodynamic characteristics of the store-pylon combination in the presence of the wing-fuselage combination.

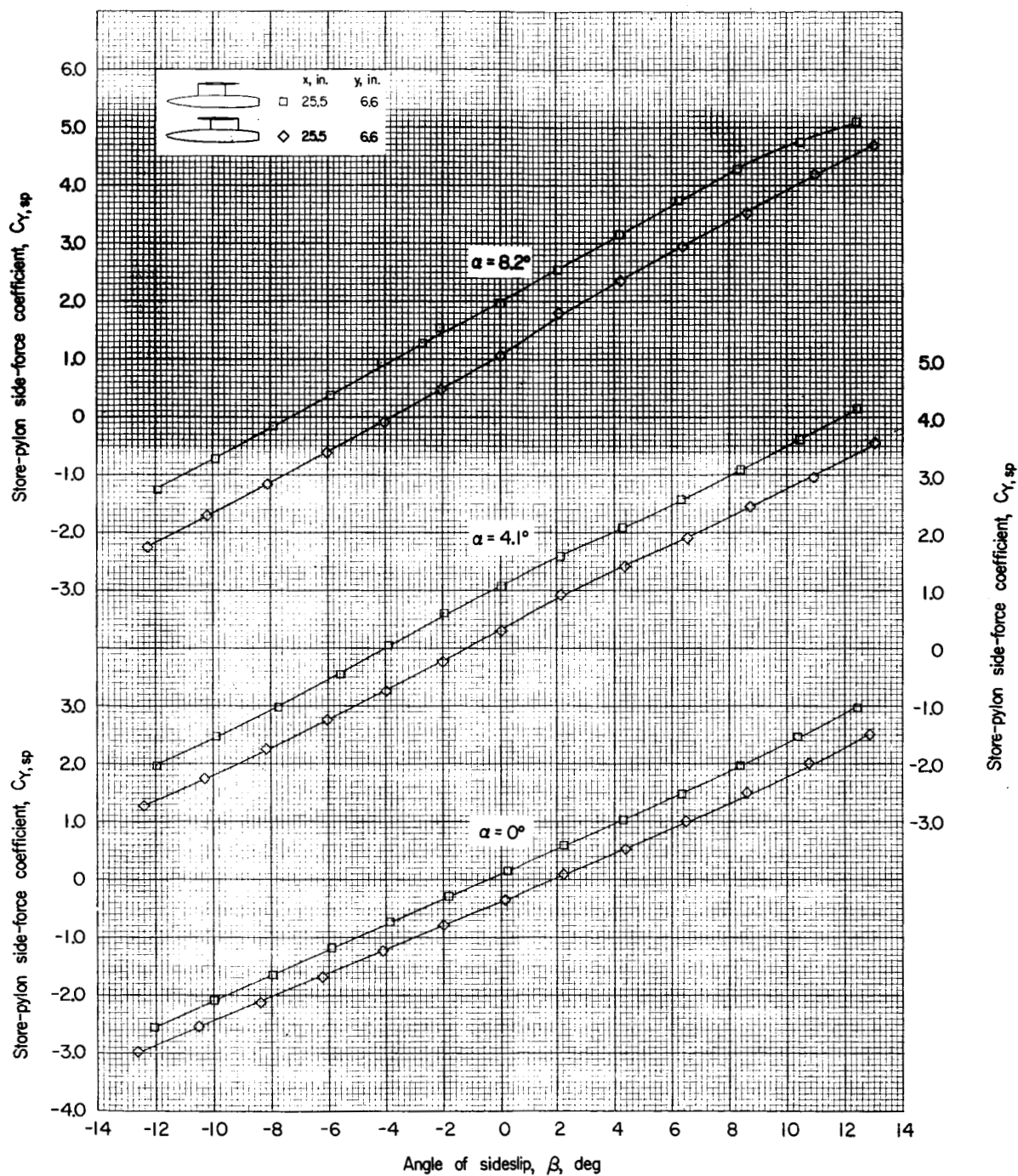


(b) Variation of $C_{n,sp}$ with β .



(c) Variation of $C_{M,sp}$ with β .

Figure 31.- Concluded.



(a) Variation of $C_{Y,sp}$ with β .

Figure 32.- Effect of pylon location on the aerodynamic characteristics of the store-pylon combination in the presence of the wing-fuselage combination.

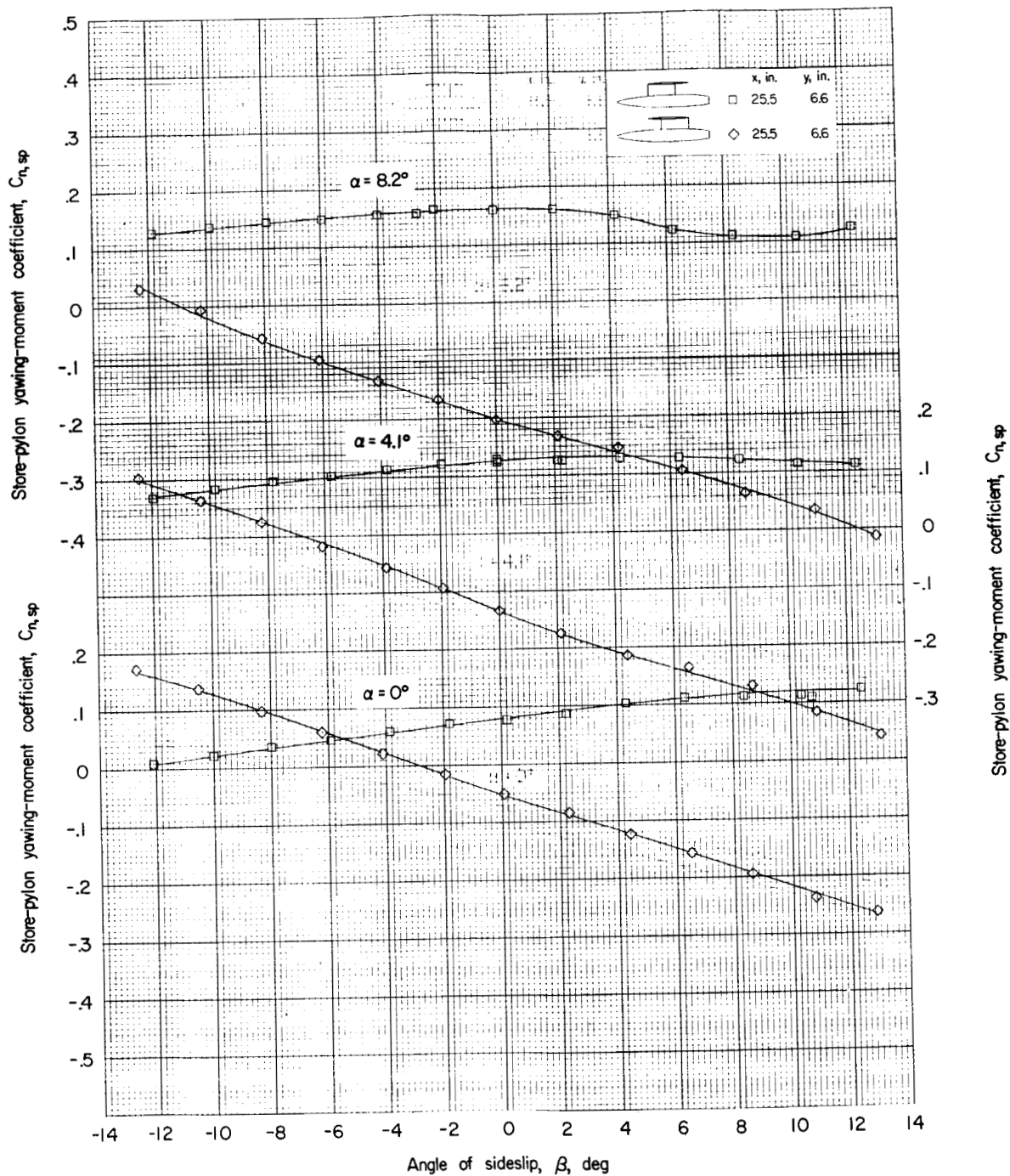
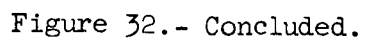
(b) Variation of $C_{n,sp}$ with β .

Figure 32.- Continued.



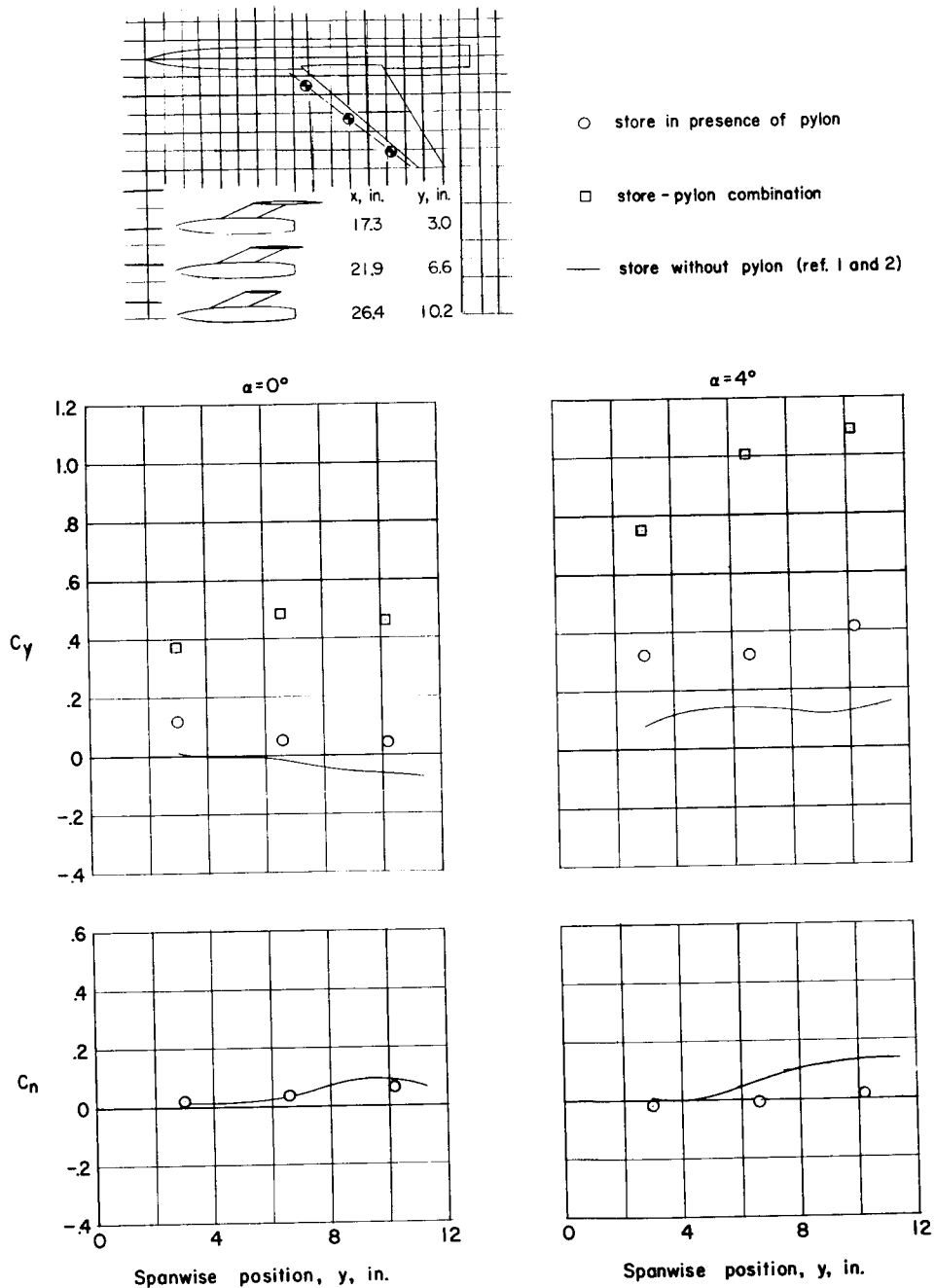
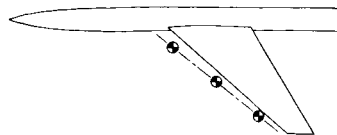
(a) C_Y and C_n .

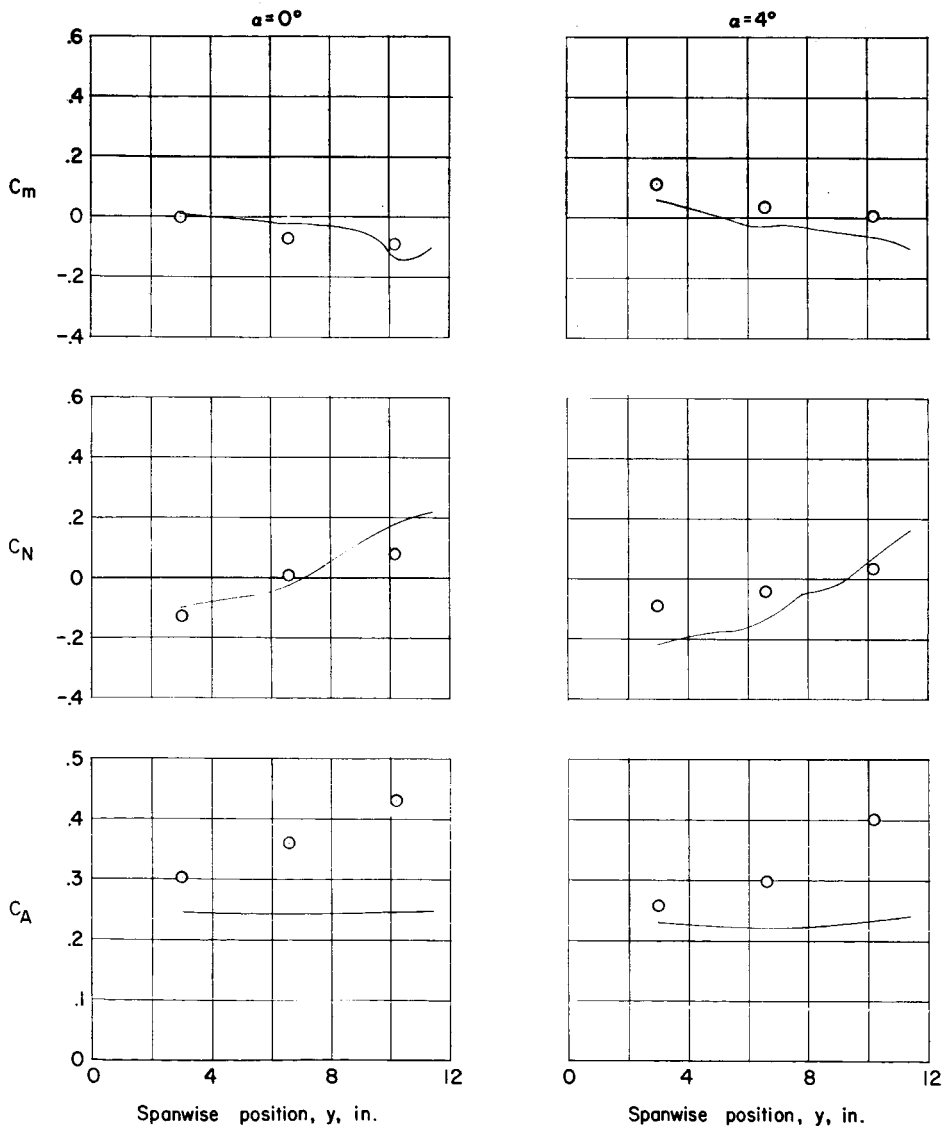
Figure 33.- Spanwise comparison of the store and store-pylon coefficients.



	$x, \text{ in.}$	$y, \text{ in.}$
	17.3	3.0
	21.9	6.6
	26.4	10.2

○ store in presence of pylon

— store without pylon (ref. 1 and 2)



(b) C_m , C_N , and C_A .

Figure 33.- Concluded.

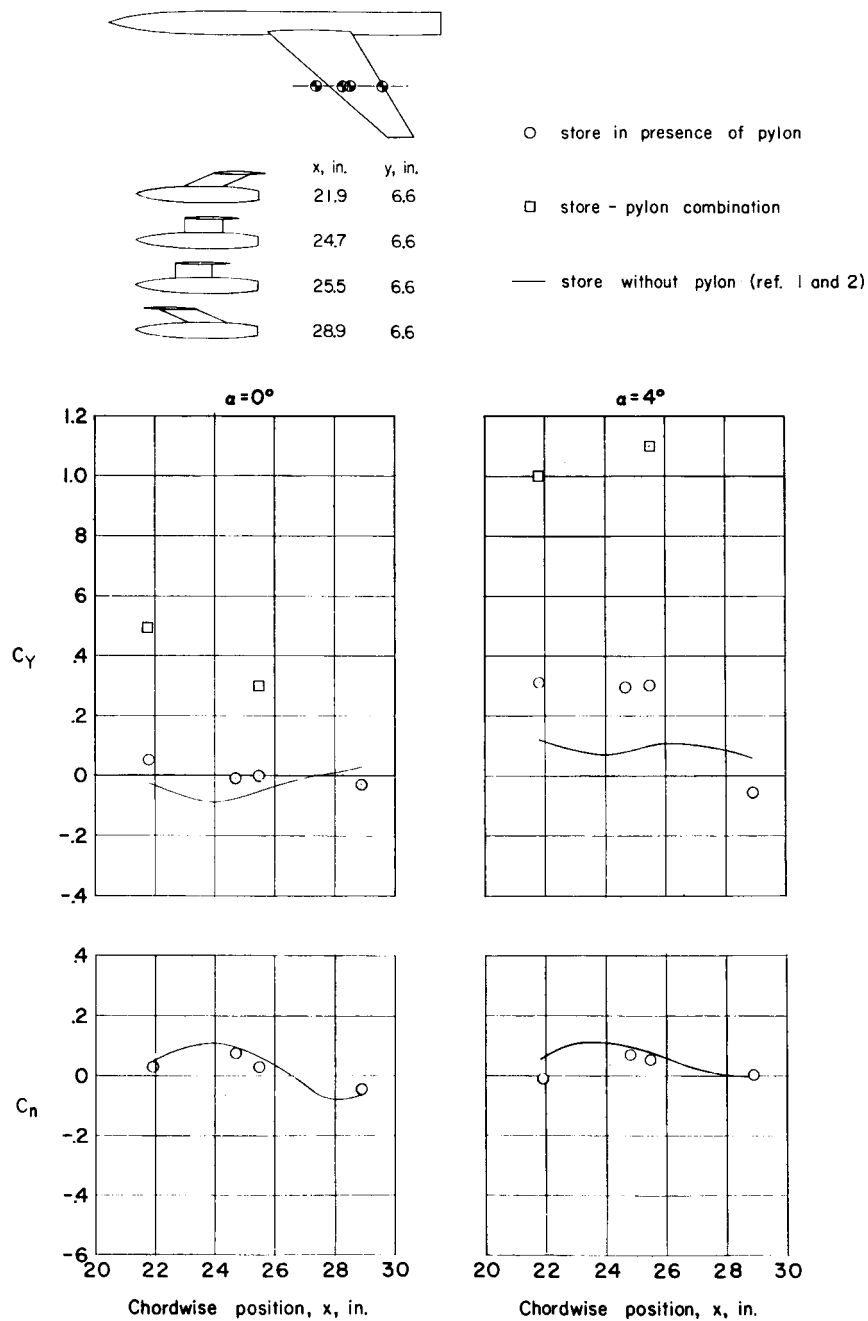
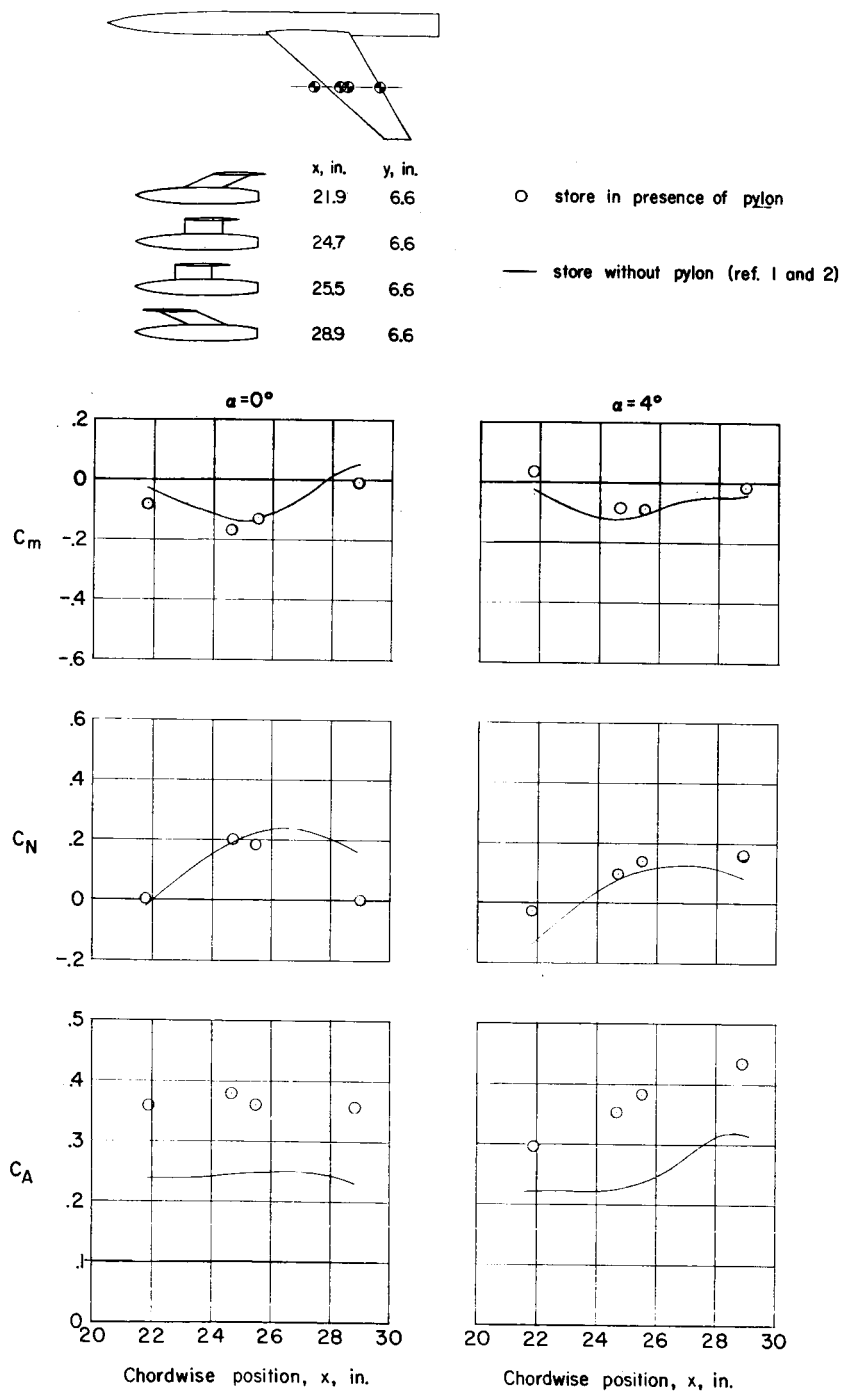
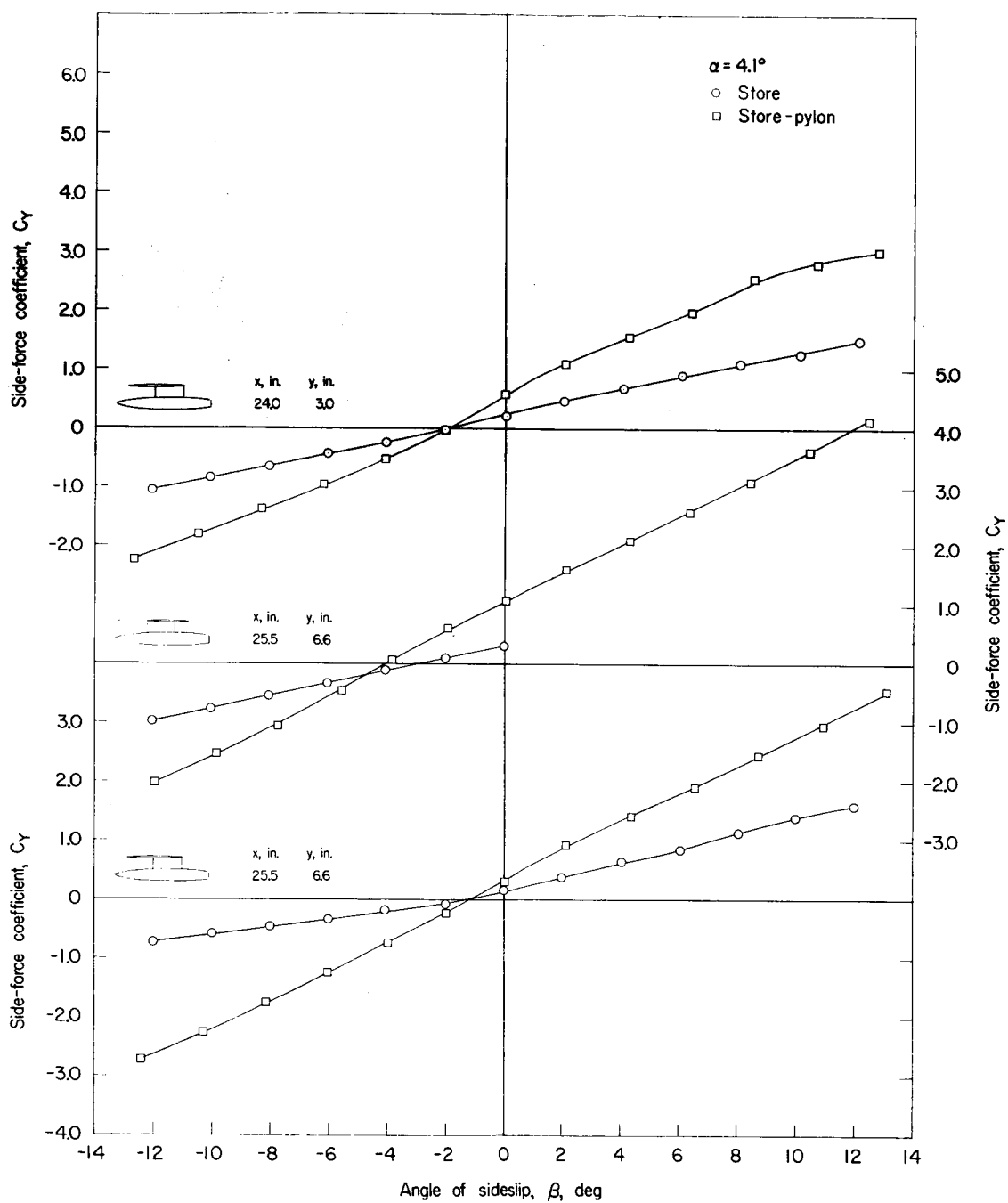
(a) C_Y and C_n .

Figure 34.- Chordwise comparison of the store and store-pylon coefficients.



(b) C_m , C_N , and C_A .

Figure 34.- Concluded.



(b) Unswept pylon.

Figure 35.- Concluded.

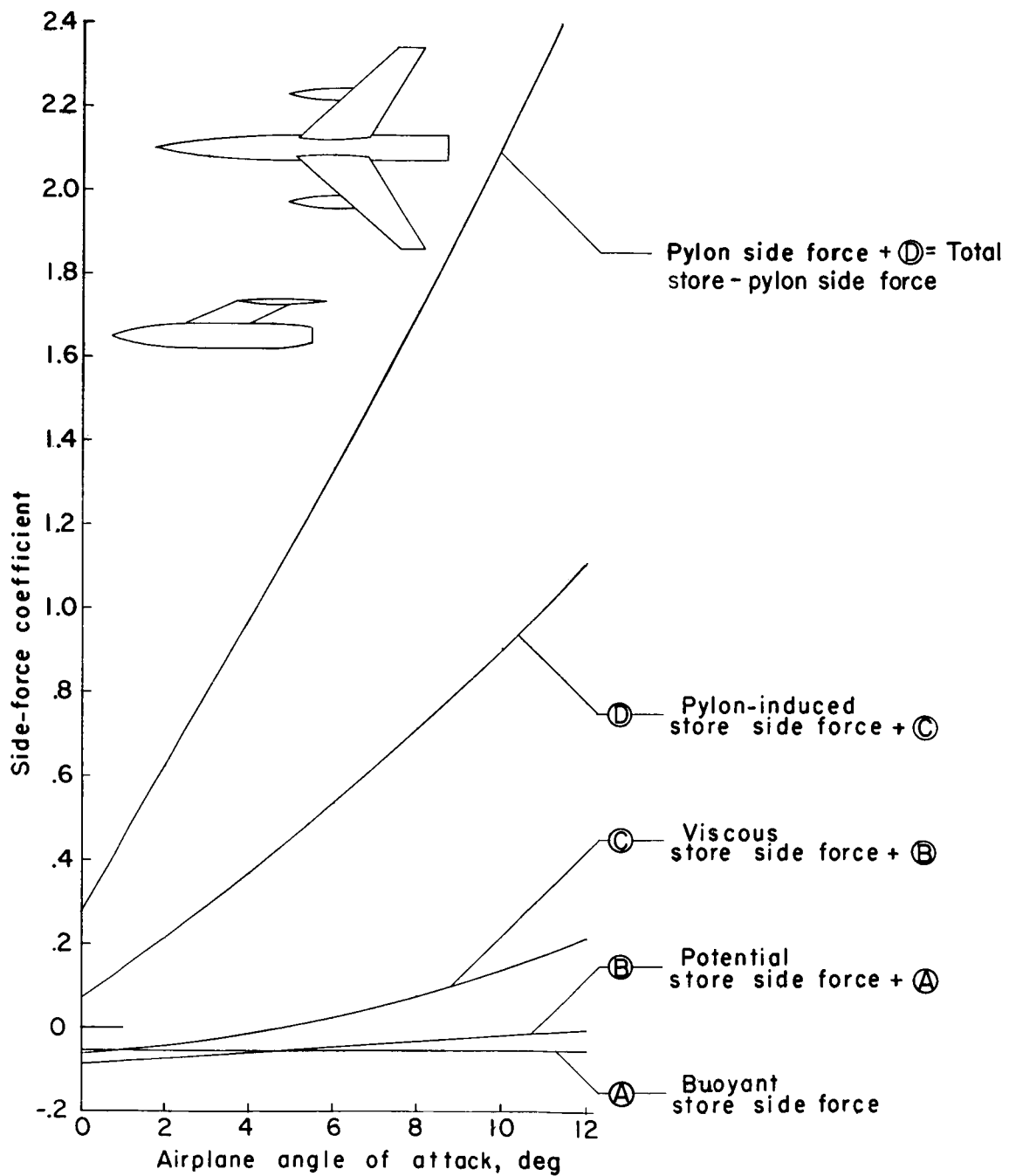
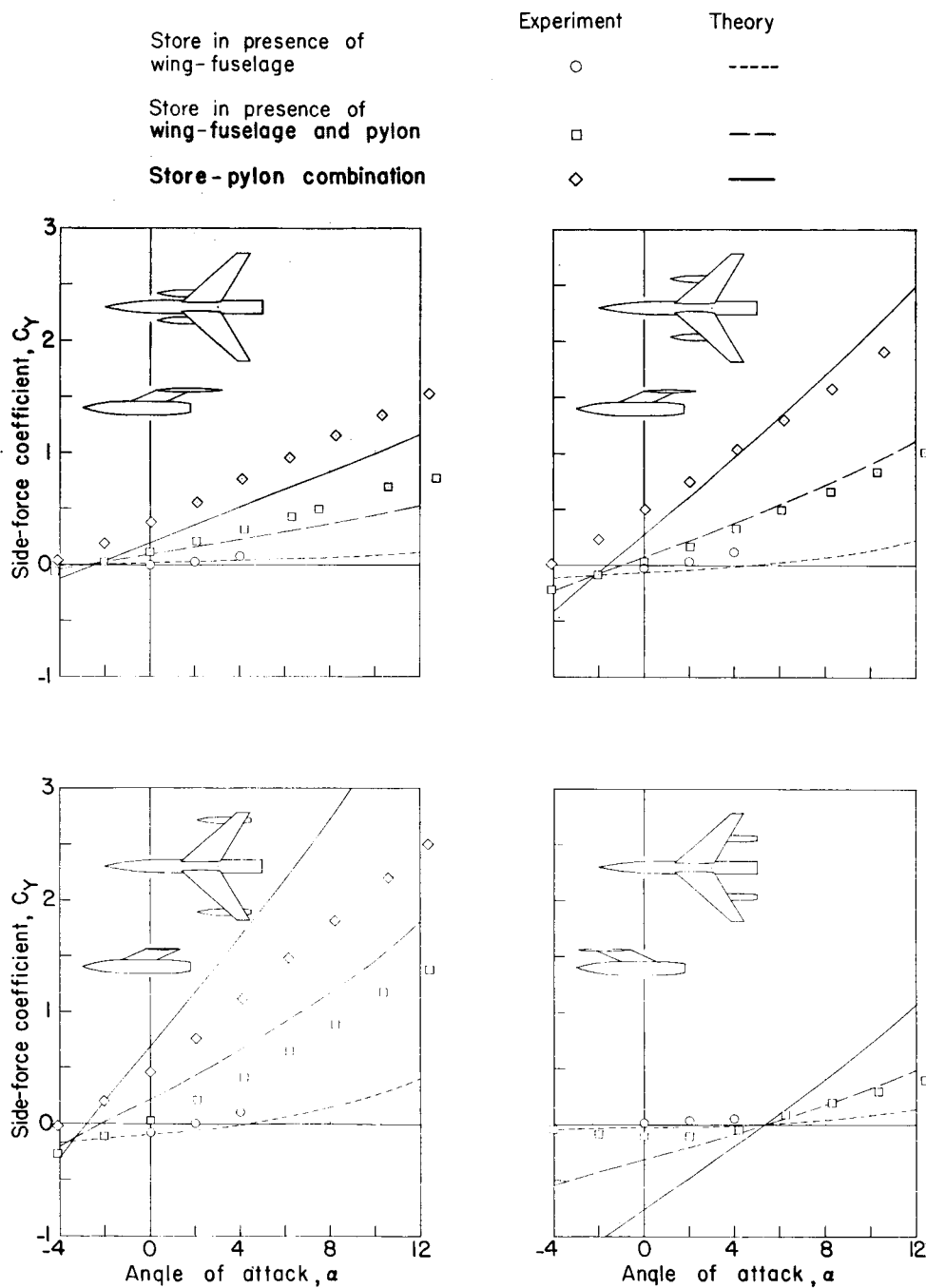
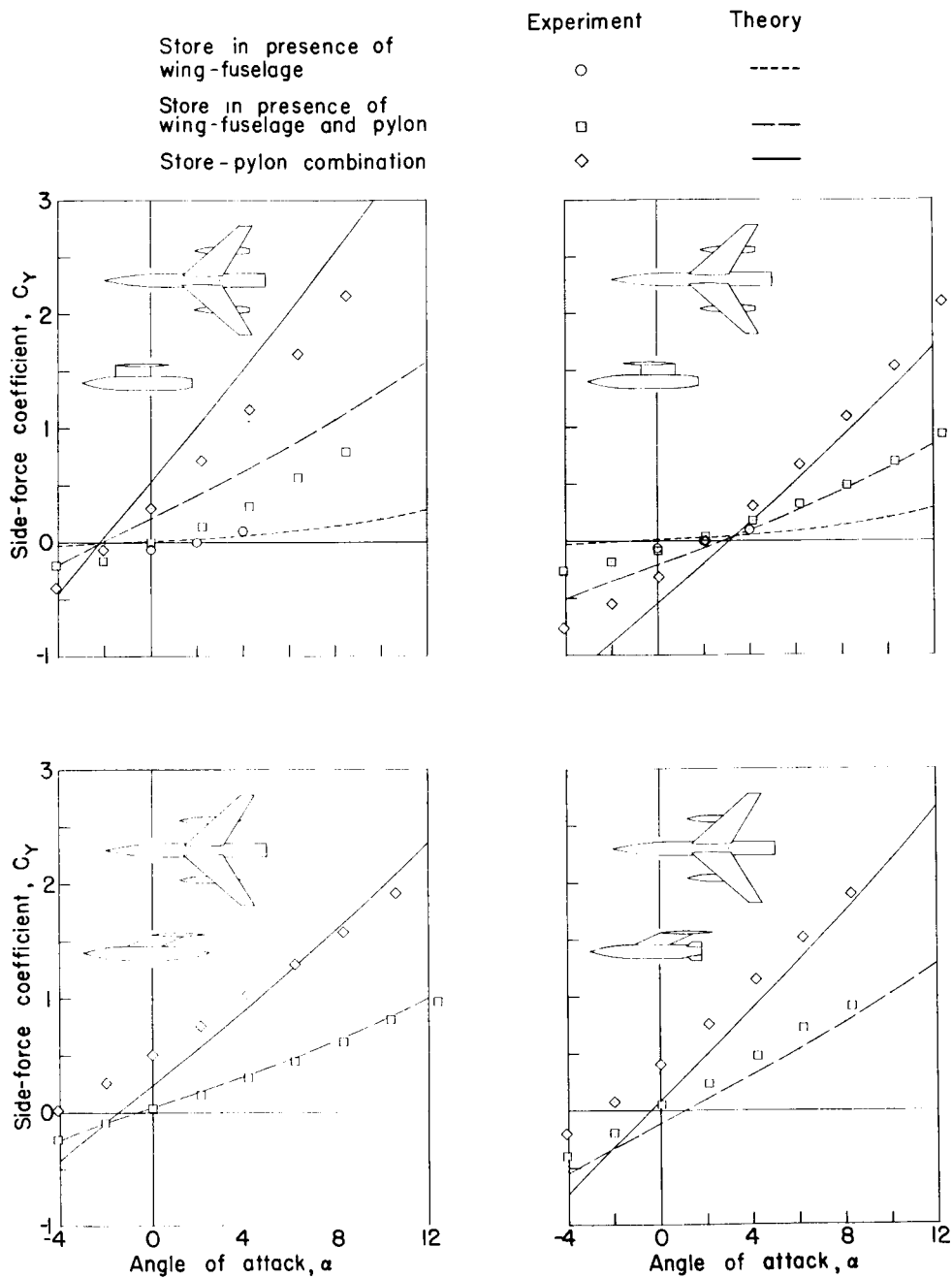


Figure 36.- Relative contribution of the various theoretical components of store-pylon side force.



(a) Effect of spanwise positions and pylon sweep.

Figure 37.- Comparison of theoretical and experimental side force.



(b) Effect of fins, store tail cone, and change in pylon location.

Figure 37.- Concluded.

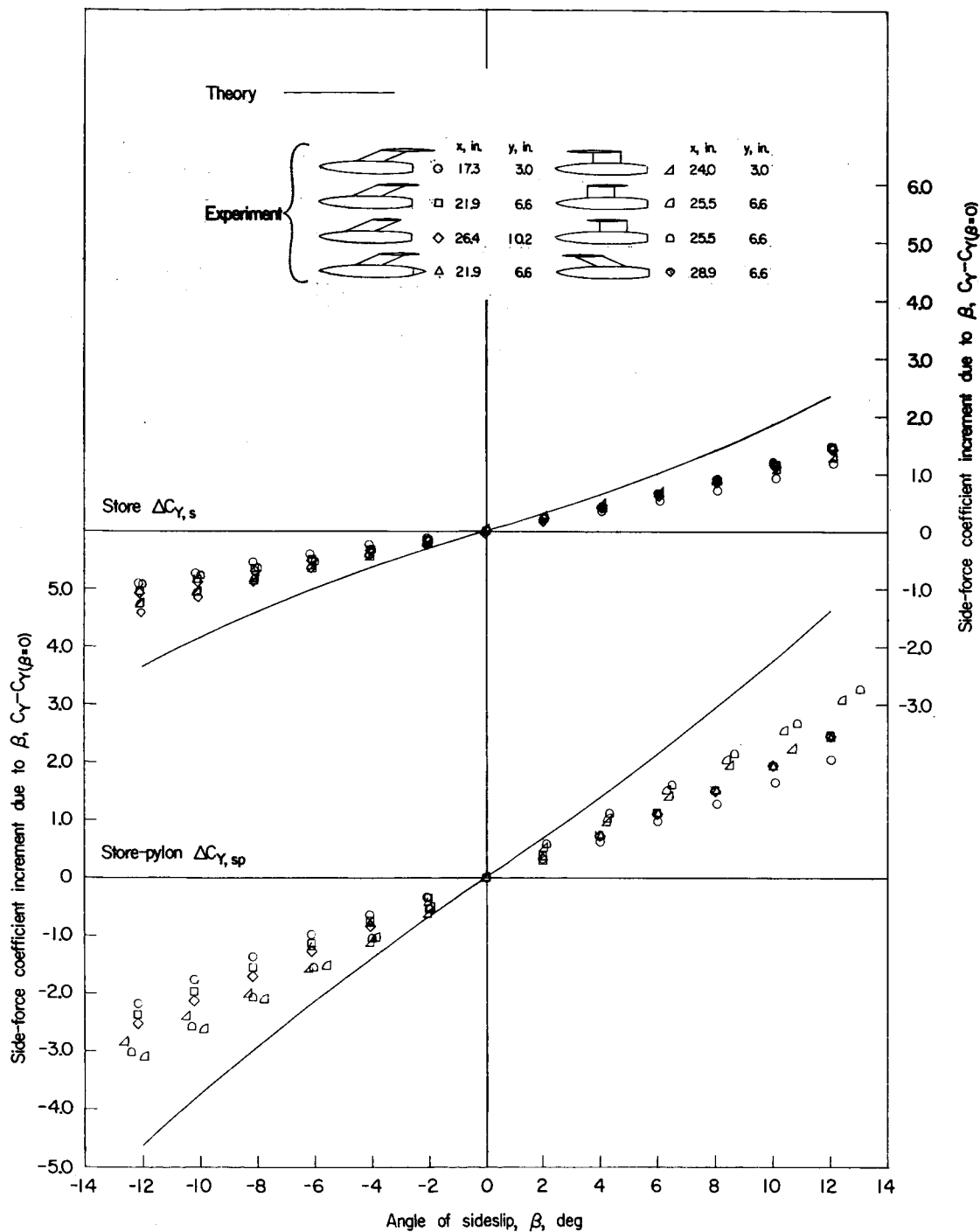


Figure 38.- Comparison of theoretical and experimental side force.
 $\alpha = 4^\circ$. (Signs reversed on store angle of sideslip for ease of comparison.)